EUROPEAN ORGANIZATION FOR NUCLEAR RESEARCH (CERN)

LHCb-PUB-2015-008
10th July 2015

LHCb Scintillating Fibre Tracker Engineering Design Review Report: Fibres, Mats and Modules

The LHCb Scintillating Fibre Collaboration

Abstract

During the Long Shutdown 2 of the LHC, the LHCb collaboration will replace the current Outer and Inner Tracker by a single tracking detector, based on 2.42 m long scintillating fibres with a diameter of 250 μm, readout by silicon photo-multipliers (SiPM). The fibers are arranged in mats of 6 fibre-layers with a width of 130.65 mm. Eight fibre mats will form a module and are sandwiched between honeycomb and carbon fibre composite panels to provide stability and support over the module length of 4.85 m. At either end of the module are the interfaces to the SiPMs and the front-end electronics. The active detection area of the Scintillating Fiber Tracker (SciFi) of 360 m^2 will comprise 144 single modules arranged in 12 detection planes.
This document summarizes the engineering design of the fibre mats and of the modules including the interfaces to the SiPMs and the mounting to the detector frames. Mechanical and detector properties of several prototype modules are discussed. The production procedure of the fibre-mats and the modules is introduced and time and cost estimates are given. Details of the mounting of the SiPM inside a cold-box as well as the connection to the front-end electronics is subject of a separate EDR. Detector frames are also excluded from the discussion in this document.

Contents

1 Introduction **1**
1.1 Requirements . . . 1
1.2 Design of the Scintillating Fibre Tracker . . . 3
1.2.1 Fibre and fibre mats . . . 4
1.2.2 Module design . . . 5
1.2.3 Number of individual SciFi components . . . 5
1.3 Production of fibre mat and modules . . . 5
1.4 Detector assembly and installation . . . 7
1.5 Test modules and prototypes . . . 7

2 Scintillating Fibres **10**
2.1 Specifications . . . 10
2.2 Measurements and results . . . 13
2.3 Radiation effects . . . 22
2.4 Procurement plan . . . 24
2.5 Quality Assurance . . . 25
2.6 Safety considerations . . . 26
2.7 Open issues and remaining developments . . . 26
2.8 Perspective of NOL fibres . . . 27

3 Fibre Mats **29**
3.1 Introduction . . . 29
3.2 Winding of fibres into mats . . . 30
3.2.1 Winding machine . . . 30
3.2.2 Winding Wheel . . . 34
3.2.3 Process and materials . . . 36
3.3 Mat Casting and Endpiece Gluing . . . 40
3.3.1 Components . . . 40
3.3.2 Casting and gluing tools . . . 40
3.3.3 Casting of fibre mats . . . 42
3.4 Cutting and Mirroring . . . 51
3.4.1 Transversal cut to Diamond Polish fibre ends . . . 51
3.4.2 Longitudinal cut . . . 58

3.5 Demonstrators and Measurements . . . 59
3.6 Quality Assurance . . . 66
3.6.1 Online monitoring during winding . . . 67
3.6.2 Optical scan of fibre mat cross section . . . 67
3.6.3 Optical scan after longitudinal cut . . . 69
3.6.4 Metrology . . . 70
3.6.5 Tests with ionizing particles . . . 70
3.7 Open issues and remaining development . . . 71

4 Fibre Modules **74**
4.1 Module Assembly . . . 76
4.1.1 Beam-pipe module . . . 79
4.2 Module Components . . . 81
4.2.1 Endplugs . . . 81
4.2.2 Half-Panels . . . 83
4.2.3 Material Budget . . . 86
4.2.4 Tooling . . . 87
4.3 Finite element calculations . . . 91
4.4 Survey strategy and integration of targets . . . 95
4.4.1 Survey results of the 5 m dummy module . . . 95
4.5 Production plan and logistics . . . 97
4.5.1 Sites . . . 97
4.5.2 Schedule for Production . . . 97
4.6 Shipping and Logistics . . . 97
4.7 Quality Assurance . . . 98
4.8 Safety considerations . . . 98
4.9 Open issues and remaining developments . . . 99

5 Interfaces **100**
5.1 The Module and ROB . . . 100
5.1.1 ROB . . . 100
5.1.2 SiPMs, Fibre Mats and and Endpieces . . . 101
5.2 The Module and the C-Frames . . . 103

6 Test Beam Results **106**
6.1 Experimental Setup . . . 106
6.2 Calibration . . . 107
6.3 Analysis . . . 107
6.3.1 Results . . . 108
6.3.2 Attenuation length . . . 108
6.4 Conclusion . . . 111

7 General Planning, Production Schedule and Costs **114**
7.1 General Planning . . . 114
7.2 Production scheme and task sharing . . . 115
7.2.1 Winding Centres . . . 115
7.2.2 Module assembly centres . . . 116
7.2.3 Quality Assurance . . . 117
7.3 Summary of Costs . . . 117

8 Appendix **119**
8.1 Laser Setup . . . 119
8.2 Fibremat straightness with a Sr-90 source . . . 120

References **124**

Chapter 1

Introduction

The upgrade of the LHCb detector [1], which will take place during the Long Shutdown 2 (LS2), from the end of 2018 until the end of 2020, will extend significantly the physics reach of the experiment by allowing the detector to operate at a higher instantaneous luminosity of $2 \times 10^{33}\,\mathrm{cm}^2\ \mathrm{s}^{-1}$. At the same time a triggerless 40 MHz readout will increase the efficiency for a wide range of hadronic B decay channels. Today, the LHCb main tracking system consists out of an Inner Tracker, built from silicon strip sensors, and an Outer Tracker, using 5 mm straw-tubes for the particle detection. To cope with the expected high particle multiplicities after LS2 both detectors will be replaced by a high granular, uniform, low-mass Scintillating Fibre Tracker (SciFi). The location of the new SciFi detector within LHCb is shown in Fig. 1.1. The conceptual design of this tracking detector is described in Ref. [2].

1.1 Requirements

The main tracking stations (T-stations) should continue the tracklets found in the upstream detectors (Velo and UT) after passing the magnetic field. In addition the T-stations should provide standalone track reconstruction for particles without signals in the upstream detectors. The tracking algorithms require a high hit efficiency, good spatial resolution in the bending plane of the magnet (x coordinate), and low material budget in the acceptance. The detector must be able to operate for the full lifetime of the upgraded LHCb detector ($50\,\mathrm{fb}^{-1}$) to ensure that the performance of the track reconstruction is good enough for the duration of the experiment. The main requirements for the SciFi detector are:

- The detection efficiency for single hits or clusters of hits should be close to 99%.
- The rate of accepted dark counts (DCR) should be, at any location of the detector, well below the signal rate ($< 10\%$).
- The detector should be readout at a rate of 40 MHz. The digitization should have no dead-time.

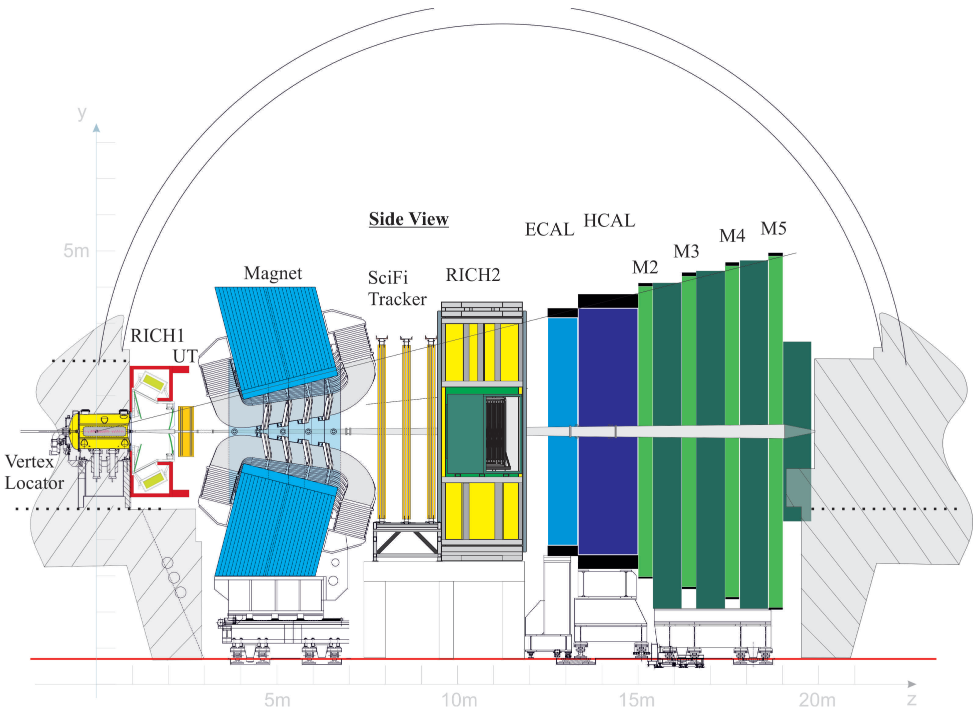

Figure 1.1: Schematic side-view of the planned upgraded LHCb detector. UT = Upstream Tracker. SciFi Tracker = Scintillating Fibre Tracker.

- The single hit spatial resolution in the bending plane of the magnet (x direction) must be better than 100 µm. The required resolution in vertical direction (y direction) is about 1 mm and can be achieved by stereo-layers (u, v layers) rotated by $\pm 5°$ with respect to the vertical layers (x-layers). The chosen layer arrangement ($3 \times$ x-u-v-x) is not subject of the EDR.

- To achieve the spatial resolution, a precision alignment of the detector modules will be made using particles. This procedure will be complicated if the shape of the single detector elements is not well known or unstable in time. The construction principle of the mats and modules thus assumes that the fibres inside a single module (8 mats) are straight and aligned better than 50 µm in the x-direction, and the fibre layers are flat within 300 µm in the z-direction. This requirement will ensure that the the spatial resolution can be obtained over the large area.

- As we assume a track alignment of the single modules the absolute position of the modules is not too relevant. However, time variations of the module positions and the module shape should be avoided.

- The SciFi material in the acceptance region should be minimized such that the effect of multiple scattering in the tracker is smaller than the effect due to the material upstream of the magnet. This is achieved when the radiation length of a SciFi detection layer, X, is in the order of 1% of a radiation lengthX_0. The material should also be minimal since the hadronic interaction of charged particles with the detector material is a source of tracking inefficiency.

- The detector should be able to operate with the required performance for an integrated luminosity up to $50\,\text{fb}^{-1}$. The irradiation profile due to the ionizing particles is very inhomogeneous and follows roughly an $1/r^2$ distribution. The parts of the scintillating fibres in the most irradiated region around the beam pipe will have seen a total ionizing dose of 35 kGy. The ionization dose will change the transparency of the scintillating fibres and decrease the attenuation length for the scintillating photons. At the same time the SiPMs mounted at the outer detector edge will have seen a neutron fluence of up to 6×10^{11} neutron (1 MeV equivalent)/ cm^2[1].

1.2 Design of the Scintillating Fibre Tracker

The SciFi will cover the detection area from the edge of the beam-pipe to distances of about 3 m in the horizontal and 2.4 m in the vertical direction with a single detector technology based on 250 μm scintillating fibres. In total 12 detection planes arranged in 3 stations (T1, T2, T3) are foreseen. As can be seen in Figure 1.2 the 12 detection planes are sub-divided in half-planes, each containing 6 individual, and (with the exception of the innermost beam-pipe modules) equal detector modules. The modules contain 2.42 m long scintillating fibres with a diameter of 250 μm which are arranged in 130.65 mm wide and 2.4 m long fibre-mats (also called submodules) of 6 staggered layers of fibres. The fibres will be read-out by arrays of silicon photo-multipliers (SiPMs) with a channel widths of 250 μm and a channel height of 1.62 mm. The SiPM are mounted on a cooling bar inside so-called Read-out Boxes (ROB) at the top and bottom edge of the detector. The cooling bar together with the SiPMs is precisely positioned with respect to the fibre ends. The precise SiPM mounting on the fibre matrix will provide the position of the through-going particles. To suppress dark noise of the SiPMs after being irradiated, the SiPMs are cooled to -40°. The lower part of the readout-boxes, called cold-box, contain all the cold parts and should insulate the cold SIPMs and the cold-bar against the outside. The conceptual design of this cold-boxes and their interfaces to the modules is not part of this EDR, but because for completeness is described in section 5.1.

To increase the number of scintillation photons seen by the SiPMs the fibre ends in the middle of the detector are equipped with a thin mirror to reflect the light towards the readout ends.

The individual fibre modules will be mounted on to a C-frame as indicated in Fig. . The C-frames are not part of the EDR. However the suspension of the modules is discussed in section 5.2.

[1] Assumes shielding of the neutrons by a layer of polyethylene in front of the calorimeter.

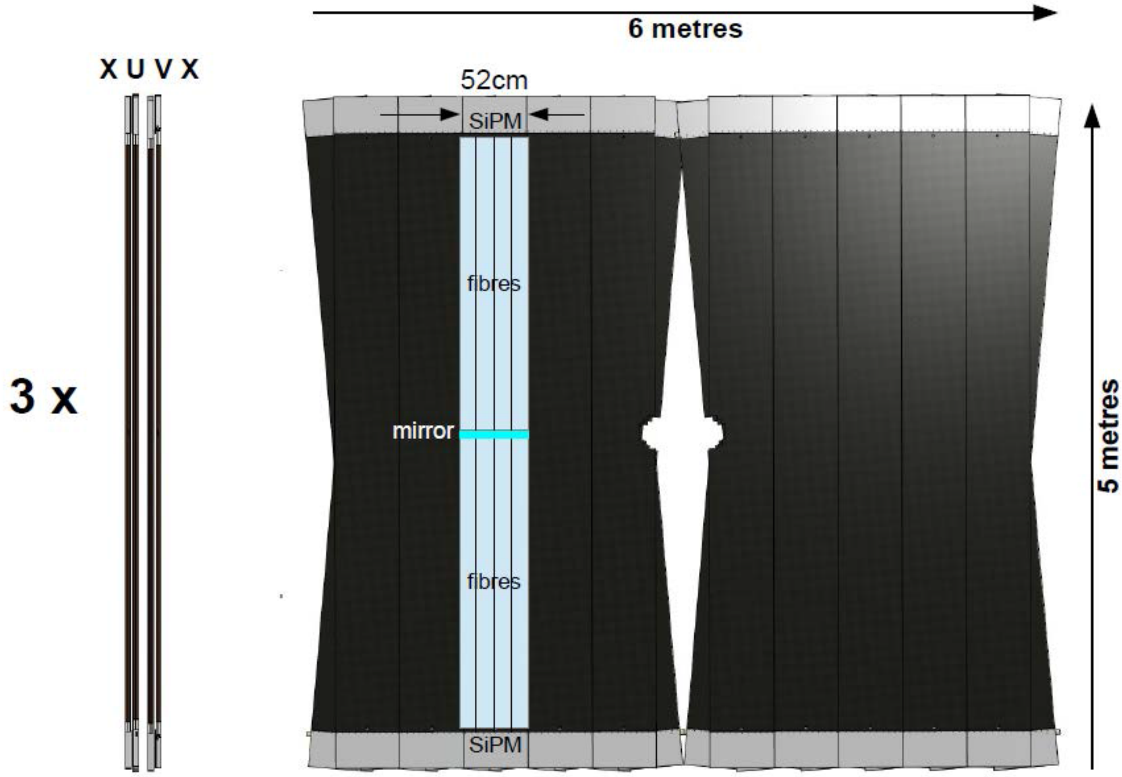

Figure 1.2: Schematic yz- and xy-view of one of the planned SciFi Tracker stations. It is composed out of 4 stereo-layers with vertical (x) and rotated (u,v) fibre orientation. Each the layers is composed out of two half layers with 6 individual fibre modules.

1.2.1 Fibre and fibre mats

The plastic scintillating fibres of 250 μm diameter with an attenuation length larger than 3 m are used. The attenuation length is crucial to ensure a high number of photons also for hits far away from the SiPMs.

Fibre mats are produced by winding 6 layers of fibres on a threaded winding-wheel with a diameter of approx. 82 cm. The winding puts the fibres in a regular hexagonal matrix with a fibre pitch of 275 μm. Fibre diameters exceeding 300 μm can lead to local defects in the winding pattern and affect the spatial resolution. Epoxy is used to bond the fibres to each other. After the curing of the epoxy the fibre-mat is cut and removed from the wheel.

The fibre mats, once removed from the winding wheel, are fragile objects and easily break or split during handling and transport. Considering the number of fibre mats that will have to be produced (≈1300) and the fact that they will need to be produced at multiple sites by different institutes and transported for module assembly, a simple and robust method was developed to protect the mats by casting them in a thin layer of epoxy.

During the glue casting plastic endpieces to connect to the SiPMs are added. On the far end (with respect to the SiPM) a plastic piece to carry a mirror (reflective foil) is added. Finally the fibre mats are cut to their final dimensions and tested.

A key element of the presented technology are the alignment pins which are added during the winding process to the fibre mat at precise locations (by filling holes on the winding wheel with epoxy). For the further machining of the mats as well as for the positioning of the mats in a module the pins are clicked into precisely machined grooves of the assembly templates or the handling tools. No optical alignment of the mats is necessary. The alignment pins ensure that the fibres follow exactly the machined grooves.

1.2.2 Module design

Modules are built from 8 mats sandwiched between two half-panels. The half-panels are made of 20 mm high honey-comb sheets laminated on the outer side with carbon-fibre skins. The two half-panels surrounding the fibre mats result into a symmetric module design. In this way one limits internal stresses which would deform the modules. As described above, a precise template will allow the exact positioning of the fire-mats with respect to each other before gluing the supporting panels to the mats. So called end-plugs surround the endpieces and are used to mount the modules on the C-frames and to connect the readout-box. An exploded view and cross-section along the 4.85 m length of a module are shown in Fig. 1.3.

Beside the standard modules we foresee special beam-pipe modules with a circular cut-out in the middle. With the exception of this cut-out the beam-pipe modules will follow the design of the standard modules. The exact cut-out geometry is still subject of optimization and therefore the special modules are not discussed in this EDR.

1.2.3 Number of individual SciFi components

The total number of different SciFi components (modules, mats, individual channels, SiPMs) required for the planned SciFi detector is listed in Table1.1. Cost increases and a larger number of detector modules than in the TDR, forces us to abandon the production of spare modules. In case spare modules are needed the outer modules of the first tracking stations shall be used as such.

However to produce 144 fully working detector modules we need more fibre mats than the 1152 mats listed in Table 1.1. To account for losses and not perfect mats we will produce about 1300 mats.

1.3 Production of fibre mat and modules

The serial production of fibre mats (1300) and the modules (144) for the SciFi is foreseen to start in January 2016 and should finish in August 2017.

For the production of the 1300 fibre mats a total of 10000 km of scintillating fibre is needed. A high fibre quality (correct diameter, on defects, large optical attenuation length,

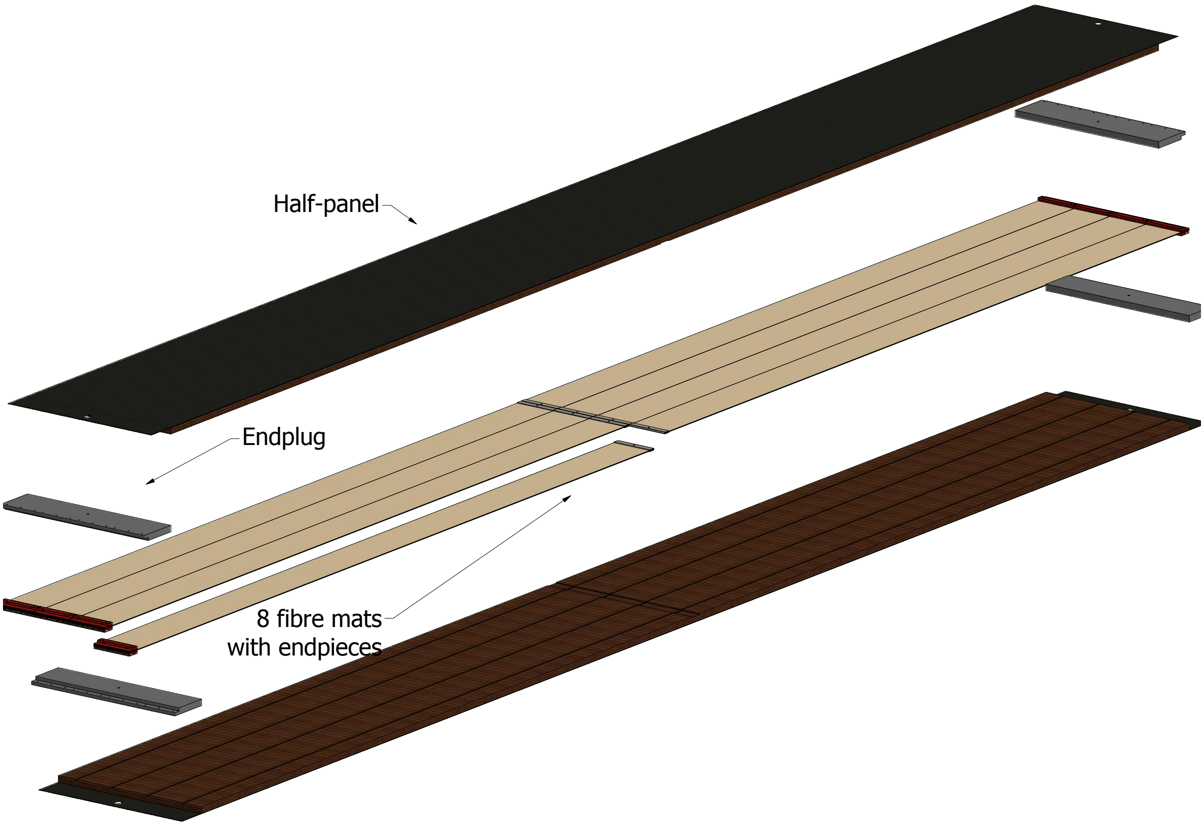

Figure 1.3: An exploded view of a finished module.

high photon yield, radiation tolerance) is the condition to build a fibre detector with high efficiency and excellent spatial resolution. All fibres therefor undergo a careful quality check before being distributed to the Winding Centres (Sect. 2.5).

The mat production, the casting, the gluing and machining of the end-pieces, and the necessary quality assurance tests of the finished mats will be done at four Winding Centres. A Winding Centre should produce 4 mats per week assuming a single shift per day. The mats will be shipped to two Module Assembly Centres.

The first step in the Module Assembly Centers is the cutting of the mats along their long edge to their final width. The mats are positioned inside a gluing template. With the gluing of the first half-panel the mat positions are fixed. The second half-panel is added to build a symmetric and stiff module. The modules will be tested and shipped to CERN where the detector assembly will take place.

The fibre mat and module production scheme as well as the production schedule is discussed in section 7.2.

In parallel with the engineering of the detector components and the production tools,

Table 1.1: Components of the SciFi

Number of detector layers	12
Total number of modules	144
Standard modules	120
Beam-pipe modules	24
Number of mats per module	8
Total number of mats	1152
Number of channels per mat	512
Number of channels per module	4096
Total number of channels	590k
Number of SiPM arrays per mat	4
Total number of SiPM arrays	5008
Total number of Readout/cold boxes	288

quality assurance (QA) procedures have been developed. In addition a flexible database to store the production and quality data has been setup. When producing the full-size prototype (demonstrator, see Sect. 1.5) the QA procedures have been used to determine the mat and module properties (see Sect. 3.6 and 4.7). The information has been recorded in the specific production and QA data-base.

1.4 Detector assembly and installation

After arriving at CERN the modules will be re-tested and will be mounted on the C-frames as illustrated in Figure 1.4. Each of the 12 C-frames carries two stereo-layers. For the exact positioning of the modules, precise spheres mounted on the C-frames and sliding in special mounting holes inside the endplugs of the modules will be used. The readout boxes are added. The C-frame assembly at CERN should start in July 2017. All C-frames must be ready for installation in August 2018.

Once fully assembled and equipped with electronics (includes careful testing of the readout electronics) the C-frames are lowered into the experimental cavern and are installed in LHCb (see Figure 1.4).

1.5 Test modules and prototypes

A series of small and full size prototypes have been built and different tests have been performed:

- Several small 5-layer prototype modules have been studied in a pion beam in October and November 2014. One of the small prototypes had the size of 130 mm × 2.5 m, comprised a single mat and was built following the concept of this document. In the

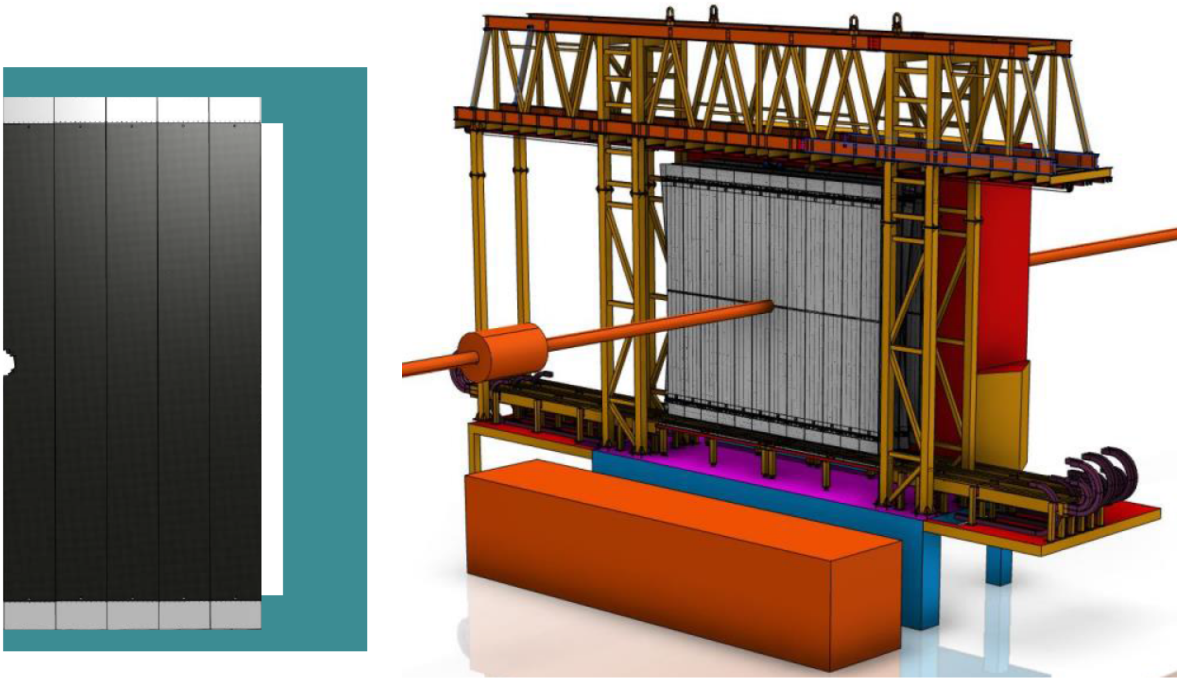

Figure 1.4: Left: Sketch to illustrate the modules mounting (x laxer) on a C-frame. The C-frame carries on each of its sides a layer. Right: Installation of the C-frames on a support bridge in the LHCb experiment.

2014 test-beam also a small module with a 6-layer mat built with a slightly different technique (coverlay technique) was tested.

- A small 6-layer module (130 mm × 2.4 m) was studied intensively in a pion test beam in May 2015 (**May test beam module**). The module was built following the EDR concept. Efficiency and resolution results are reported in section 6.

- A full size (0.5 m×4.8 m) mechanical dummy module has been built and its mechanical properties have been determined (**full size dummy**). This module is constructed with the tools and following the procedures described in this document. Only the fibre mats have been replaced by equally thick plastic sheets. All other parts are as described in this document.

- A full size (0.5 m × 4.8 m) prototype module has been constructed (**demonstrator**). This module contains 8 6-layer fibre mats. The production of the components have been documented. The quality of the fibre mats was examined. Due to time-constraints only basic mechanical measurements have been performed on the finished modules.

Due to the construction of the module from 8 individual fibre mats we consider the efficiency and resolution results obtained with the **May test beam module** as representative for the full size modules. Measurements with a full size module using beams with limited beam spot sizes will not provide additional information.

Chapter 2

Scintillating Fibres

2.1 Specifications

The specifications of the scintillating fibres described in this section are based on the document [3]. They are driven by the following main requirements on the SciFi tracker performance:

- The SciFi tracker is designed to detect particles with high hit efficiency and a spatial resolution of better than 100 μm in the direction orthogonal to the fibre axis.
- It is conceived to allow for a clear matching of the detected particles with the LHC bunch crossings which occur in intervals of 25 ns.
- The tracker is expected to operate in the radiation field of secondary particles generated by the LHC beam collisions. The field is highly non-uniform and concentrated in a cylindrical region around the LHC beam axis of 0.5 m diameter. This coincides with the region from where the scintillation light has to travel the longest distance to the photodetectors (up to 2.4 m). Fluka simulations predict the maximum integrated ionizing dose to which the fibres are expected to be 35 kGy. It is mainly composed of charged hadrons.

In the following we describe the required specifications, grouped in material related, geometrical, mechanical, optical, radiation related and other aspects.

The scintillation material

The performance requirements of the SciFi tracker described above, call for a scintillating plastic material with short scintillation decay time, high intrinsic light yield per absorbed energy, low specific density and low nuclear charge number such as provided by a Polystyrene based scintillator.

- Scintillation decay time $\tau_d < 3$ ns

- Light Yield $Y_l > 7000$ ph/MeV
- Specific density $\rho < 1.1$ g/cm^3
- Nuclear charge number $A < 12$

Geometry

The scintillating fibre shall have a round cross section with an average total diameter D of 250 μm. As shown in Fig. 2.1, it shall consist of a scintillating core and a cladding structure, which is discussed in more detail below. To maintain a high active volume fraction, the thickness of the cladding structure shall not exceed 6% of the total diameter. The statistical variation of the total diameter shall be smaller than $3\sigma/D = 4\%$ (or $\sigma = 3.3\mu$m for $D = 250\mu$m).

While the producers have no difficulties to fulfil the above specifications averaged over a fibre of several km length, all fibre samples tested in the past year showed local variations of the fibre diameter which are outside the statistical limits. These *bumps and necks* are related to the production process and environment, details of which are not disclosed by the producers.

Experience from winding fibre mats indicates that bumps up to 300 μm diameter have only a local quasi-negligible impact on the winding pattern. Bumps exceeding 300 μm can lead to regional defects in the winding pattern which may affect hit efficiency and spatial resolution.

We therefore request the fibres to be free of bumps exceeding 300 μm. In case the producers are not fully meeting this requirement, steps can be taken to remove faulty sections from the fibre as described in 3.2.

Necks with diameters below 200 μm are suspected to weaken the strength of the fibre and may compromise the light transport along the fibre. The fibres shall therefore also be free of such defects.

The deviation from roundness D_x/D_y , where D_x and D_y are measured in any two orthogonal directions, shall not differ from unity by more than 5%. The fibres shall have a

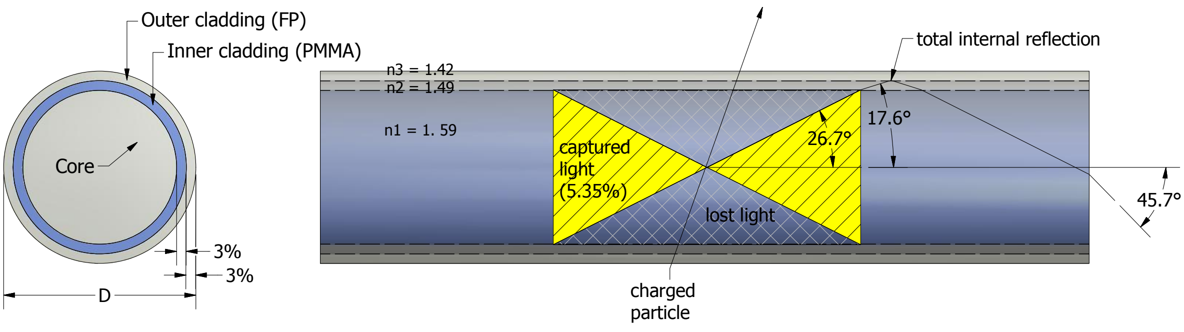

(a) end view

(b) side view

Figure 2.1: Schematic representation of the light transport in a double cladded fibre.

smooth surface, free of cracks, scratches and discolouration. When unspooled, the fibres shall be reasonably straight and free of twist.

Mechanical

During processing and assembly in the SciFi detector, the scintillating fibres undergo a number of quality control, cleaning, winding and cutting steps. These entail bending and local stress to the fibres. The fibres shall tolerate bending to a radius of curvature of 25 mm without short or long term loss of performance. The fibres shall tolerate cutting with appropriate tools (e.g. single point diamond tools or diamond blade saw) and machining parameters without cracking or other mechanical damage.

Optical specifications

The emission spectrum of the scintillating fibre shall lie in the wavelength interval from 400 to 550 nm. Peak emission as measured from short (unirradiated) fibre samples shall be around 450 to 500 nm to match the foreseen sensitivity spectrum of the SiPM photosensors.

The optical attenuation length of the scintillating fibre, prior to possible damage by ionization radiation (see below), shall exceed $\Lambda_{att} = 350$ cm, averaged over the wavelength range of the emitted scintillation light. Λ_{att} is defined by the light intensity relation $I(x)/I_0 = e^{-x/\Lambda_{abs}}$, measured at a distance between 100 - 300 cm from the photodetector, such that light propagation in the cladding and by helical paths in the core are irrelevant. The non-read fibre end shall be blackened to avoid light reflecting back due to Fresnel reflection at the fibre-air interface. A dedicated set-up built for the measurement of the attenuation length is described in the LHCb note [4].

To ensure a high trapping fraction of the scintillation light inside the fibre core, the fibre shall provide a numerical aperture of $NA = nsin\theta > 0.71$ where n is the refractive index of the core material ($n = 1.59$ for polystyrene). This corresponds to a half opening angle of the transported light cone of 45.7° (once the light has left the fibre, see Fig. 2.1). This requirement can generally only be achieved by a double cladding structure. The optical parameters of the fibre shall be uniform within 10% over the full length of the fibre.

For the application in the SciFi detector, the crucial quantity is the detectable light yield at the fibre end following the passage of a minimum ionizing particle. This parameter can only be determined using ionising radiation, i.e exposing the fibre to a particle beam or a radioactive source. Fibre producers are generally not equipped to perform such a measurement. As described in the section 2.2, for the SciFi project a set-up based on an energy filtered Sr-90 source has been developed which allowed to measure the scintillation yield in photoelectrons. Details of the set-up are described in the LHCb note [5]. A corresponding measurement protocol and acceptance limits will be agreed with the producer(s) to assess this quantity during series production.

Radiation related aspects

Plastic scintillators which are exposed to substantial doses of ionising radiation show a decrease in light yield which is attributed to two major causes: (1) degraded transmission properties of the base plastic and (2) a degradation of the scintillating and wavelength shifting fluors. While the second cause can usually be avoided by the choice of modern robust fluors that are added to the base scintillator material, the loss of transparency of the polystyrene core is a fundamental problem to which the SciFi team devoted a number of irradiation campaigns with different particles and energies. It must be clear that any irradiation experiment can only be an approximation of the *real world* in terms of dose, dose rate, dose distribution, and environmental parameters.

Apart from this transparency loss which is described in more detail below, we require the scintillating fibre to be radiation hard in the following sense:

- The scintillation light yield shall not be affected by an ionizing dose of up to 50 kGy.
- The mechanical and geometrical properties of the scintillating fibre shall not change for an ionizing dose of up to 50 kGy.

The producers are generally unable to measure and guarantee these parameters. Furthermore also for the client it is very difficult to verify the quality of a received fibre in a limited time. The SciFi project intends to set up in the coming months an x-ray based irradiation set-up in which fibre samples can be exposed to O(kGy) doses within a few days. This will allow to spot any production related effects (change in the composition of or impurities in the core, cladding or fluor materials). An open and efficient communication with the producer is the only way to detect degradation as early as possible.

Other aspects

The fibres shall be delivered on spools which allow for efficient and damage free unspooling, i.e. fibres must not be buried under other fibres. The minimum length of fibre on one spool shall allow the winding of a 6-layer mat, i.e. be 8 km or more. To use the raw material economically, the length per spool should be a half or a third of the total length given by a fibre pre-form.

2.2 Measurements and results

Throughout the R&D phase of the SciFi tracker, most studies were performed using the fibre SCSF-78M from Kuraray. As proven by the measurements below, this fibre generally meets the above requirements. The various irradiation tests are described in section 2.3. A remaining issue related to local diameter variations and the prospects of solving or mitigating it are discussed in 2.7.

A few measurements were performed on blue emitting BCF99 fibres specifically prepared Saint-Gobain (formerly Bicron). Following the large observed gap between the measured attenuation length and the SciFi requirement, the producer was not prepared to invest effort to improve the quality.

A recent development concerns the production of so-called NOL fibres, which are based on nanostructured organoluminophores. This innovative concept, which promises higher scintillation yield than conventional fibres, and results of the characterisation of first NOL samples, are described in section 2.8

Optical attenuation length

A set-up, as shown in Fig. 2.2 has been conceived and built which allows measuring the optical attenuation length Λ_{att} of fibre pieces of up to 3.3 m length in a fast manner [4]. Simple operation and a speedy result were main requirements as the set-up will be used during series production when large numbers of samples need to be characterised. The wavelength shifting dye in the fibre is locally excited by a symmetric arrangement of 4 UV-LEDs (Bivar, 390 nm) which can be shifted along the fibre. One end of the fibre is read by a Si-PIN photodiode of type Newport 818-UV, the other end is blackened by a chemically inert paint to avoid Fresnel reflections which could affect the results.

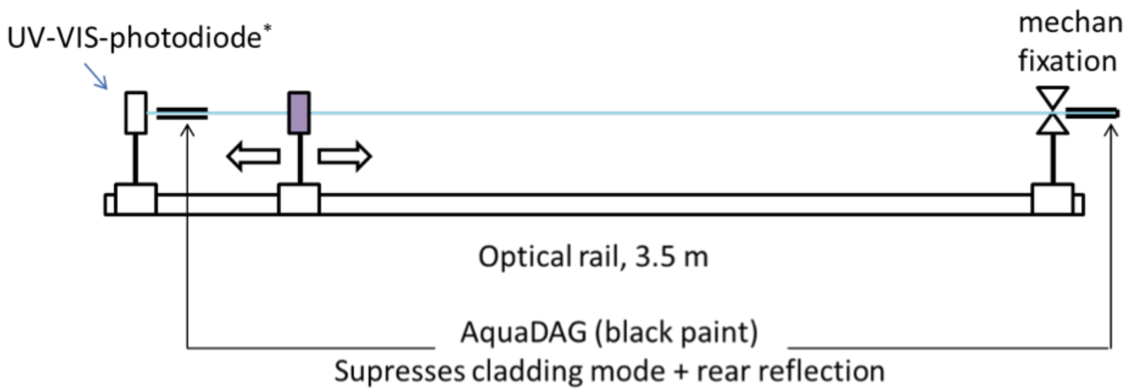

Figure 2.2: Schematic representation of the set-up for the measurement of the attenuation length.

Attenuation measurements exhibit typically two distinct exponential terms:

1. A relatively steep term (short attenuation length) which is attributed to losses of cladding light and non-meridional rays;

2. A more flat term (long attenuation length) which describes the losses of light which propagates in a regular manner in the core.

The above described set-up leads to reproducible results. Repeating a measurement of the same fibre sample several times gives results well within 5%. Samples taken from the same fibre spool may exhibit differences in the attenuation length of 10-15%. This is believed to reflect the variation of the fibre properties on a spool rather than an instability

Table 2.1: Evolution of attenuation length parameter in recent years.

year	Λ_{att}(m)
2010	3.7
2013	3.0
2014	2.6
2015	3.7

of the set-up. Visual inspection of fibres close to the emission point shows that the light losses along a fibre are by far not fully uniform. The observer finds localised bright spots, randomly distributed along the fibre, where larger quantities of light seem to escape from the fibre.

Kuraray operates a similar set-up, however the readout is based on a photomultiplier tube with bialkali photocathode, which has a significantly more blue-dominated sensitivity than a Si-PIN diode. A simple model indicates that the PMT readout should lead to 10% lower Λ values than a Si-PIN readout.

For direct comparison with attenuation length measurements performed at the fibre producer, we perform a single exponential fit to the data range from 100 to 300 cm. This range avoids interference with the steep term which has typical attenuation lengths of 20 30 cm, i.e. it is already sufficiently attenuated at 100 cm to be ignored.

Our initial expectations on the attenuation length were guided by measurements on SCSF-78 fibre samples purchased in the context of other projects in 2010. We measured consistently values of about 3.5 m. Fibres acquired by the SciFi project in 2013 (100 km) showed Λ values around 3 m and another delivery in 2014 (50 km)showed values of $\approx$ 2.6 m. The issue was discussed during a visit of the Kuraray production facility in autumn 2014 and corrective measures were taken (the technical details fall under a non-disclosure agreement). As shown in Fig.2.3, recent batches of 50 km fibres received in March and June 2015 gave Λ-values between 3.6 and 3.9 m. Kuraray considers the temporary attenuation length problem as understood and solved. There may be even room for further improvement.

Alternatively, at our set-up, the fibre under test can also be connected to a compact spectrometer with wavelength and relative sensitivity calibration (Ocean Optics USB2000+UV-VIS-ES and HL-2000-CAL). The fibre is excited at a distances d of e.g. 1 and 3 m and the emission spectra $E_{1m}(\lambda)$ and $E_{3m}(\lambda)$ are recorded. Dividing the recorded spectra, the attenuation length $\Lambda(\lambda)$ is obtained as $-\Delta d/\ln(\frac{E_{3m}}{E_{1m}})$.

We recently noticed a detail in this spectral measurement which had been ignored before. The spectrometer has a numerical aperture NA = 0.22 while the scintillating fibre has NA = 0.7. This means that a substantial part of the light cone exiting from the fibre end was not accepted by the spectrometer. In particular, the measurement favoured light which travelled at a small angle to the fibre axis, which gives a biases the attenuation

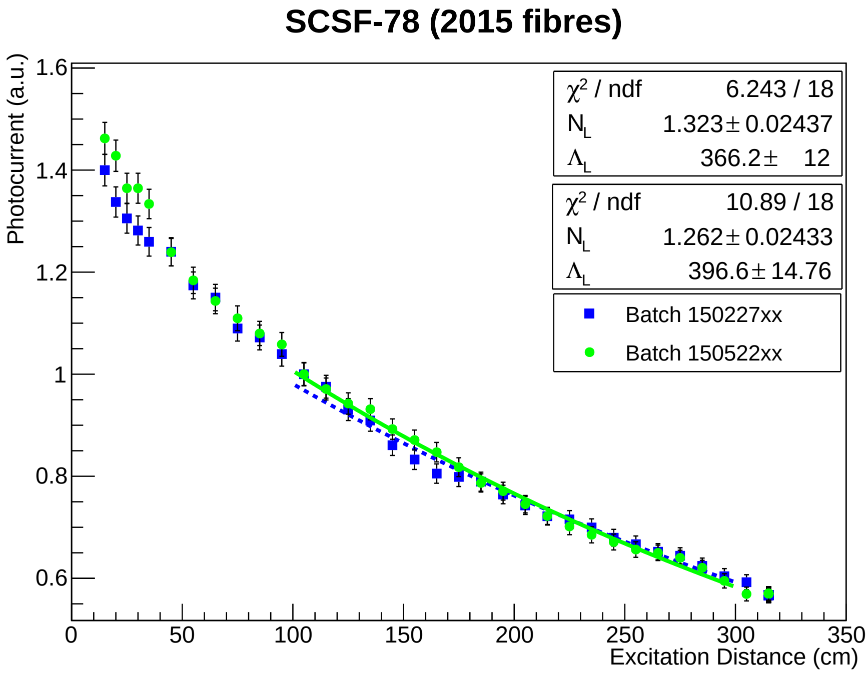

Figure 2.3: Light attenuation along a non-irradiated SCSF-78 fibres from two batches received in March and June 2015. The attenuation length is determined from a single exponential fit between 100 and 300 cm.

length toward higher values. As recently demonstrated, the problem of the unmatched NA values can be fixed by a micro lens (f = 1.4 mm). A systematic study is ongoing.

Fig.2.4 shows a plot of the spectral attenuation length with the typical feaures attributed to the excitation levels of polystyrene.

In conclusion, we consider the demonstrated performance of the Kuraray 2015 fibres adequate for the SciFi Tracker. On the other hand, every percent of improvement of the attenuation length leads to a percent higher number of photoelectrons from the inner detector region where the radiation losses are highest. We are therefore looking forward to further possible performance gains and will carefully watch this parameter throughout the full series production phase.

Scintillation yield

The intrinsic scintillation yield of a fibre, describing the number of photons emitted by the wavelength shifting dye normalised to a given energy deposition, e.g. 1 MeV, is difficult to measure. In addition, it is to a certain extent depending on the diameter of the fibre as primary photons may escape from a thin fibre prior to being wavelength shifted. Some producers provide the yield figure of 7000 to 8000 photons per MeV.

For the purpose of comparing different fibres or monitoring their quality during the R&D and the series production phases, it is sufficient to measure an effective light yield under

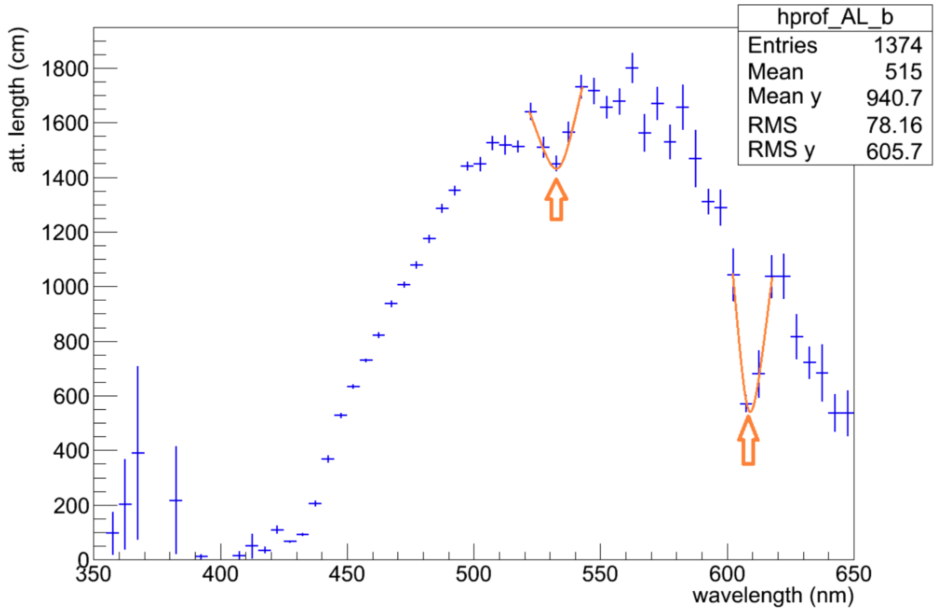

Figure 2.4: Measurement of the spectral attenuation length in a nn-irradiated SCSF-78 fibre. The enhanced absorption at $\lambda \approx 535$ and 605 nm is a well known feature, attributed to the excitation of molecular vibration levels of polystyrene.

defined and stable experimental conditions. Excitation of the fibre by an ionising particle or an x-ray photon is however mandatory. The ionising radiation cannot be replaced by UV light as this would just excite the wavelength shifting dye without assessing the scintillation process itself.

A set-up has been built which allows measuring the detected light yield, in units of photoelectrons, created by a minimum ionising particle. The parameter is related to the intrinsic scintillation yield by a constant but unknown factor, which can in principle be obtained by modelling the full set-up. Details are provided in [5].

The light yield of a single scintillation fibre of 250 μm diameter is small and therefore difficult to discriminate from noise. We therefore read the combined signal of several fibres by the same photodetector. Three fibres have proven a good compromise between sufficiently high signal amplitude and mountability.

The *fibres under test* (FUT) are vertically piled up in a channel between two plastic walls and are sandwiched between two trigger fibres, which have also a diameter of 250 μm. The two trigger fibres are individually read by photomultiplier tubes (PMT) of type Hamamatsu H7826, while the 3 FUTs are jointly read by a PMT of the same type. The waveforms of the FUT PMT are recorded and time-integrated by a digital scope. The gain of the PMT was determined by measuring its single photoelectron charge distribution. The FUT signal charge can therefore be expressed in photoelectrons.

An energy filtered Sr-90 source, usually called e-gun ([**?**]) provides a collimated beam of

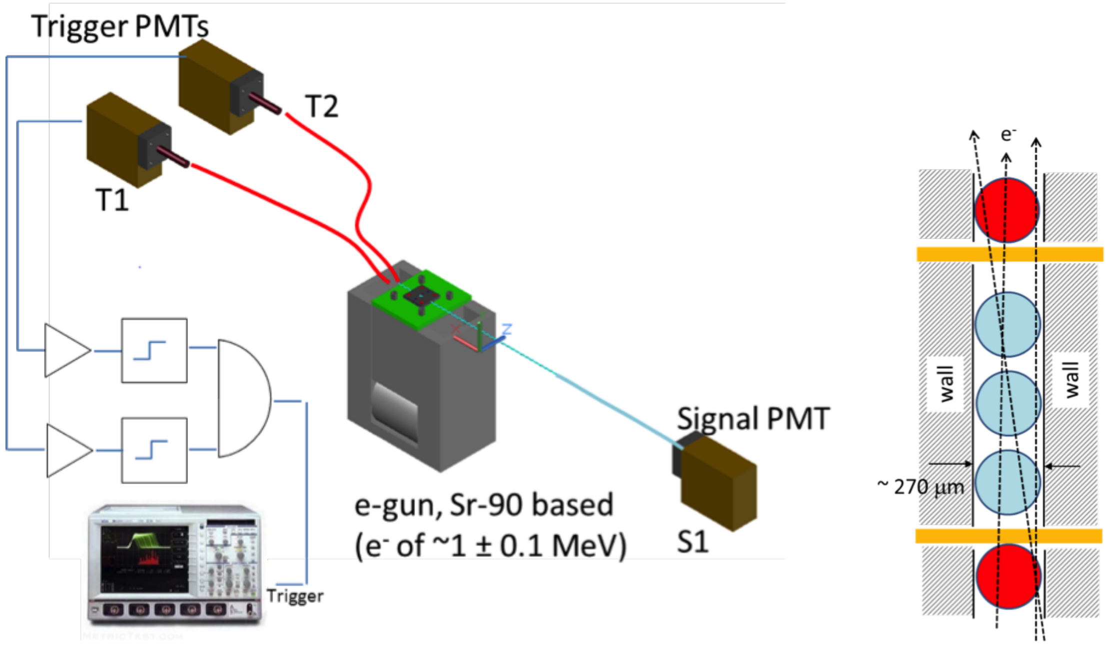

Figure 2.5: Left: Schematic representation of the set-up for the scintillation yield measurement. Right: Detail of the stacked mounting of the test fibres in between the trigger fibres.

electrons of 1.1±0.1 MeV energy, which are quasi-minimum ionising ($dE/dx \approx 2$ MeV/cm). The trigger rate is about 20 Hz.

The quality of the fibre end cut has an impact on the light output. The FUT are therefore glued into a fibre connector and machined to optical quality by a dedicated diamond tool[1].

Measurements are performed by hitting the FUT at different distances, typically, 60 cm $< d <$ 240 cm, from the readout end. The measured yields are fitted with a single exponential curve and extrapolated back to $d = 0$. The data points at $d = 60$ cm are usually not included in the fit as they are already influenced by the short component of the attenuation length.

Fig. 2.6 shows typical light yield curves of a SCSF-78 standard and 2 NOL (see sec. 2.8) sample sets. SCSF-78 fibres from different lots have given consistently 2 p.e. per fibre. It should be noted that the light yield measurements obtained in this set-up cannot be directly compared to test beam results. The main differences are the photodetectors (PMT vs. SiPM) and the effective geometry (aligned vs. staggered configuration).

Our set-up and method are similar to the approach employed by the GlueX team at Jefferson lab [?] for 1 mm SCSF-78 fibres. When correcting for the different geometries and attenuation lengths, our results agree within 10% with the one of GlueX.

[1]FiberFin 4. www.fiberfin.com

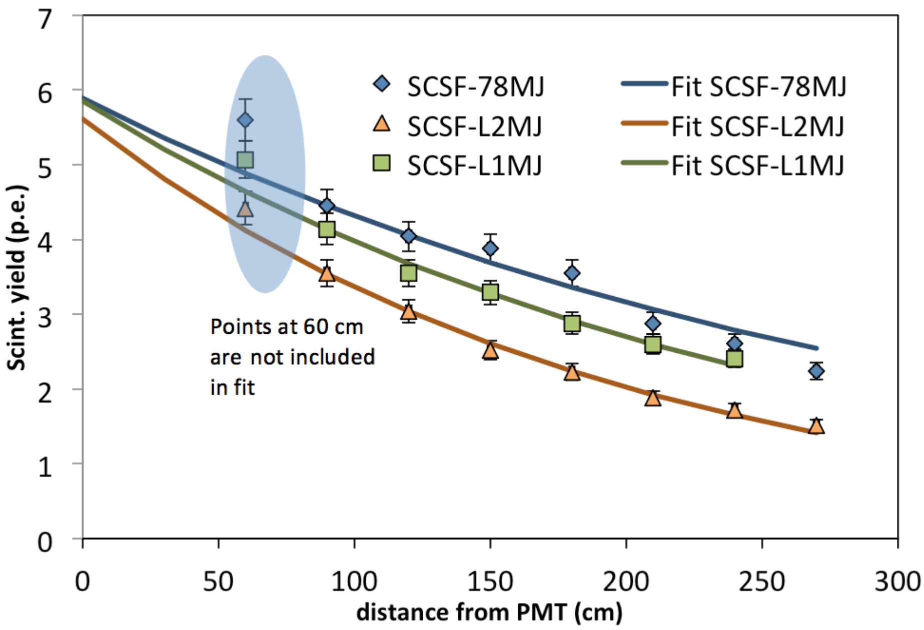

Figure 2.6: Example of light yield measurements performed on 3 sets of fibres. Every set consists of 3 fibres vertically piled up on top of the e-gun. The curves correspond to a SCSF-78 standard fibres and two NOL fibre samples (see 2.8). Extrapolation to d = 0 shows that all three fibres samples have a comparable scintillation yield of 2 p.e. per fibre. The NOL samples have a shorter attenuation length than the SCSF-78 reference fibre.

Geometrical parameters

As described in section 2.1, the geometry of our small-diameter fibres plays a particular role for the efficiency and spatial resolution of the SciFi detector. The producers measure the diameter of the fibre online during the drawing process, more or less continuously, and tune the process parameters in order to stabilise the diameter on the design value.

The RWTH Aachen group had experienced in the PERDAIX project problems with local diameter variations of the fibres. The typical length scale of these defects, most of them are bumps, ranges from 1 mm to several cm. Aachen has therefore developed a set-up which allows to rewind the fibres and scan their diameter with high precision. A similar development was undertaken at the university of Dortmund. In the meantime, based on these previous developments, the LHCb collaboration has built a slightly upgraded machine and installed it at CERN, where the major part of the fibre quality control will take place.

The principle and technical implementation of the machine, in the following called Fibre Diameter Scanner (FDS) is given in [?]. Fig. 2.7 shows a (panoramic) photo of the FDS at CERN.

The FDS unwinds the fibre from the spool, as delivered by the producer, threads it through a system of sensors and rewinds it on a new spool. During this process, the

Figure 2.7: Panoramic photo of the FDS at CERN. The total width of the set-up is 6 m.

tension of the fibre is regulated to 50 cN (50 grams) and no bending below a radius of 25 mm occurs.

The diameter measurement is performed by means of a laser micrometer, which provides two orthogonal measurement axes and reaches a resolution of the order 0.1 μm. The fastest laser micrometer currently in use measures 2400 samples per second (for every axis). A second laser micrometer, a so-called lump and neck (LN) detector, is able to detect jumps in the fibre diameter exceeding a programmable threshold (e.g. $\pm 25 \mu$m), without measuring the profile of the defect. The LN detector is used to switch the machine between a fast (> 1 m/s) and a slow mode ($\approx 0.15 m/s$), an approach which combines high throughput and high definition. In the slow mode, the fibre is scanned with a sampling interval of 40-50 μm. Fig. 2.8 shows examples of diameter variations (default $= 250$ μm) on mm and cm length scales.

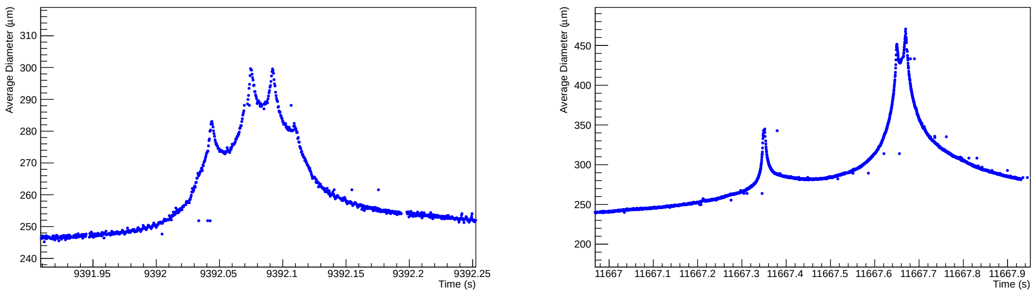

Figure 2.8: Examples of diameter measurements with the FDS at CERN at low scan speed (≈ 15 cm/s). In the left figure, a time interval of 0.05 s corresponds to 7.5 mm. Accordingly, in the right figure, a time interval of 0.1 s corresponds to 15 mm.

Status and prospects of fibre diameter variations

Measurements performed at Aachen, CERN and Dortmund point to a persisting difficulty for the producers to fully eliminate large bumps (diameter $> 300\mu$). For the producer, a high resolution measurement of the fibre diameter, online during the winding, is even more challenging because the drawing speed cannot be reduced to decrease the sampling interval. In the past, the resulting large sampling intervals have led to systematic underestimation of the bump and neck diameter or the defect remained completely undetected. This has now been fixed at Kuraray by installing a high speed laser micrometer which led to fully consistent measurements with the SciFi team. This is demonstrated in Fig. 2.9, which compares the Scan results of the same spool at Kuraray and at CERN. Spools of 12.5 km length received in 2015 showed typically 20 to 30 bumps $> 300\mu$m. Most of the bumps are just above the critical value of 300 μm, very few (< 10 %) exceed 400 μm.

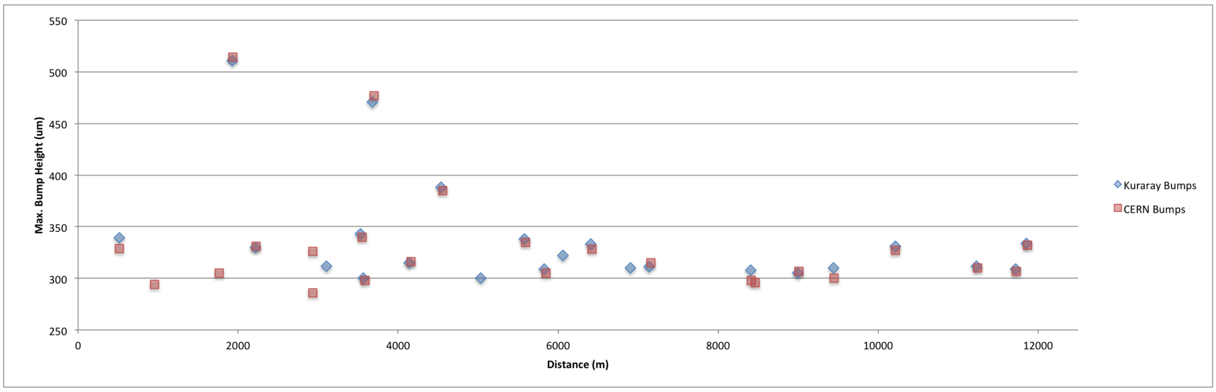

Figure 2.9: Comparison of bump position and heights of a recent fibre spool measured at Kuraray and at CERN. The agreement is above 95%.

During the past months Kuraray made continuous efforts to reduce the frequency and size of the bumps. While details fall under a non-disclosure agreement with the producer, it can be said that the improvements concern material and environmental parameters. Recently, Kuraray announced the production of a 12.5 km spool with only 4 measured bumps $> 275\mu$m of which 2 were $> 300\mu$m. The measurement was already performed before the new high speed laser interferometer became available and may therefore underestimate the number of bumps by a factor of two. Nevertheless, the result is very encouraging and brings us a big step forward to the goal of quasi bump free fibres.

It may turn out that a complete elimination of large bumps ($> 300\mu$m) is impossible to reach in the remaining time and with reasonable efforts. The threaded wheel method, which we employ for the winding of fibre mats, allows cutting out faulty fibre sections, in-situ during the winding process without degradation of the optical quality of the mat. The intervention is however labour intensive and interrupts the winding process for about a quarter of an hour. We estimate that we can tolerate one such intervention per fibre layer, i.e. we can tolerate spools with on average 1 bump $> 300\mu$m per 1.5 km fibre length, i.e on average 8 bumps per spool. A significantly larger defect rate would compromise the fibre mat production and could only be compensated by additional manpower resources.

Integrity of the cladding

Damage to the cladding structure, either due to bending to too small radius, scratching or production related issues, may result in a significant local degradation of the light transport, correlated with light leaking out of the fibre. The FDS are therefore equipped with dedicated sensors to spot damaged fibres. The principle is based on the detection of the light leaking out from the fibre at the damaged position by means of a SiPM detector mounted in a dark cell through which the fibre passes. On the CERN machine, the fibre is excited 50 cm before the SiPM sensor with a UV-LED (390 nm), while the Aachen machine relies on excitation by ambient light before the fibre enters the dark cell.

Measurements at CERN with deliberately damaged fibres showed that a cladding damage which leads to a 10 % loss of the light traversing the faulty position, can safely be detected in the FDS.

Damage of the cladding structure appears to be a rare phenomenon on Kuraray SCSF-78 fibres. It has to be admitted, that its systematic study was pushed back by the bump problem which was given highest priority. This will be corrected in the coming months.

2.3 Radiation effects

Previous studies have typically focussed on other fibres such as 3HF [?], Bicron-12 [?] and Kuraray SCSF-81 fibres. The fibre foreseen to be used in the LHCb Scintillating Fibre Tracker is the Kuraray SCSF-78MJ fibre. This newer fibre has a longer attenuation length than previous fibres and uses two different dyes[2] that result in a fast scintillation time with good light yield. Unfortunately, it has received limited study in literature, and under circumstances different from the LHCb upgrade environment, with reported results that are inconsistent or contradictory. The particular fibre type, the bonding of fibres with glue into ribbons, the dose profile along the fibres and the dose rate profile results in a complex system where the absolute magnitude of the radiation damage becomes difficult to judge purely from results in literature. As such, a campaign of measurements to cover to the total expected dose received in LHCb was undertaken.

Irradiation of SCSF-78MJ

The maximum expected dose after 10 years deposited in the scintillating fibres in the LHCb upgrade ranges from 35 kGy near the beam pipe decreasing exponentially down to 50 Gy 2.5 m away. Achieving this dose profile with similar dose rates over this length of fibre was not possible in a lab setup due to beam and time constraints, and, as such, an attempt was made to achieve comparable results in multiple separate measurements. To achieve the higher doses greater than 1 kGy, fibres were irradiated in proton beams where the dose rate was considerably higher than expected in the LHCb upgrade environment. To achieve doses lower than 1 kGy, the fibres were irradiated using x-ray or gamma sources

[2] assumed to be p-Terphenyl (PT) and Tetraphenyl Butadiene (TPB) based on spectra and decay times.

with lower dose rates. In the proton and x-ray irradiations, several fibres were grouped and epoxied onto plastic holders to simulate the similar environment of the tracking detector. Sections of the fibre were then irradiated step-wise to a dose profile similar to the LHCb upgrade. A summary of the measurements and doses achieved is shown in Table 2.2.

Table 2.2: Summary of irradiation experiments.

Beam Type	Facility	Doses (kGy)	Dose rate (kGy/h)
24 GeV/c protons	CERN PS	3, 22	1.7, 0.4
24 MeV protons	KIT	9 – 60	$1.8 \cdot 10^3$
F^{18}(e^+ to 511 keV γ)	CERN/AAA	0.5	$\sim 2 \cdot 10^{-2}$
35 kV x-ray	Uni. HD	0.1, 0.2	$3.5 \cdot 10^{-3}$

Measurements were made of the attenuation length before and after irradiation using a UV LED source to stimulate the fibres. The CERN PS measurement also used a Sr-90 beta source to measure the light yield and attenuation length. In all measurements, the light output was measured with a calibrated PIN diode, as well as with a photospectrometer to examine the wavelength dependent transmission damage.

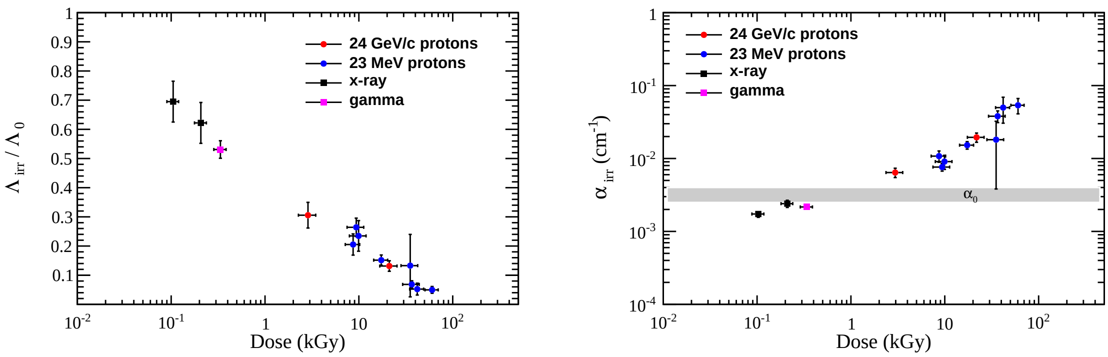

(a) combined data for Λ_{irr} (b) combined data for α_{irr}

Figure 2.10: The combined attenuation length data as measured with a PIN diode are shown with statistical errors versus the total integrated ionisation dose from four different fibre irradiation studies.

In general, the results agree with previous measurements of other fibre types over a similar range of doses [6]. A rather rapid onset of damage to the transmission is seen at lower doses, seen on the left in Figure 2.10. If the increased loss of light is attributed to additional scattering or absorption within the fibre due irradiation, the new attenuation length can be described as $\Lambda_{irr} = \frac{1}{\alpha_0 + \alpha_{irr}}$. A plot of the reduced attenuation length, Λ_{irr}, as well as the attenuation coefficient, α_{irr}, as a function of integrated ionizing dose for the irradiations conducted for the LHCb upgrade are seen in Figure 2.10. From the results seen in the LHCb Scintillating Fibre Tracker irradiation measurements, including wavelength

intensity measurements, the total expected loss of signal near the highly irradiated region around the beam-pipe is expected to be nearly 40%. A more detailed analysis, based on the spectral attenuation length is currently under way.
As explained above, except of the x-ray irradiation, all other irradiation tests took place at a significantly higher dose rate than the one expected in LHCb (at most 10 Gy /day). We therefore intend to perform during the LHC Run 2 (from now until 2018) in-situ irradiation tests in the LHCb cavern. A complete test beam module which consists of a 2.5 m long fibre mat glued in between two honeycomb panels, is foreseen to be irradiated with hadrons at a location close to the LHC IP8. Initial calculations (FLUKA) show that appropriate positioning of the module could lead to a dose profile which resembles the final one in the SciFi tracker. While it would be desirable to read out the module online during the exposure, the expected neutron damage of the SiPM detectors rules out this option, unless dedicated shielding and low temperature operation can be implemented. We favour at this moment a passive irradiation and extract the module during technical stops for measurements of the attenuation length.

2.4 Procurement plan

The construction of the SciFi detector is expected to last 18 months. We foresee delivery of fibres on spools with 12.5 km of usable fibre length. Typically, spools contain an excess length of several hundreds of metres, however without guarantee for the correct fibre diameter. The length is related to the fibre pre-form size of 25 km preferred by the potential suppliers.

The winding of our base unit, a 6-layer fibre mat, requires approximately 8 km. Two spools allow the winding of 3 mats. Based on a total mat number of approximately 1300, the total amount of fibres needed is close to 10'000 km.

In June 2015, a market survey has been conducted by CERN in view of the planned procurement of 12'500 km of scintillating fibres. The market survey, which is a formal way to identify qualified companies, preferentially in the CERN member states, will be followed by a call for tender in early autumn 2015, such that the supply contract can be awarded before the end of the year.

The volume mentioned in the market survey is an approximate figure, assuming a 25% margin for production yield and spare fibres. The market survey also mentions an option for an additional delivery of 2500 km. The exact quantity (and options) will be fixed in the supply contract.

Further to notification of the award of contract, the supply shall be delivered to CERN according to the following provisional schedule: start of delivery in January 2016 at an average rate of 100 km per week. The delivery shall rise to a rate of 250 km per week by March 2016 and shall be maintained until Q1/2017.

In a meeting with one of the potential suppliers, a production and procurement scenario has been discussed. It appeared that the capacity of the supplier would allow to produce the required quantity during the envisaged period, however little margin would exist for additional volume or re-making of fibres which were turn out to be of non-optimal or insufficient quality. It is assumed that the full quantity of 12'500 km can be produced in a period of 18 months.

It is understood that a small pre-series of several 100 km of fibres will be needed already in late autumn of 2015 in order to commission and optimise the operation of the winding centres (winding, casting, cutting, etc.).

2.5 Quality Assurance

The quality assurance for the fibres requires a continuous and tight collaboration with the producer. CERN will be in charge of procuring the fibres and ensuring the QA, before the fibres are distributed to the 4 winding centres (see 3).

The fibre QA will be integrated in a global QA database, briefly mentioned in sec. 1 and currently under implementation.

Details of the QA procedures at the production site and acceptance criteria will be part of the supply contract and hence need to be negotiated with the supplier. In the following we describe our plans, which have been discussed informally with one of the potential suppliers. Our plans are based on the assumption that the supplier buys the ingredients (like styrene monomers, dyes, cladding material) in relatively large quantities. All fibres produced from the same set of base ingredients form a batch.

The supplier maintains detailed records of the production parameters and keeps witness samples of all base materials of a batch for a possible later failure analysis.

The supplier verifies the mechanical and geometrical compliance of the fibres. This includes in particular a continuous measurement of the diameter profile and identification of deviations by more than $\pm 25\mu$m from the default value of 250 μm We aim for receiving only spools with less than 8 bumps exceeding a diameter of 300 μm

The supplier measures the attenuation length of samples from every spool and guarantees values in excess of 3.5 m, derived from a single exponential fit to the attenuation data which was measured between 1 and 3 m from the photodetector.

We assume that the fibre production volume of 1 week, i.e. typically 250 km, will be shipped to CERN with a minimum delay. Upon arrival at CERN, samples will be taken for reception tests. We foresee the following tests using the equipment and measurements described above:

- Visual inspection (cleanliness, surface quality, bending test).
- Optical attenuation length. During production ramp-up, measured on every spool. Afterwards on 10-20 % sample basis or at start of a new batch (change of any of the base ingredients).
- Scintillation yield. During production ramp-up, measured on 20% of spools. Afterwards on 5-10 % sample basis or at start of a new batch.

- Diameter and cladding scan. During production ramp-up, all spools are scanned. If full coherence with the data of the producer is obtained, the rate can be reduced to a sample basis of 10 %

- Irradiation test. At a start of a new btach, fibre samples are foreseen to be irradiated with X-rays to doses of a few hundred Gy.

Definite acceptance of a delivery shall be declared within 1 month after reception, except at a start of a new batch. In the latter case, up to 2 months are needed to perform the qualification tests.

2.6 Safety considerations

Scintillating fibres are made from polystyrene and are as such flammable and may burn under the emission of dense and toxic smoke. Following CERN safety instruction IS-41, polystyrene is in principle banned from use in underground areas. The total mass of the scintillating fibres is approximately 0.5 ton, which is significant. As in other equivalent cases, derogation will be asked for in combination with dedicated safety measures. In the SciFi project, the fibres will be enclosed in gas and light tight enclosures made from self extinguishing honeycomb panels and CF-reinforced skins, which retard fire and suppress the contact of the fibres with oxygen. In the worst case, a fire extinguishing system, already in place for the current Outer Tracker, may need to be reused.

Precautions have also to be taken for the storage of larger quantities of fibres in labs or storage areas

2.7 Open issues and remaining developments

We consider the following issues requiring further studies or efforts on the side of the manufacturer(s):

- Diameter variation of the fibres. As described above, the fibres delivered in 2014 and 2015 showed all rates of bumps $> 300\mu$m in excess of our limit 1 bump per 1.5 km. We continue our tight cooperation with the producer and, particularly after the recent announcement, we are confident that the bump rate can in the coming months be further reduced achieving the target. If against our expectations, the goal can't be achieved, we will need to compensate this by a higher effort during fibre winding or by allowing in the outer detector region fibre mats with winding imperfections.

- Availability of a very reduced number of suppliers. The market situation for scintillating fibres is uncomfortable from the client perspective. The handles on price, quality and delivery plans are not very effective. While the situation is not new and had to be handled by other large scale projects, LHCb's quality and volume requirements push the supplier to the technical limits. We see no alternative to our strategy of open cooperation and exchange with the supplier.

2.8 Perspective of NOL fibres

Recently a Russian group from the Enikolopov Institute of Synthetic Polymeric Materials of the Russian Academy of Sciences developed a novel type of plastic scintillator, in which so-called Nanostructured Organosilicon Luminophores (NOL) are admixed to the polystyrene (PS) matrix [7]. Unlike in traditional plastic scintillators, where the activator and wavelength shifting dyes are independently and randomly distributed in the PS matrix, the NOL approach couples activator and wavelength shifters via bridges of Silicon nanoparticles to dendritic antenna structures. The close geometric correlation of activator and wavelength shifting complexes is expected to reduce losses of UV photons and to increase the overall efficiency of the conversion process by profiting from non-radiative energy transfer (Frster transfer). This was demonstrated by comparing the light yield of disk-shaped scintillator samples (25 mm 0.2 mm), exposed to 5.49 MeV a-particles with that of standard scintillators (UPS89 from Amcrys-H, Ukraine) of the same geometry. The authors of [7] report for different NOL formulations up to 49% higher light yield and at the same time reduced decay time constants. A sub-set of the authors have founded a start-up company LumInnoTech[3] which intends to bring these dyes to the market.

If similar light yield gains as observed on scintillator disks could be reproduced in scintillating fibres, NOL fibres would be a highly interesting alternative, particularly for the inner part of the detector, where the radiation damage of the fibres is the highest.

On our initiative, LumInnoTech and Kuraray started to collaborate end of 2014 on the production of NOL based fibres. In spring 2015 we received the first two NOL fibres samples with 250 μm diameter and double cladding produced at Kuraray. Details of the formulation are protected by non-disclosure agreements. The production of these first samples was compromised by the non-availability of large enough quantities for the standard preform size used by Kuraray. In addition, the chosen concentration of the dye was a guess which will need to be carefully tuned in future batches for optimum results. Measurements on our set-ups at CERN indicated that the scintillation yield of these samples was comparable to SCSF-78 standard material, however the attenuation length was reduced compared to standard material. This was in agreement with relative light yield measurements by LummInnoTech and attenuation length measurements by Kuraray. We consider these results interesting enough to continue this development as a side activity. We received 4 more blue emitting NOL fibre samples in May 2015.The best of these samples achieved comparable scintillation yield and attenuation length as the SCSF-78 reference fibre. In a third iteration, the formulation of the NOL fibres are now being fine tuned in order to achieve high scintillation yield without compromising on the transparency. Furthermore, also the production of NOL fibre samples with cyan and green peaked spectra are foreseen. Given the spectral transparency of polystyrene and the

[3]http://www.luminnotech.com

fact that radiation damage affects primarily blue light, such fibres could provide a further advantage in the central high dose region of the tracker.

Chapter 3

Fibre Mats

3.1 Introduction

The scintillating fibre mats are the active component of the SciFi Tracker and must be assembled very precisely and with high quality. Single scintillating fibres with a diameter of 0.250 mm are arranged to staggered multi-layer fibre mats to achieve a sufficient light yield at the photodectector. It has been found that six layers are required. To produce these mats, a threaded winding wheel with a diameter of approx. 0.82 m is used. A layer of fibre is produced by laying down the fibre on the turning wheel with a pitch of 0.275 mm. The accuracy of the first layer is guaranteed by the thread machined in the surface of the wheel. Each successive layer uses the fibres below as a positioning guide, and is therefore shifted by half the horizontal pitch with respect to the layer below.

A schematic of the fibre mat is shown in Figure 3.1. The top drawings shows a raw fibre mat before cutting the long sides. The pyramid structure is ideal here. The bottom drawing shows two mats placed adjacent to each other with specified gaps to allow for production tolerances and SiPM array placement. A mat width of 130.60 mm is shown in the figure, rather than the nominal 130.65 mm, as this is closer to the demonstrator mats produced for the EDR.

The geometry of the fibre mat is defined by several constraints. The width of each fibre mat must correspond an integer value of the SiPM package width, including tolerances. Four arrays were judged to be a good width for handling and production, which corresponds to 130.65 mm. This allows for 130.4 mm of active fibre matching the active SiPM area and 0.125 mm of dead fibre on each edge from cutting. The length of the mat is determined by the need to cover the acceptance of the LHCb detector. The full height of the plane is 4.85 m, which requires that the fibre mats are half this length, covering the top half and bottom half of the detector plane with a 2 mm gap in between to account for tolerances. The final length of a finished mat will be 2,424 mm. To cover the 12 detector planes needed for the SciFi tracker, approximately 1,300 fibre mats will need to be produced. To guarantee the straightness of the fibre mats during the production of the modules so called alignment pins will be glued to the fibre mats during the winding process (see section 3.2.2). The packing and alignment of multiple mats into full detector modules is discussed

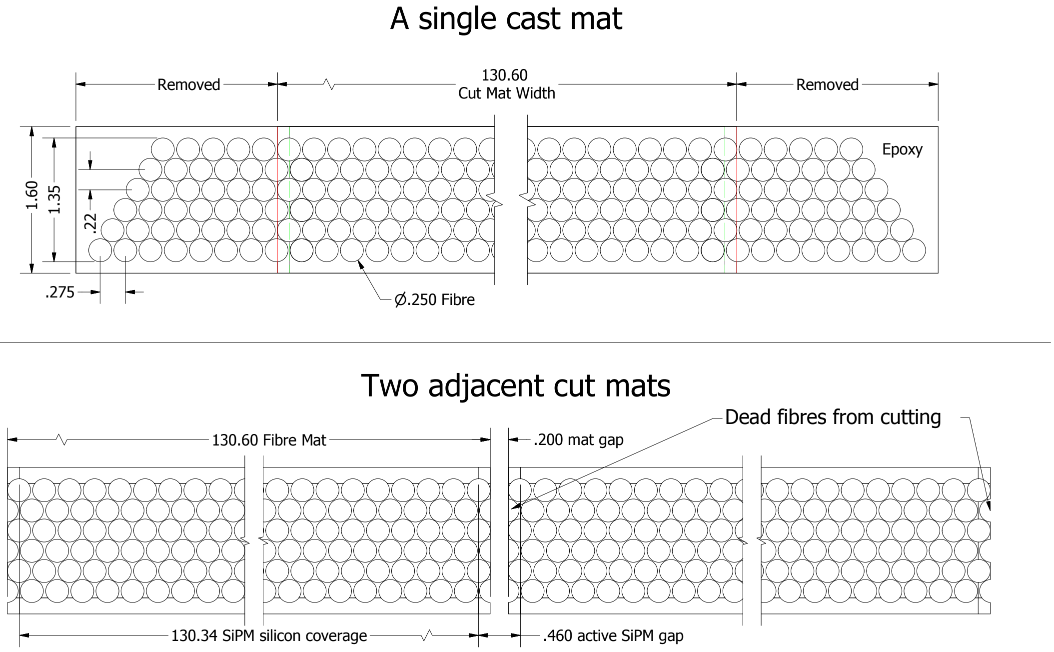

Figure 3.1: (top) Schematic of a cross-sectional cut through an single uncut cat mat. (bottom) Two cut mats adjacent to each other in a module with the gaps indicated. A mat width of 130.60 mm is shown, rather than the nominal 130.65 mm.

in Chapter 4.

3.2 Winding of fibres into mats

Based on the experience of producing shorter fibre mats at RWTH Aachen for balloon and other experiments, a similar principle is being used to produce fibre mats for LHCb. Pre-qualified fibres are aligned to the grooves of the winding wheel under a controlled tension. An epoxy loaded with TiO_2 is applied during winding, such that hardening epoxy holds the fibres together.

3.2.1 Winding machine

Based on the experience with a winding machine at RWTH Aachen and a prototype machine developed at TU Dortmund a new machine was developed for the serial production. To ensure a high quality and all safety features during operation an external company was charged with the construction of a machine which can handle the serial production of the fibre mats. The machine developed by STC-Elektronik GmbH is shown in Fig. 3.2.

The main function of the machine is to place the fibre on a turning threaded wheel (for detailed information see Sec. 3.2.2) which positions the fibres of the first layer. The fibre is provided by a feeding spool and guided by the help of several small spools to the winding wheel. To maintain a small angle of the fibre entering the first guiding wheel a rotating cylinder is used. Afterwards the fibre passes a dancer roller arrangement (see Fig. 3.3 (a))

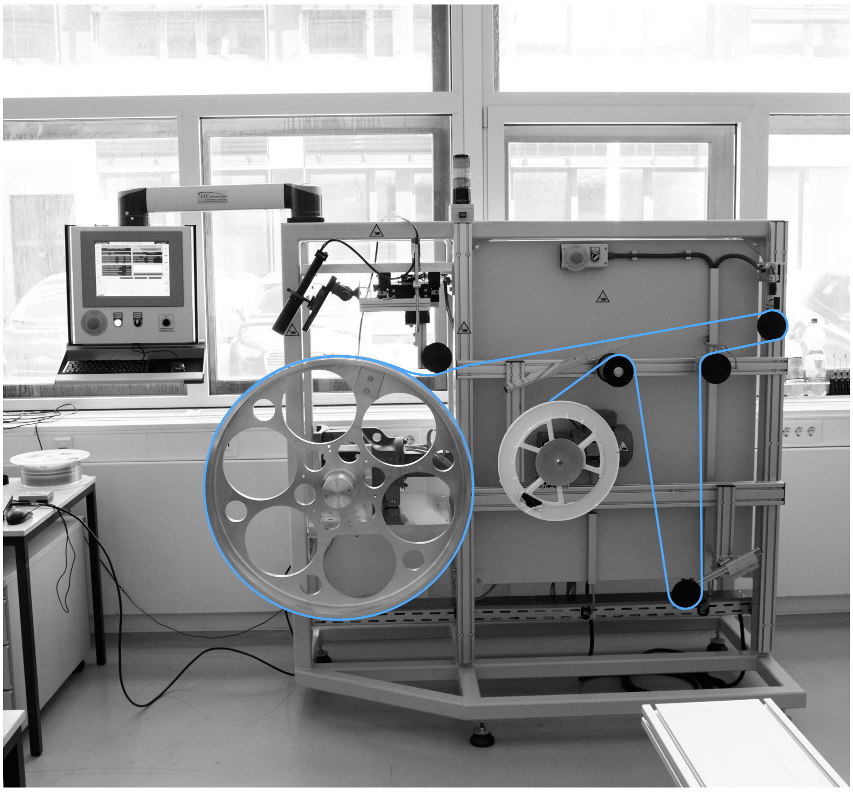

Figure 3.2: Winding machine for the serial production. The blue indicates the path of the fibre.

which is used to define the fibre tension. In addition the dancer roller arrangement controls the speed of the feeding spool. The tension can be adjusted mechanically with a weight. To measure the applied tension the fibre is guided through a load cell. The correct position of the fibre on the wheel is provided by a linear slide which carries a small guiding spool (see Fig. 3.3 (b)). This linear slide moves along the width of the winding wheel with the correct pitch.

The machine was received end of April 2015, the tests performed so far indicate that the performance of this machine corresponds to the requirements of the fibre mat production. The whole mechanical part is well-thought-out. All guiding spools are mounted in a way that the fibre can be placed easily. Also the winding wheel is mounted in a way, that an exchange is very simple and to be done in a few minutes.

Especially the software part of the machine provides a lot of adaptability during the production of a fibre mat. There are different modes available for the different steps of the fibre mat production (winding of a layer, glue coating, glue curing). The mode which are foreseen for the glue coating and the glue curing just provides the turning of the wheel with a selected speed. For more variability the speed can be selected with a potentiometer. For placing the fibre the machine provides a special mode which unwinds the fibre simultaneously from the feeding spool with the right speed. The most important

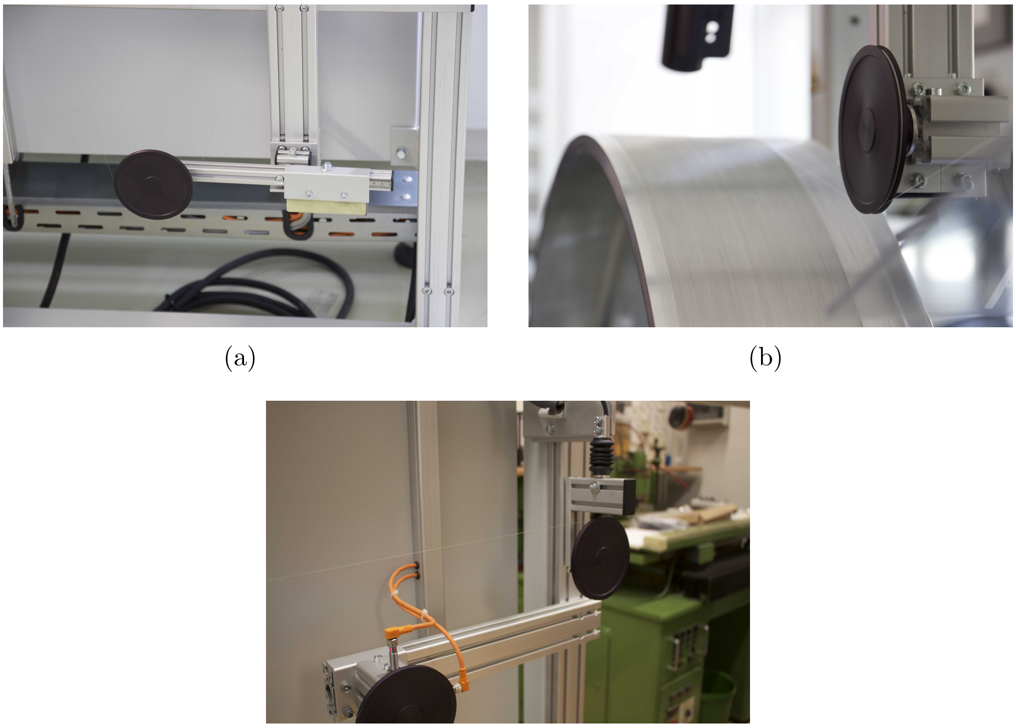

(a) (b)

(c)

Figure 3.3: (a) Dancer roller arrangement. (b) Positioning spool. (c) Load cell.

and variable mode is the one for winding a fibre layer. To ensure a good quality of the fibre mat the positioning of the fibres has to be monitored the whole time (see section 3.6). If a miss-placement occurs the machine is able to stop and turn the wheel in the opposite direction to correct the positioning of the fibre. In this case the linear slide with the positioning spool moves with the pitch in the opposite direction too, to ensure furthermore a precise positioning of the fibre. Also the speed is variable adjustable with a potentiometer. This is especially beneficial for the first turns of a layer or after correcting an error, where the positioning is usually a little bit difficult. Another feature of the machine is, that the position of the positioning spool can be corrected during the winding of a fibre layer. This could be necessary to prohibit a wrong positioning of the fibre. All parameters of the machine which are useful for the fibre mat production can be set manually and variable for an efficient fibre mat production. A view of the control panel can be found in Fig. 3.4.

In addition a special feature is implemented which allows to read the file of the quality control of the fibres. In this file all diameter defects are listed. The machine knows the current position at the fibre spool and is able to stop automatically if a diameter defect (bump or neck) approaches. The operator can then have a look at the fibre to decide whether the defect needs to be cut out.

The fibre mats for the demonstrator module were not produced using the machine described before, because the first serial winding machine was not available early enough

Figure 3.4: Control panel of the winding machine.

for this purpose. The prototype machine is based on the same principle. The fibre is guided on the threaded wheel by a positioning spool while the tension of the fibre is kept constant (see Fig. 3.5). The main differences are:

- the winding wheel is not interchangeable
- the tension is controlled with a loose spool
- the positioning spool moves in steps of 275 µm instead of a continuous movement
- the overall machine mechanics is less rigid
- the software fulfils basic needs only
- no measurement and automatic documentation of parameters

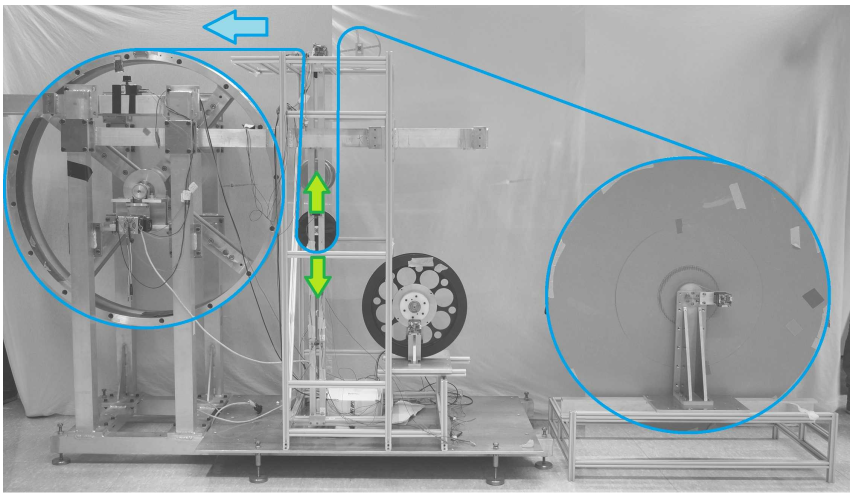

Figure 3.5: Fibre winding machine prototype used to wind the mats for the demonstrator.

3.2.2 Winding Wheel

The circumference of the winding wheel determines the maximum length of the fibre mats that can be produced. In consequence the diameter of the winding wheel has to be chosen in a manner that also accounts for the cutting notch. Given the length and width of a ready cut fibre mat of 2424mm × 130.45mm, the respective dimensions of the wheel are chosen to be 817 mm × 140mm (diameter, width). The oversize of length and width is needed for the cutting and final machining to the nominal dimensions of the fibre mat. The winding wheel is made of the aluminium alloy Al7075 which is typically used for aircraft, space and moulding applications. Its strength is among the highest of aluminium alloys and resembles the one of stainless steel. It is very robust, process save and typically not glueable. As an alternative, a hybrid stainless steel wheel with aluminium spokes is under production.

Into the surface of the cylinder a thread-like groove with a pitch of 275 μm is cut on a numerically controlled lathe or milling machine. The depth of the groove is 100 µm. The engraved profile can be seen in figure 3.6. In addition small holes, i.e. alignment pin holes (diameter: 3 mm, length: 6 mm) are milled which follow the central thread line. The distance between two holes is 245.97 mm. The holes are filled with glue before the winding of the first fibre layer is started. They later on form the alignment pins on the back of the fibre mat (see figure 3.6g). When the first layer of fibres is wound onto the winding wheel the groove helps positioning the fibre. At each side of the grooved region a margin of 1.5 cm is kept. Here as many threaded holes as the future mat will have layers are placed in circumferential direction for the fixation of the beginnings and ends of the fibre of each layer. Near these holes a notch runs in transverse direction over the full width of the wheel. It facilitates at a later stage the cutting of the fibre mat.

Starting from a monolithic aluminium block, most of the aluminium is machined off to keep the wheel light weight. For the winding process the winding wheel is mounted on a winding machine (see section 3.2.1). Figure 3.6 shows the winding wheel with the thread-like grooves and the holes for the creation of the alignment pins

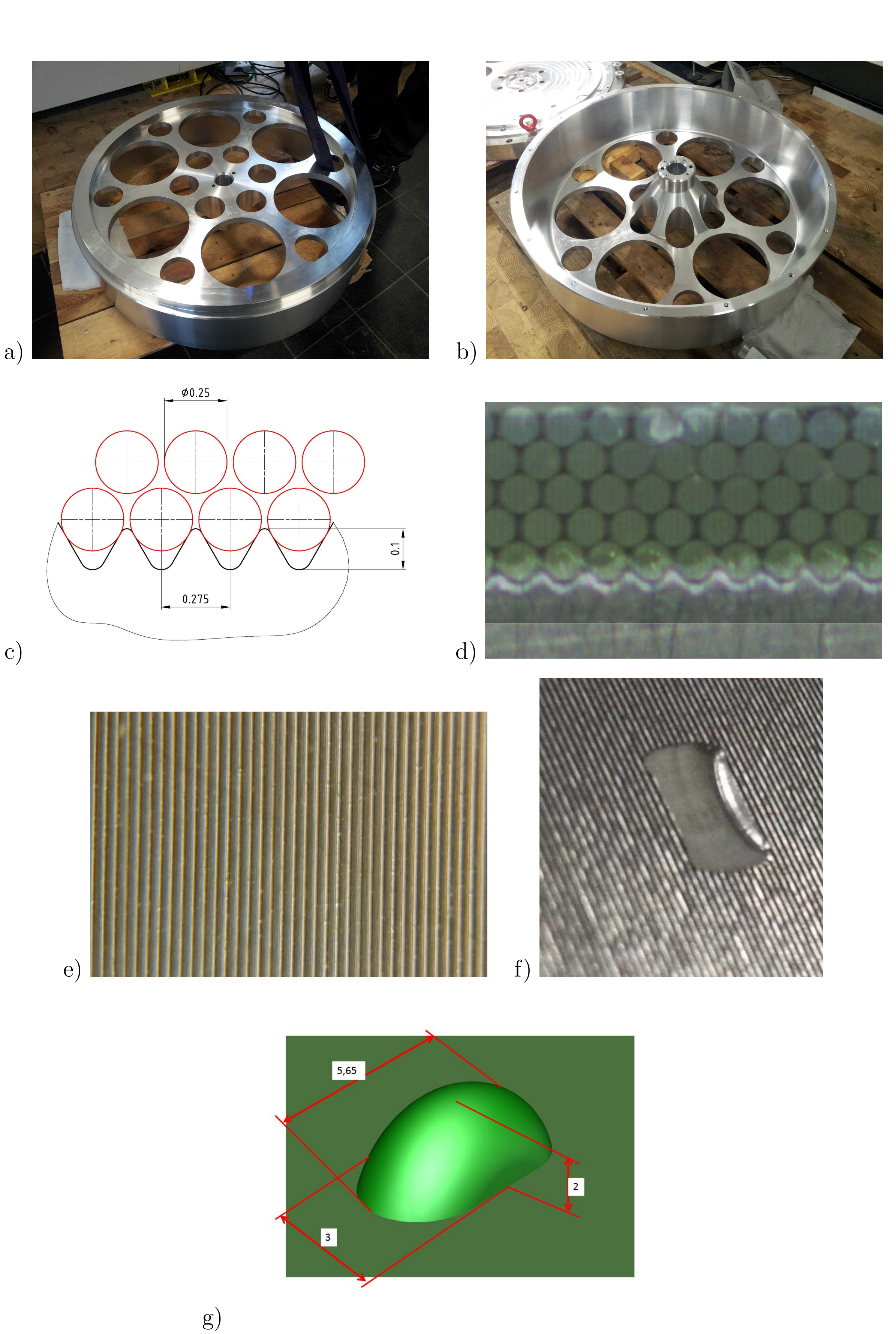

Figure 3.6: a) and b) winding wheel, c) schematic profile of winding grooves, d) visible produced profile of winding grooves and fibre windings on wheel, e) zoomed photo of winding grooves, f) zoomed view of milled alignment pin-hole in groove, g) drawing of resulting alignment pin after winding on wheel with alignment pin-holes in groove.

3.2.3 Process and materials

The production of a fibre mat comprises numerous steps.

- Preparation of the winding wheel
- Pin gluing
- Winding of first fibre layer
- Application of glue
- Winding and gluing of layers 2 to 6.
- Glue curing
- Removal of mat from wheel

Preparation of the winding wheel A clean wheel is the basis for a high quality fibre mat. After cleaning the wheel and ensuring that the grooves in the winding wheel are free from dust and glue from the prior fibre mat production a layer of sealer needs to be coated. After this, five layers of release agent are applied. This shall guarantee, that the fibre mat comes off the wheel nicely and undamaged. These and additional preparations (e.g. check of fibre stock, cleaning the small spools) are done the day before winding.

Preparation of glue The fibre mat productions starts with the preparation of glue for the pins. After preparing the wheel and after the winding of one layer, new glue has to be mixed. This ensures that the glue is always in good and reproducible condition. The used glue is a two component epoxy glue (Epotek Epoxy 301-2). So in this step the resin and hardener of the epoxy plus titanium dioxide (20 % by weight) are needed. This glue is non outgassing and has a potting time of 8 h. For measuring the right amount of each component scales and syringes are used. To guarantee a smooth mixing of the three components a special mixing machine under vacuum is employed. Afterwards, the mixer has to be cleaned with isopropanol.

Pin glueing The alignment pins are made from glue and are used e.g. for the positioning of the fibre mats in the casting tool (see sec. 3.3). To ensure a regular pin with a smooth surface the pin holes get filled up with a syringe (see picture 3.7). Furthermore, the surrounding wheel surface is coated with a thin layer of glue. This shall help that the glue stays in the holes. In addition the winding of the first layer in the region of the pin holes is done with extra caution. If required, a small extra portion of glue can be added to top up the pin holes. Once the holes are totally covered by fibres the winding procedure can proceed at normal speed until the end of the layer.

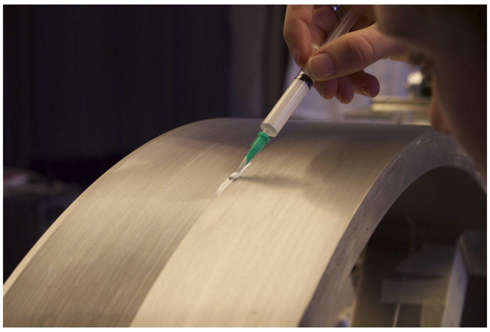

Figure 3.7: Filling the pin holes with glue with the help of a syringe.

Winding For each fibre layer, the beginning of the fibre is fixed with a screw on the edge of the winding wheel (see Fig. 3.8(b)). For the first turns the wheel rotates slower to ensure that the fibres find their right position in the thread. Afterwards the rotation speed of the winding wheel can be increased. Till now a winding speed of 0.2 turns per s was used (40 min per layer without interventions), it is assumed that this speed can be increased with the serial winding machine. At the end of a layer the fibre is cut and fixed with a screw. To wind the next layer, the fibre is again fixed on the starting edge. Depending on the quality of the used fibres interventions during the winding are needed. Therefore the winding process needs to be followed carefully. To simplify the survey we foresee an optical survey system (see section 3.6). In case a fibre jumps to a wrong position the winding is stopped and the error is corrected. Bumps which are to thick can be cut out. For this the fibre is fixed at the position of the vertical cut with instant glue. The new fibre is glued right in line to it. The fact that the light guidance is interrupted at this position is irrelevant because this part of the mat will be cut anyhow. This intervention takes about 15 min.

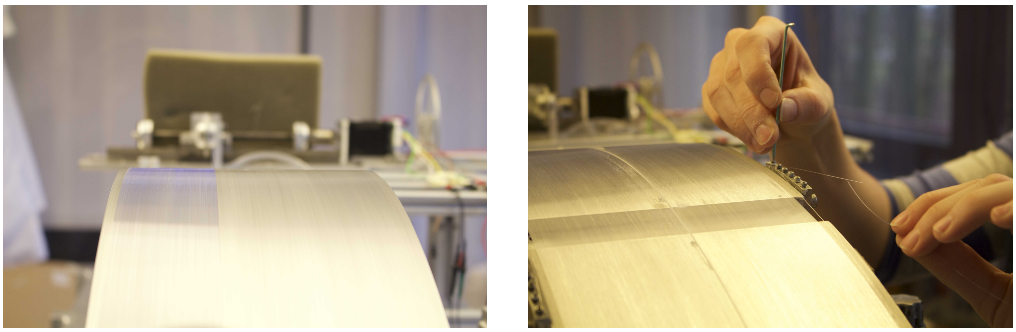

(a) (b)

Figure 3.8: (a) winding a fibre layer (b) fixing the fibre end with a screw on the wheel

Layer gluing On each fiber layer a thin film of TiO_2 loaded epoxy is added. The thin and homogeneous film used in the layer glueing should not affect the positioning of the fibres of the next layer. To ensure the thin and homogeneous epoxy layer a wiper is used (see Fig. 3.9).

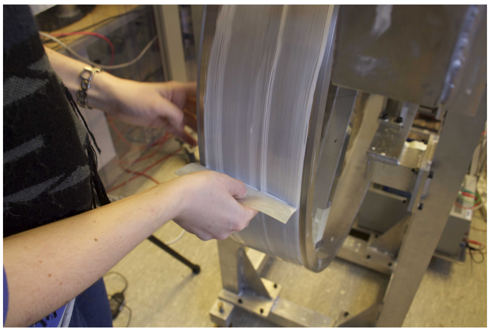

(a)

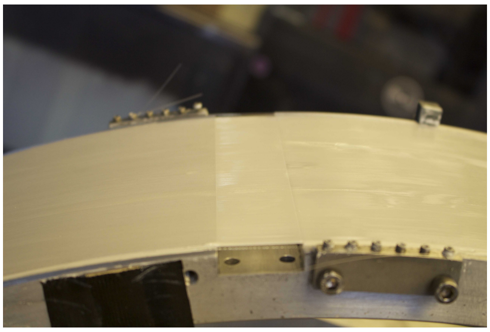

(b)

Figure 3.9: (a) Applying glue on the top of a fibre layer with a wiper. (b) Thin and homogeneous layer of glue on top of the fibres.

Curing Once all fibre layers are finished and the last layer of glue is added, the epoxy needs to cure. This glue curing takes 36 h. For the first 12 h the winding wheel has to rotate to prevent the build-up of glue drops.

Taking off the mat After the curing time, the fibre mat can be taken off the wheel to be flattened. For this the fibre mat will be cut at the position of the cutting notch perpendicular to the fibres. Because of the tension of the fibres during the winding, the fibre mat will shrink if released. For this reason, the cut needs to be done at once over the whole width. A cutting tool (e.g. a hot wire) with the right width enables this. In addition clamps with the right width are used to force the mat to stay in its position on the wheel. After cutting the fibres the clamps need to be taken off simultaneously and quickly. This guarantees that all the pins come out off the pin holes at once and without getting sheared off.

Cleaning the wheel After the mat is taken off, the wheel has to be cleaned. As a clean wheel is important the cleaning has to be done carefully and accurately. All grooves have to be freed of glue remains and dust.

A list of needed materials and price estimates for the different winding steps can be found in Tab. 3.1.

Table 3.2 lists the needed time for the different productions steps. It is split in *preparations*, *winding* and *post production*. Only the winding-steps need to be performed with the wheel mounted on the winding machine. The steps in brackets can be performed in parallel to other steps and don't account for the sum. The listed times assume the current speed of the procedures and might be optimized in the future.

Table 3.1: Material list with price estimates.

material	number	price/item	price/mat
fibres (Kuraray)	8 km	0.2 Euro / 1 m	1600 Euro
glue (Epotek 301-2)	65 g	620 Euro / 2 kg	20 Euro
TiO2	16.5 g	0 Euro / 1 kg	0 Euro
release agent (Mikon 205)	50 ml	25 Euro / 500 l	3 Euro
sealer (Mikon 199)	10 ml	40 Euro / 500 ml	1 Euro
ethanol	150 ml		? Euro
wiping cloths			1 Euro
syringe			1 Euro

Most of the steps require one person only. For some procedures it is preferred to have a second person available. Working with two wheels (1 mat per day) will only be possible with two persons.

Table 3.2: List of time needed for each production step.

preparations	1+13.5 h
release agent	60 min
wait in between	90 min
wait for release agent	12 h

winding	7.3+36 h
winding preparations	30 min
prepare glue	10 min
filling alignment pin holes	20 min
glue layer 0	5 min
clean mixer	(5 min)
winding layer	6×50 min
prepare glue	(6×10 min)
glue layer	6×10 min
clean mixer	(6×5 min)
documentation	10 min
glue curing	36 h

post production	2+0 h
mat take off	30 min
clean wheel	90 min

3.3 Mat Casting and Endpiece Gluing

Fibre mats are still fragile after taking them off the winding wheel. They have a tendency to split between adjacent fibres. Fibres near the edges are particularly prone to becoming separated from the ribbon. For this reason, the ribbon is cast in a bath of glue to ensure a thin protection film around the mat, which also creates a precise flat surface. In addition, the mats must have SiPM arrays precisely aligned to the fibre, such that no light is missed or the position incorrectly recorded.

The various components and jigs that are needed to assemble a finished cast mat are described in the following along with available details regarding costs and production tolerances.

3.3.1 Components

Fibre Mats Approximately 1300 fibre mats are produced on several winding machines and made ready to be cast. It contains the alignment pins formed on the winding wheel from glue that follow the central axis of the fibre mat which are important for aligning the module at several steps.

Endpieces Two paired endpieces, one on each side of the mat, are made from polycarbonate or some other amorphous thermoplastic.
The endpiece halves on the readout side have a length of 60.5 mm, a width of 130.45 mm, two 6 mm drill holes for the alignment in the casting jig and the lower half three 2 mm precision holes in the front face for the SiPM mounting and alignment (see figure 3.10a and c). The lower half of the endpiece communicates the alignment of the central axis of the fibre mat to the SiPMs.
The endpiece on the mirror side has a length of 15.5 mm, a width 130.45 mm and two 6 mm drill holes for the alignment in the casting jig (see figure 3.10). This second paired endpiece supports the mirror glued to the fibres at this end.
Both endpieces protect the ends of the fibre mat from damage during handling, processing and assembly. In addition they limit the heat load to the cooling system, given their thin profile which allows space for added insulation and increases the distance from parasitic heat sources, such as the endplug.
Approximately 2600 in all will be needed. The endpieces cost 16 CHF per piece. Tolerances are given in technical drawing (see figure **??**). All not given tolerances in the drawing correspond to DIN2768m.

Mirrors Each cast mat will be mirrored as the last step during mat production. The mirror is an aluminized mylar foil with a reflectivity of 80±5% (see dedicated note [8]). It is bonded square and flush to one diamond milled end of a finished sub-module with epoxy (EPOTEK 301 - 90 min potting time). The cost of mirroring is neglible.

3.3.2 Casting and gluing tools

The casting jig consists of two parts, the first one is a mold made of an aluminium plate

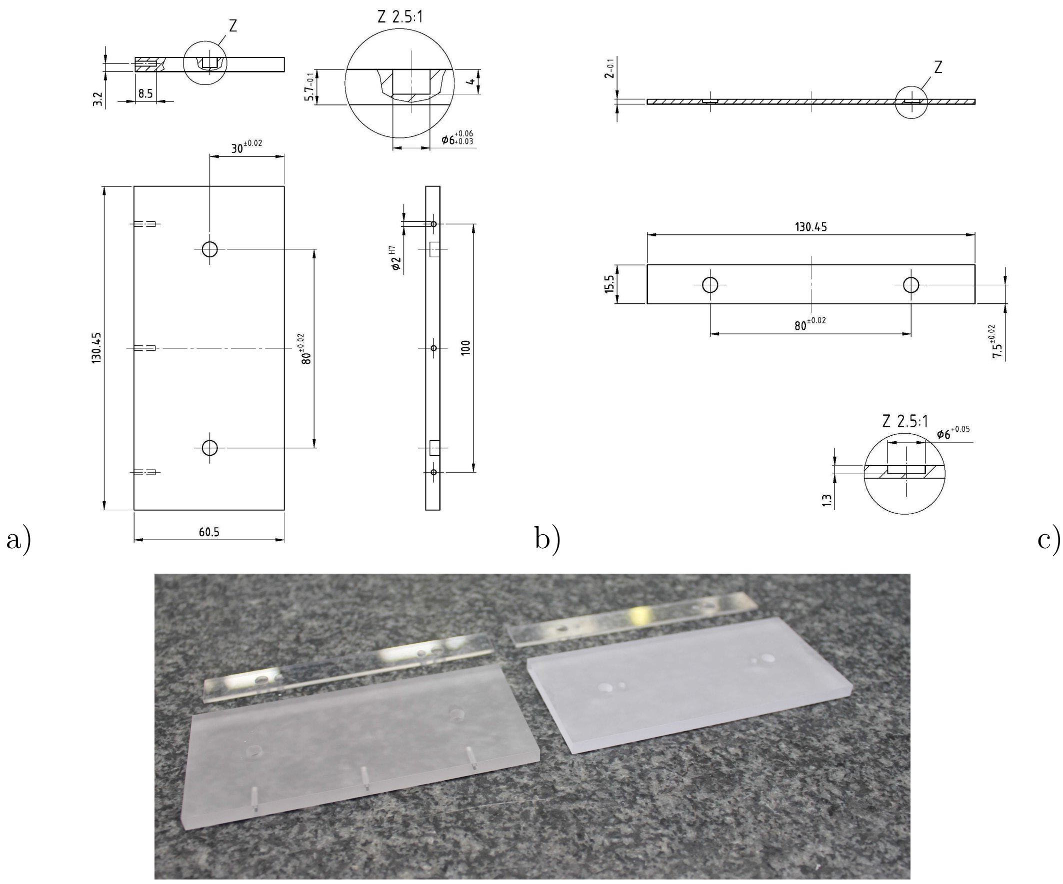

Figure 3.10: A drawing of the endpiece a) on readout side and b) on mirror side of a fibre mat.c) A photo of the endpiece on readout side and on mirror side of a fibre mat.

which is mounted on a lifting jack (see figure 3.11a), the second one is a cover made of 10 mm thick glass reinforced by a aluminium frame to visually control the casting process. The outer dimensions of the mold are: length 3000 mm, width 880 mm and height 842 mm. During the casting process the jig is rotated in an almost vertical position (see figure 3.11b). To cover the fibre mat with glue the Al-plate is countersunk to a depth of 1.6 mm. The aluminium casting mold plate contains two pockets and alignment pins for the endpieces, as well as long pin grooves to receive the mat pins and align the mat (see figure 3.12). The endpieces are therefore aligned in the casting mold with respect to this common reference system. Once the casting glue is hardened, the endpieces are centered and fixed to the fibre mat throughout the module assembly process. The measured straightness of the casting jig showed a deviation from a straight line of better then ± 50 μm (see figure 3.12 bottom).
The casting jig long grooves for the aligment pins of the fibre mats have additional holes for ejector pins. They are needed as support during the unforming of the fibre mat out of the jig after the casting

The cover is sealed by a rubber O-ring against the aluminium body. The aluminium body has two additional feedings, one serves as supply for the casting glue, the other one as a connection for a vacuum pump.
Tools: 4 casting jigs per winding center, cost estimate: 5000 Eur/casting jig

A **multi purpose jig** is developed to glue the upper endpiece halves (see figure 3.13). The lower jig halves hand over the precision to the upper half of the jig to position the upper endpiece with a high precision of ± 30 μm with respect to the lower endpiece. In addition this jig can be used to support the fibre mats during the optical cuts, quality assurance scans and measurement operations, as wells as the gluing of the mirrors.
Tools: 4 multi purpose jigs per winding centre, cost estimate: 1500 Eur / multi purpose jig

3.3.3 Casting of fibre mats

The sequence of work of the casting process consists of various steps (see table 3.3). Before each casting process the aluminium body, the glass cover and the rubber O-ring need to be cleaned and treated with a release agent (step1). The next two steps are the preparation of the fibre mat and the placement of the spacing lines (80 μm fishing line) on it (see figure 3.14a). These distance holders of 80 μm height guarantee the proper positioning of the fibre mat in the mold. If the measured height of the uncasted fibre mat is less then

a) b)

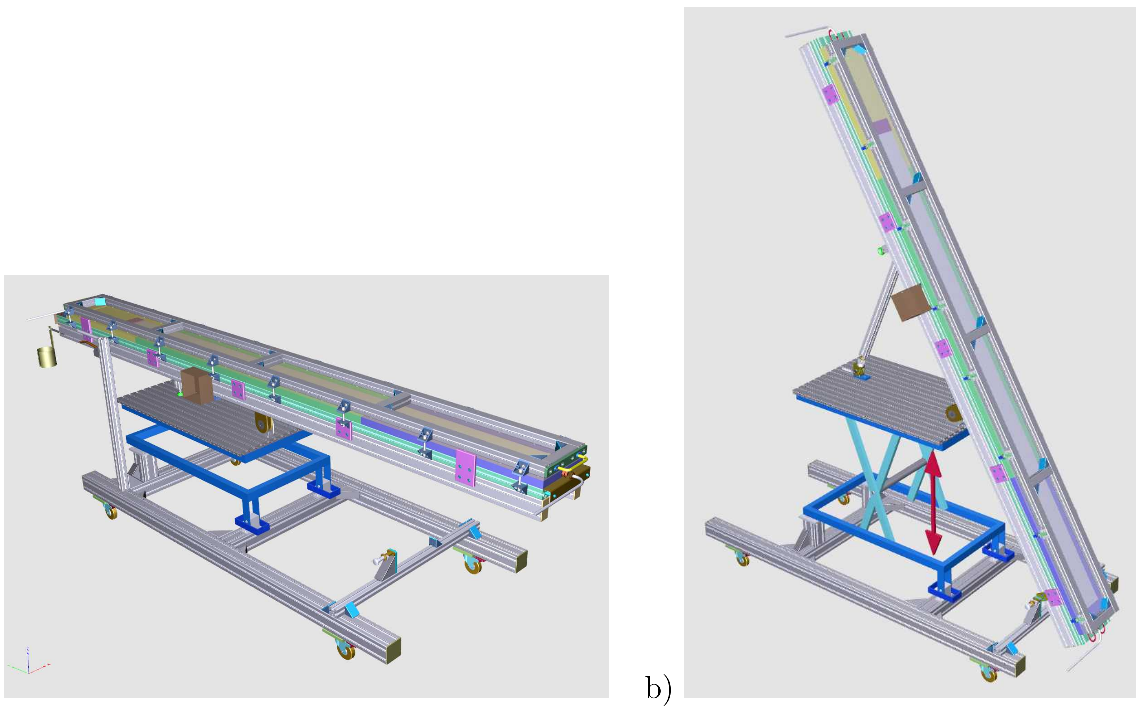

Figure 3.11: a) Casting jig in working position, b) Jig in casting position

Hole Position	y [mm]	Deviation from straight line [µm]
Endpiece 1	168.484 (+40.000)	-54
1	208.531	-7
2	208.544	6
3	208.542	4
4	208.555	17
5	208.550	12
6	208.526	-12
7	208.494	-44
8	208.515	-23
9	208.565	27
10	208.559	21
Endpiece 2	168.569 (+40.000)	31

Figure 3.12: Photo of aluminium body of casting jig (top), pocket for endpiece readout side (middle left), long alignment grooves (middle) and pocket for endpiece mirror side (middle right). Measurement of casting jig straightness (bottom)

the nominal value of 1.4 mm, the distance holders in between fibre mat and glass cover are choosen due to the measured deviation of the nominal value of the fibre mat height. After the preparation of the lower endpiece halves (step 4) they are placed, aligned and sealed with Latex WLAM2211 CCM55 in the mold (see figure 3.15). The endpieces are aligned in the aluminium body of the jig with respect to the fibre centre by holes.The lower readout endpiece half aligns the SiPM arrays.

To cast the fibre mats they are placed in the aluminium body of the casting jig made (see figure 3.16). The fibre mat is positioned by means of its pins that are positioned into the long grooves in the casting jig. The spacing lines which have been placed on the fibre mat before ensures the separation distance between endpiece, fibre mat and glass cover within 30-40 micron tolerance and allows the glue to fill in this space for a good bond.

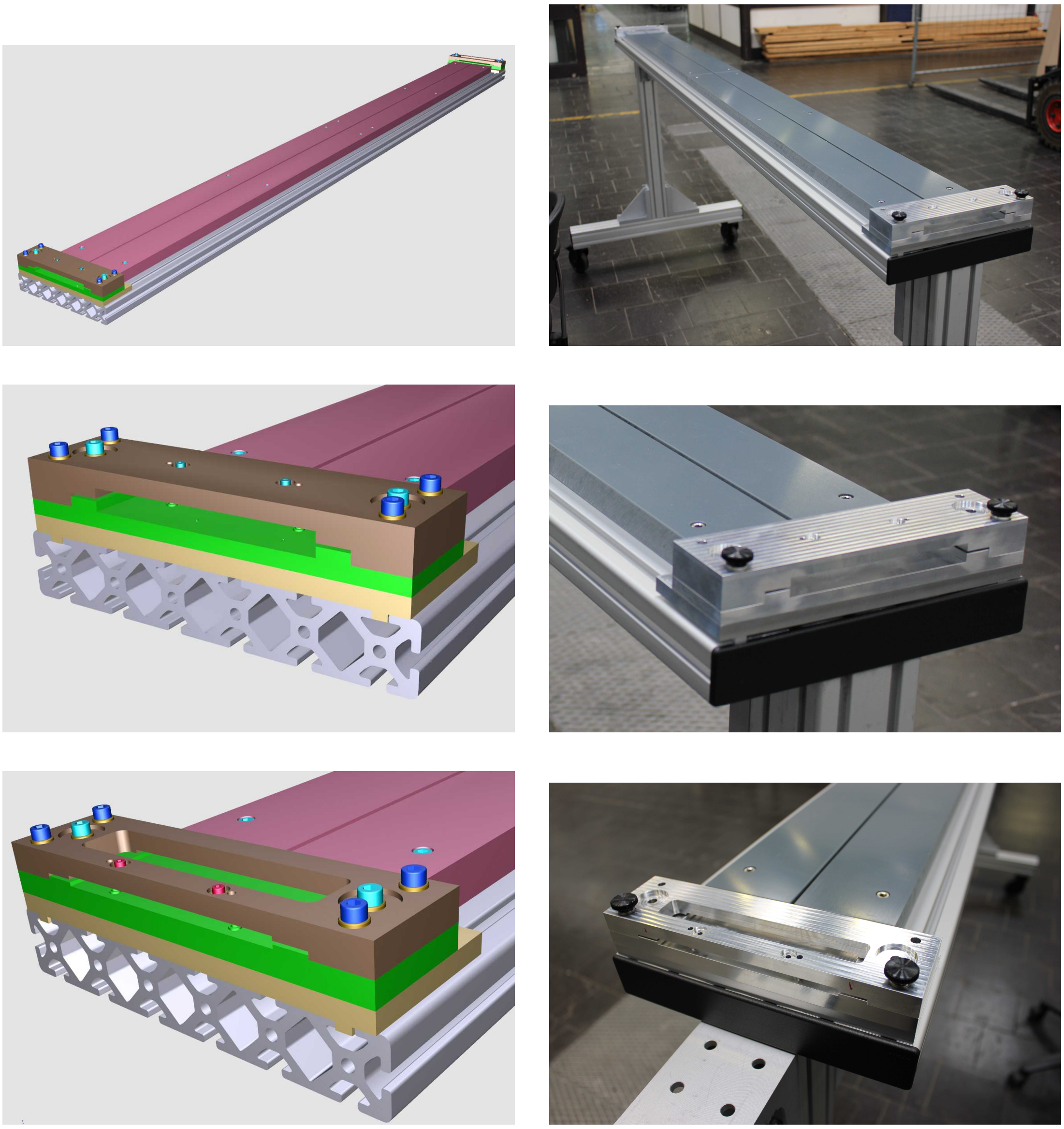

Figure 3.13: Multi Purpose Jig: Drawing and photo of jig (top), drawing and photo of bracket endpiece readout side (middle), drawing and photo of bracket endpiece mirror side (bottom)

The mould is closed by means of a glass plate and placed in a vertical position. The glue is filled into the casting jig from bottom to top. During the filling a running vacuum pump is connected to the top connection to support air bubbles which are enclosed in the glue to climb up faster with respect to the curing time of the glue.
After 3 days of curing the casted fibre mat can be taken from the casting jig. An unformed casted fibre mat, the lower endpiece halves on readout and mirror side glued to the mat and the resulting alignment pins on the fibre mat are shown in figure 3.17. The width of the alignment pins were measured to be (3.00 - 0.04) mm and cross checked with a high

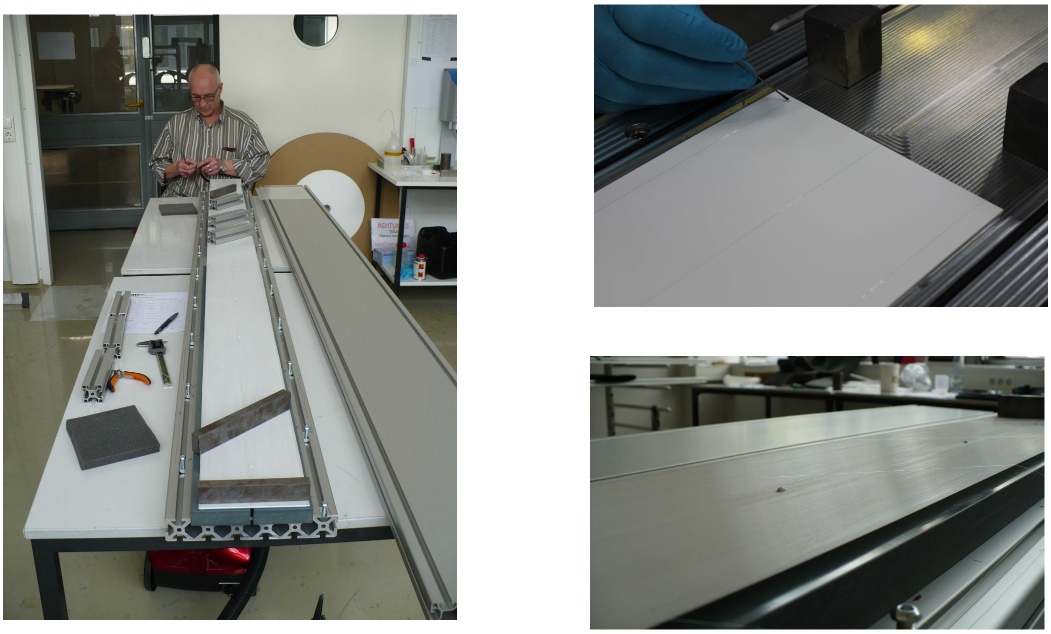

Figure 3.14: Step 2: Preparation of fibre mat with spacing lines

Figure 3.15: Step 5: Placing of endpiece on readout side (left) and mirror side (right) in casting mold and sealed with Latex

precision milled test gauge which has a slit of (3.00 + 0.005) mm (see figure 3.17 lower right). No casted alignment pin exceeded the required width of 3.0 mm.
The height of an uncasted fibre mat should be 1.4 mm. The measured height of the uncasted fibre mats are (1.33 ± 0.02 mm). The deviations is due to the variing thickness of the used individual fibres. The nominal height of a casted fibre mat is 1.60 mm. The measured heights of the casted fibre mats are (1.63 ± 0.03 mm). The deviations result from the tolerances of the aluminium body and the glass cover of the casting jig and the processing itself. Measurements on the mechanical properties of the casted fibres mat are summarized in section 3.6.
After this casting the resulting fibre mat is robust and handleable without fear of damage.

Figure 3.16: Step 9: Filling of glue into casting jig

Table 3.3: Summary of steps to cast a fibre mat.

Step	Item	Time	People	Materials	Cost/mat
1	clean and prepare jig	150 min	1	release agent	10 EUR
2	prepare fibre mat	10 min	1		
3	place spacing lines onto mat	80 min	1	fishing line 80 μm, glue	
4	prepare lower endpiece halves	10 min	1	endpiece, WLAM2211 CCM55	30 EUR
5	place lower endpiece halves in jig	20 min	1		
6	place and adjust fibre mat in jig	10 min	2		
7	close casting jig	30 min	2	casting jig	
8	mix glue with vacuum mixer	10 min	1	Epotek 301-2FL, vacuum mixer	150 EUR
9	fill the casting jig with glue	60 min	1		
10	curing time	3 days	-		
11	unform fibre mat from mold	20 min	2		
12	check of mat geometry	15 min	1		
Total	process time 415 min + 3 days	issue time 415 min			190 EUR
Tooling costs		4 casting jigs per winding center			20000 EUR

Optimization of the process parameters is ongoing. Two lines are followed: First is optimization of process parameters to reduce the curing time of the fibre mats in the casting jig (see figure 3.18). A first dummy was casted successful using the glue

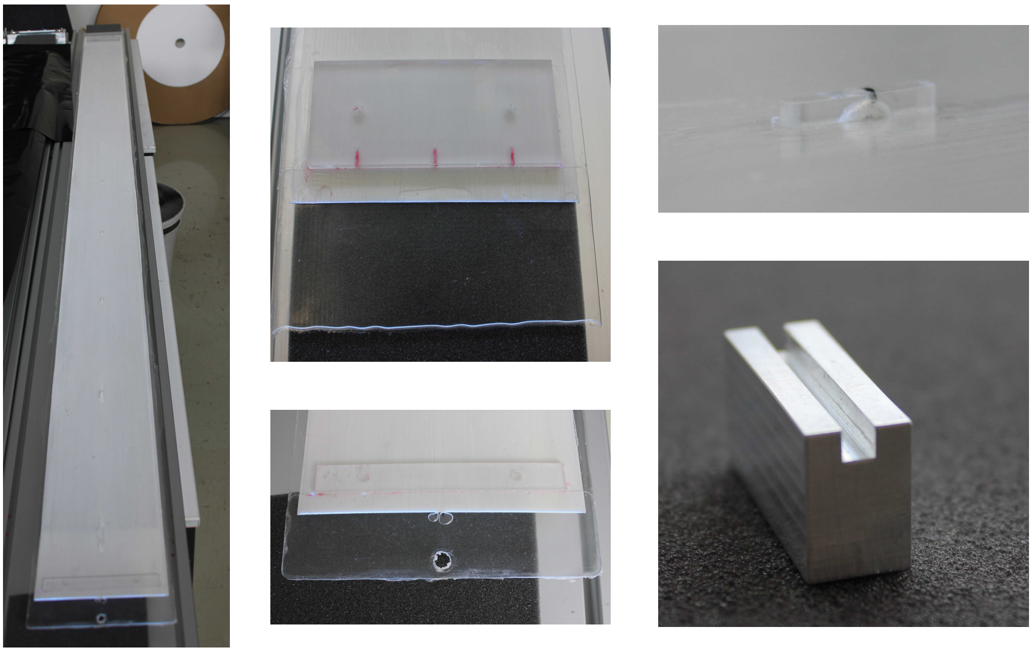

Figure 3.17: Step 11: Casted fibre mat after unforming from casting jig (left), lower endpiece half readout and mirror side (middle two), zoomed view of a casted alignment pin (upper right), precision gauge for quality assurance of alignment pin width (lower right).

Figure 3.18: Optimization of casting process parameters: Casted dummy with EPOTEK 301, zoomed view of one alignment pin.

EPOTEK 301 which has a 90 min potting time compared to the glue EPOTEK 301-2FL used for the casting of the 8 fibre mats for the first module. Almost all bubbles managed the way along the diagonal spacing lines to the edge regions which are cutted away with the longitudinal cut (see section 3.4). Using this glue would save 1 day of curing time.

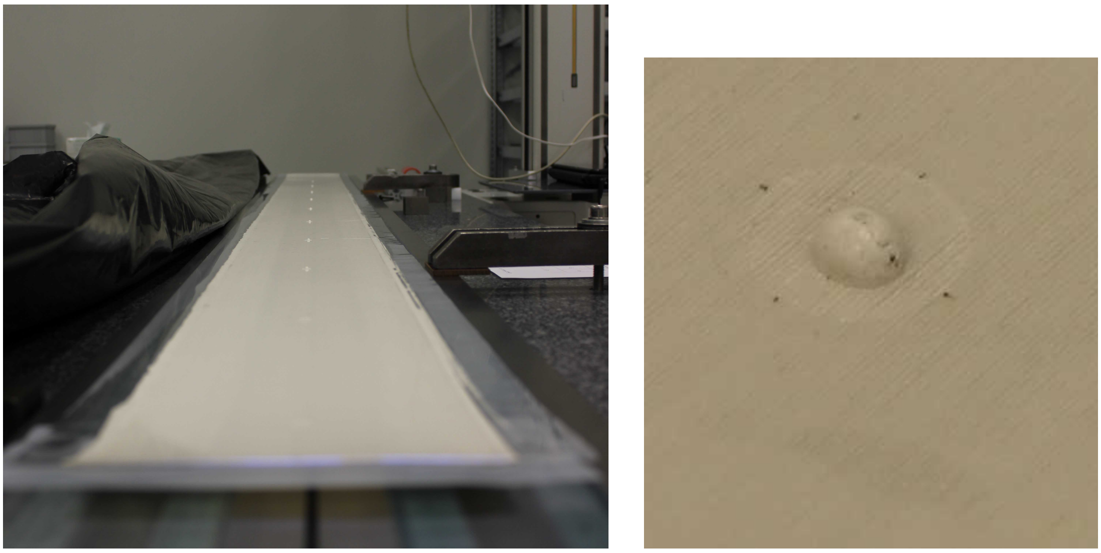

Figure 3.19: Optimization of casting process: Foil casted fibre mat (left), zoomed view of one alignment pin (right).

Secondly, an alternative to the glue casting could be the foil casting which would have the advantages of less production steps, lower costs, lower material budget, casting with a light tight foil, but with the disadvantages of a not well defined thickness of the foil casted fibre mat and less protected alignment pins (see figure 3.19).

3.3.3.1 Glue endpieces

The upper endpiece halves are added after the casting, but before the diamond milling, in a second aligned bonding step. The casted fibre mat is placed on the multi purpose jig (see figure 3.20) The upper endpiece halves are bonded to the fibre mat opposite the endpieces bonded during the casting. These are aligned via the multiple purpose jig and bonded with an epoxy that has a short potting-time.

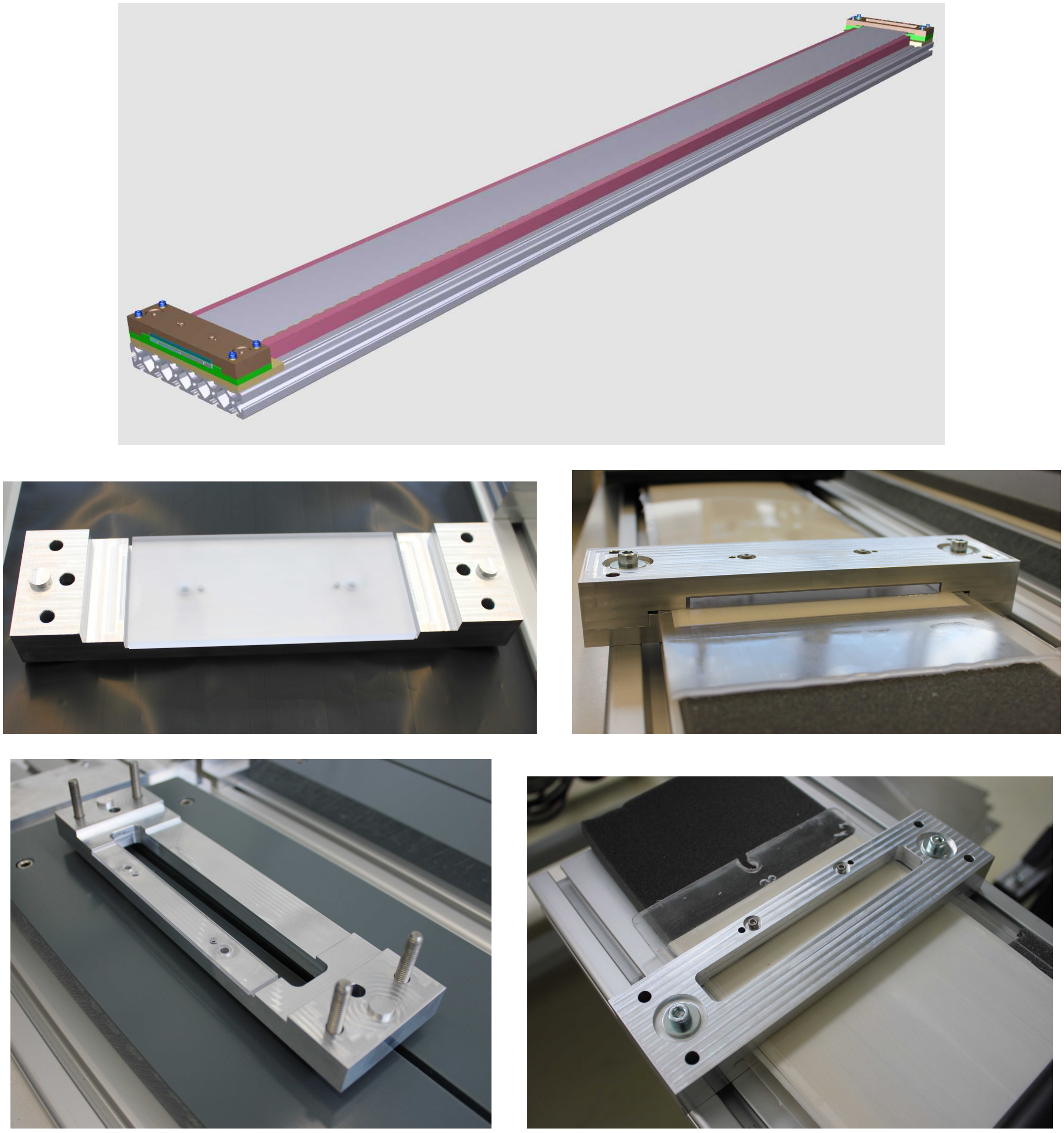

Figure 3.20: Drawing of upper endpiece halves gluing to fibre (upper). Photos of prepared upper endpiece halves (clear polycarbonate material) in brackets (middle) and during bonding process to fibre mat aligned in multiple purpose jig (lower). The blue glow is from the fibre mat, which has the bottom endpiece already glued in the casting jig on the bottom.

Table 3.4: Summary of steps for glueing the 2nd endpiece.

Step	Item	Time	People	Materials	Cost/mat
1	prepare multi purpose jig	10 min	1	jig	
2	place fibre mat on jig	5 min	2	mat, jig	
3	prepare upper endpiece halves	10 min	1	endpiece	30 EUR
4	prepare glue	10 min	1	5ml glue	15 EUR
5	align and glue	10 min	1		
6	apply pressure, remove leaking glue	30 min	1		
7	curing	18 h	-		
Total		75min + 18 h			45 EUR

3.4 Cutting and Mirroring

3.4.1 Transversal cut to Diamond Polish fibre ends

Figure 3.21: Tools: Saw blade for pre-cut (left) and a diamond head for final optical cut (right).

A precise diamond milling of the end of the cast fibre mats and endpieces is done to provide a smooth flat surface against which the SiPM window is pressed so that the SiPMs can detect the majority of the light which is produced and transported in the scintillating fibre in direction to the SiPMs. The diamond cut finish all ensures maximal optical transmission. The feed and rotation speeds of the milling head has been optimised to ensure that the fibres are not damaged through melting and the endpieces are not distorted.

The sequence of work of the transversal cut has the following steps (see table 3.6): The multi purpose jig is used now as a cutting jig which has to be positioned in place at the milling machine (see figure 3.22 upper plots). The fibre mat is placed and fixed on the cutting jig. The mat is aligned on the jig with its reference holes in the endpieces (see figure 3.22 middle plots). Then a pre-cut is done using a saw blade to cut away the overlength of the fibre mat close to the final length (see figure 3.22 lower left). The speed of the saw blade during the pre-cut is 250 m/min. The feed value is 0.001 mm/tooth. The pre-cut is first done on the readout end. Then the optical cut using a diamond head (see figure 3.22 lower right) is done. The speed of the diamond head is 200 m/min during the optical cut. The feed value is 0.003 mm/tooth and the infeed depth is 0.03 mm. After turning the jig, the pre-cut and the optical cut are done on the mirror side. In the next step the length of the fibre mat is measured (see figure 3.23). If the mat still has an overlength, the step with the optical cut and the measurement of the length is repeated. The measured lengths of the 8 EDR casted fibre mats is shown in table 3.5 and fullfil the required length of $(2424 + 0.1 - 0.3)$ mm.

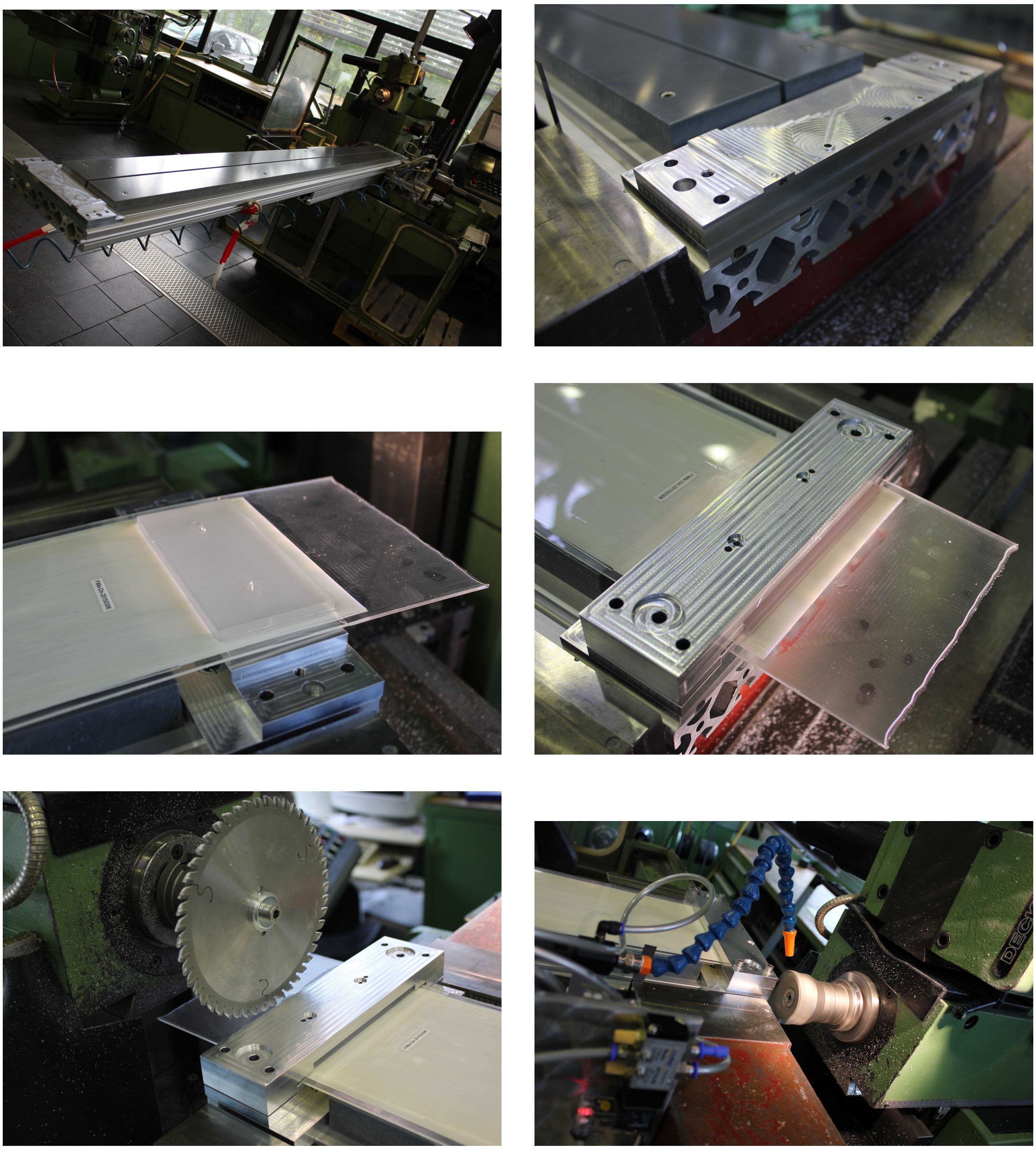

Figure 3.22: Cutting jig positioned in place at milling machine (upper left), cutting jig lower endpiece bracket half at place (upper right). Positioning (middle left) and fixation (middle right) of fibre mat on cutting jig. Pre-cut with a saw blade to cut away overlength of fibre mat (lower left). Optical cut with diamond head (lower right).

As a criteria for the quality of the optical cuts the surface roughness and its uniformity of the scintillating fibres was measured using a high precision microscope (see figure 3.24) and the light yield of a fibre mat with SiPM-readout was measured in a cosmic teststand.

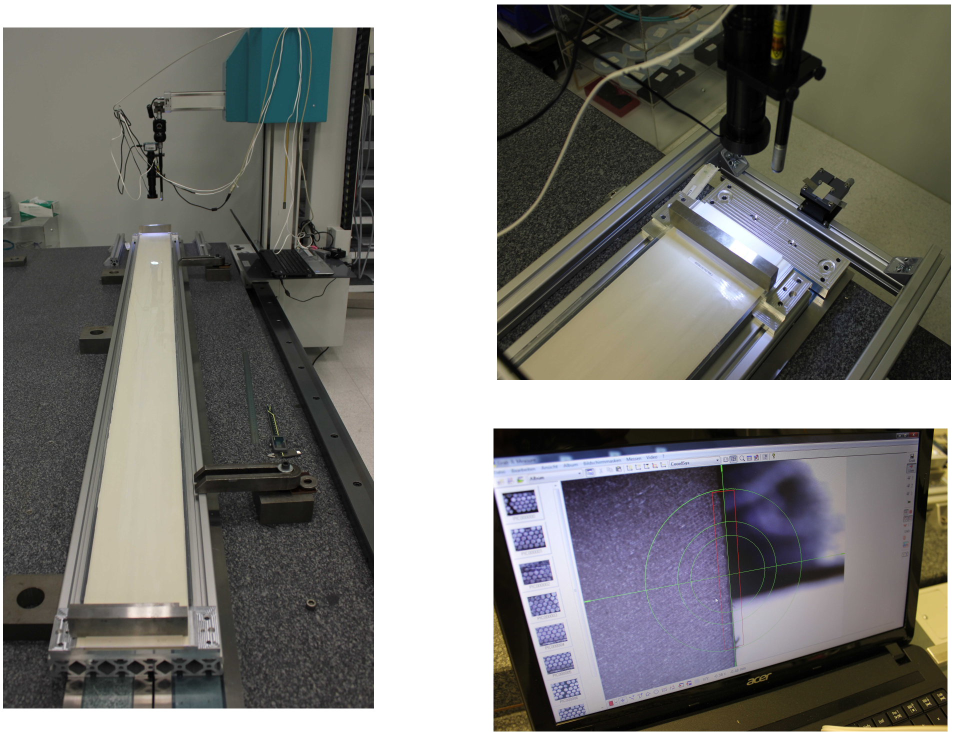

Figure 3.23: Measurement of final length of fibre mats

Table 3.5: Measurement of final length of 8 EDR fibre mats.

EDR Mat	Length after optical cut (mm)
FiMa-Do.20150213	2423,960
FiMa-Do.20150218	2423,901
FiMa-Do.20150303	2424,022
FiMa-Do.20150306	2423,911
FiMa-Do.20150313	2423,926
FiMa-Do.20150318	2423,780
FiMa-Do.20150410	2423,690
FiMa-Do.20150505	2423,900

The uniformity and the surface roughness of 390 nm in average using a saw blade improved to 250 nm in average using a diamond tip milling head. The measured light yield increased by 10 %. Therefore the diamond tip milling head is the chosen tool for the optical cut.

The quality control of the casted fibre mats after optical cut is a scan of the fibre mat readout and mirror side (see section 3.6).

Tools for transversal cut: Standard milling machine per winding centre. 8 Saw Blades

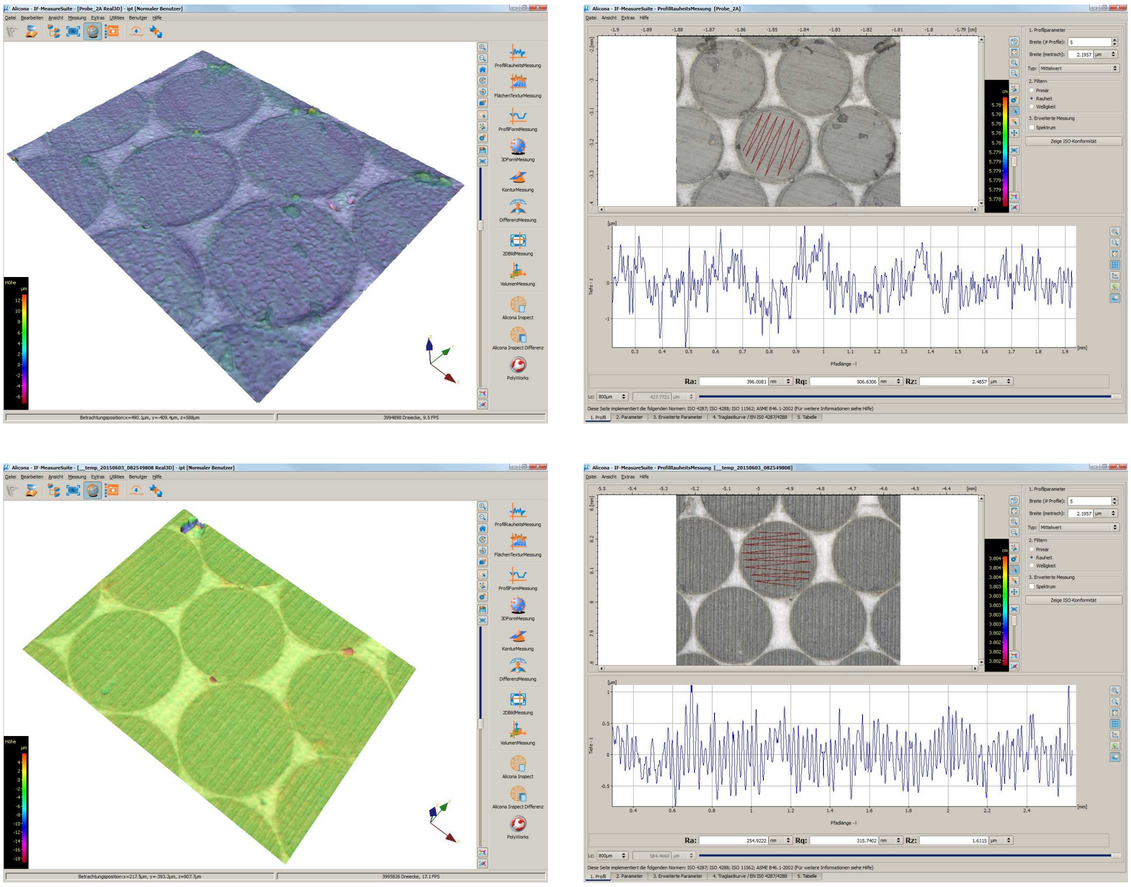

Figure 3.24: Measurement of surface roughness of fibres after the cutting with a saw blade (upper) in comparison to the cutting with a diamond milling head (lower).

(with 1 saw blade 20 fibre mats can be cut) per winding centre plus backup, cost estimate 540 EUR. One Diamond milling head per winding centre plus backup (2 x 1000 EUR) and maintenance of diamond milling head after cutting of 20 fibre mats for another 20 mats, cost estimate: 2 x 1000 Euro plus 12 x 300 EUR. Multi purpose jig as cutting jig to hold mat ends during milling, cost 1500 EUR.

After the optical cut and the quality assurance measurements the gluing of the mirror to the casted fibre mats is the last production step in the winding centres.
The sequence of work of the mirroring has the following steps (see table 3.7):
The multi purpose jig is used now as a gluing jig. The fibre mat is placed, aligned and fixed on the gluing jig. (see figure 3.25 upper left). The surface of the fibre ends at the mirror side are cleaned using isopropanol (see figure 3.25 upper right). After the preparation of the mirror (see figure 3.25 middle left) the mirror is fixed to an stainless steel bar with a kapton tape (see figure 3.25 middle right) and glued to the fibre mat (see figure 3.25 lower left). After overnight curing the kapton tape is loosened. In the last step the mirror overlength has to be cut away so that the mirror covers exactly the endpiece of the fibre

Table 3.6: Summary of steps to diamond cut the fibre mat ends.

Step	Item	Time	People	Material	Cost / mat
1	Align mat on cutting jig	5 min	2	jig	
2	Precut readout side	15 min	1	sawblade	4 EUR
3	Optical cut readout side	40 min	1	diamond head	23 EUR
4	Precut mirror side	15 min	1	sawblade	
5	1st optical cut mirror side	40 min	1	diamond head	
6	acclimatisation	240 min			
7	Measurement of final length	10 min	1		
8	Final optical cut mirror side	40 min	1		
Total		170 min	1		27 EUR

mat (see figure 3.25 lower right).
Tools for mirror gluing: mirroring foil, multi purpose jig as gluing jig, cost estimate: 1500Euro / jig.

Table 3.7: Summary of steps to attach mirror.

Step	Item	Time	People	Material	Cost/mat
1	Align fibre mat in jig	5 min	2	multi purpose jig	
2	prepare mat	5 min	1	isopropanol	
3	prepare mirror	15 min	1	mirror, scalpel	
4	prepare glue	10 min	1	5ml glue	15 EUR
5	glue mirror	10 min	1	mirror	-
6	curing time	18 h	-		
7	cut mirror	10 min	1	scalpel	
Total		55 min + 18 h	1		15 EUR

After the mirror gluing, the fibre mat is ready for shipment to the module production centre (see figure 3.26 lower right).

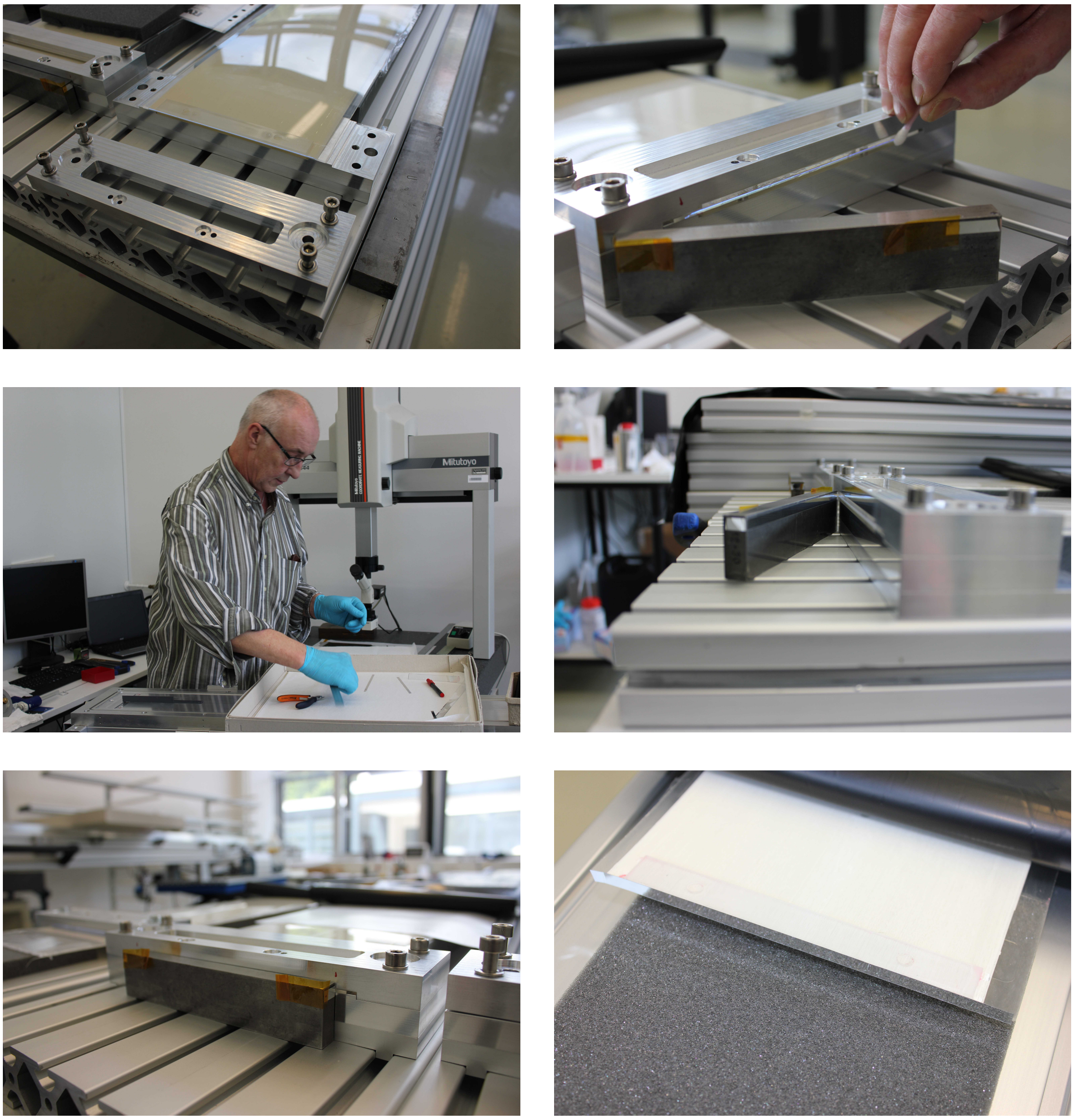

Figure 3.25: Fixation of fibre mat in gluing jig (upper left), Cleaning of fibre mat (upper right), Preparation of mirror (middle left), Fixation of mirror (middle right), Gluing of mirror to fibre mat (lower left), Mirror glued to fibre mat on mirror side after overnight curing (lower right).

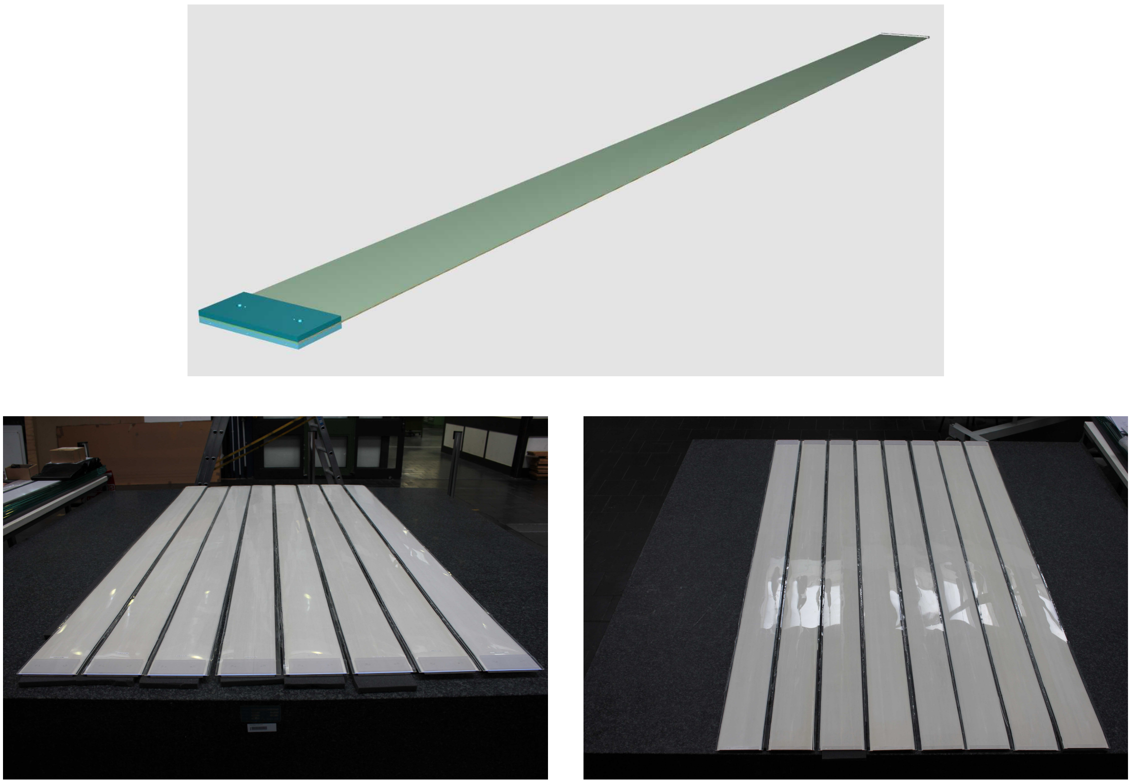

Figure 3.26: Drawing of a finished casted fibre mat with endpieces and mirror (upper), The 8 EDR fibre mats after winding at winding center TU Dortmund and after casting, transversal optical cut, quality assurance scans and mirror gluing at winding center RWTH Aachen ready for shippment to module center Uni Heidelberg (lower).

3.4.2 Longitudinal cut

To reach a minimal loss of acceptance at the boundary of two neighbouring cast fibre mats, the mats must be cut to the appropriate width with a precision of better than 150μm to ensure the needed tolerance between the mats. To guarantee this precision, two parallel cuts are performed using a circular saw. The set-up for cutting the sub-modules is shown in figure 3.27. The choice of the blade has been taken after a series of test. The advantage of that particular mill is that it efficiently removes the chips during milling and provides a reasonable cooling due to the good thermal conductivity of the blade. The range of the milling machine is not sufficient to perform a cut over the entire length of the fibre mat. For that reason it is done in two steps. A special jig mounted on a rail system is used to move the fibre mat. A measurement of the pin position of the mats cut for the demonstrator module revealed that this cut introduced a small kink in the fibre mats (see Fig. 3.34). This can be avoided in future by a correction of the parameters in the cutting program of the milling machine.
It has been verified that the cut affects mostly fibres outside the active area of the SiPM arrays (see sction 3.5).

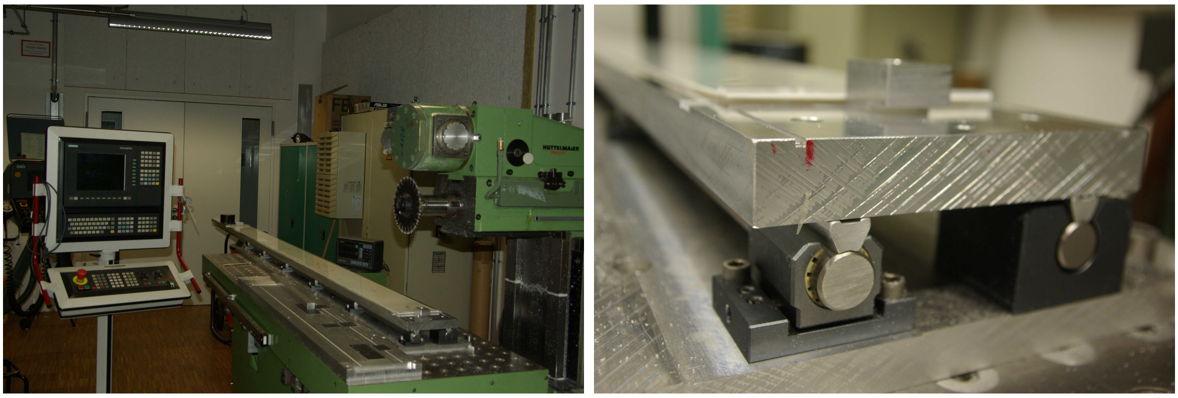

Figure 3.27: Left: Milling machine with jig used for cutting fibre mats along the fibres. The right picture shows a detail of the rail system needed to extend the range of the machine to 2.5m.

Table 3.8: Summary of steps for the longitudinal cut.

Step	Item	Time	People	Material	Cost/mat
1	Align fibre mat on jig	10 min	1 person	jig	2
2	cut fibre mat	50 min	-	blades	3
Total		60 min	-		5

Tools: Milling machine with long table (1.5m) per module assembly centre (MAC); one double blade 'Kreisfräse' / MAC. Cost estimate: 500Euro

3.5 Demonstrators and Measurements

For testing, improving and proving the procedures of the production steps of fibre mats, nine mats were produced in a mini serial production. One mat was used in a small test beam module, the other eight were used to built a full size module (see also chapter 4). This was not done in one winding centre, the responsibilities for production and quality assurance were split.

The winding of the fibre mats was performed in Dortmund with the help of the prototype winding machine, because the first serial winding machine was not available early enough for this purpose. The prototype machine is based on the same principle, the differences are explained in section 3.2.

After winding, the raw fibre mats where transported to Aachen (private transport) for further processing. The mats were casted with glue (including assembly of end pieces) and the optical cuts were performed as described before in the dedicated sections (3.3.3 and 3.4). The cross sections were optically analysed with two different set-ups. Like described in section 3.6, photographs with a dedicated set-up based on a microscope or, alternatively, on a conventional scanner were used. The fibre positions of a typical fibre mat are shown in Fig. 3.28. The distribution of distances between the adjacent fibres of this cross section is shown in Fig. 3.29. It is visible that the fibres of the first layer are positioned best because they are guided by the thread of the wheel. The width of the distribution increases as expected from layer to layer. An overview of the fibre distances for all fibre mats is shown in table 3.9. These results were obtained with the conventional scanner, because the dedicated set-up was not available for all measurements. The average mean is in very good agreement with the expected pitch. The width of the distribution is dominated by the error of the measurement but small enough to ensure that the fibre matrix is correct.

One fibre mat (FiMa-2015-Mar-13) showed a region with damaged fibres (58 fibres) in the first layer (see Fig. 3.30 & 3.31). One fibre mat developed a longitudinal crack at one end before casting. All the other mats showed no abnormality. These two defects are not tolerable in mats for the inner modules, they might still be used on the outside of the acceptance where due to a smaller irradiation doese a higher light yield is expected. It is expected that the errors occurred because of the special handling needed to ship the mats before casting. During serial production the mats will be casted after the winding with limited handling in between. No shipping will be required, it will be performed in the same room. It is less likely that errors like this occur with optimised tooling for handling the mats at the winding centres.

After applying the mirror, the mats were shipped (private transport) to the demonstrator module centre (Heidelberg). The longitudinal cut was performed as described in section 3.4. After that the pin width (see Fig. 3.32), the width of the mats (see Fig. 3.33) and the offset of the pin position to the centre of the mat (see Fig. 3.34) were measured. The pin width and the mat width are well within the specifications. The offset from zero of the pin offset is not due to the offset of the pins to the fibres, but due to the precision of the longitudinal cut. The reason for the systematic increase along the mat is known

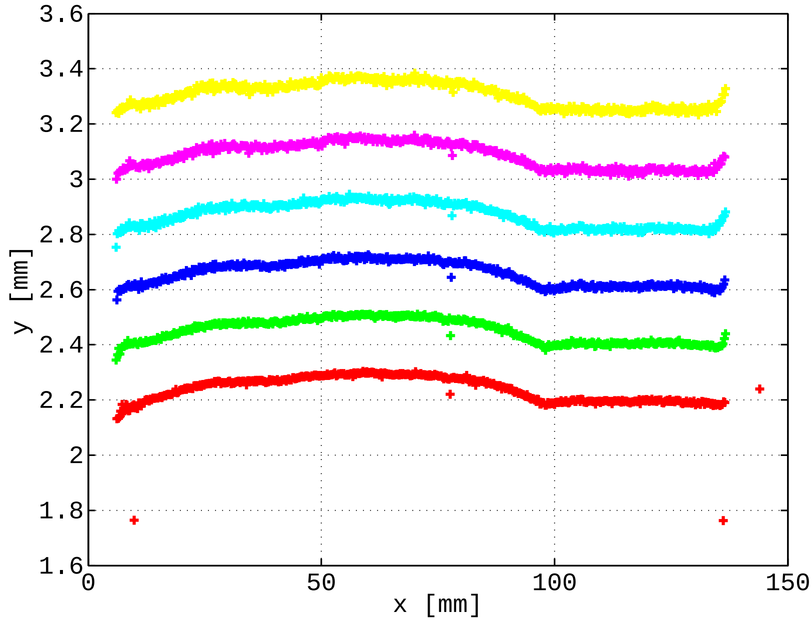

Figure 3.28: Fibre positions in a typical fibre mat. The outliers are wrongly detected circles.

and can be corrected (see section 3.4).

To determine the quality of the long cut the edge was examined with a UV-lamp as

Table 3.9: Overview of the mean and RMS of the distances of the fibres in the fibre mats. The RMS is driven by the resolution of the measurement, the results were obtained with the standard scanner.

	SiPM end		mirror end	
	mean / μm	RMS / μm	mean / μm	RMS / μm
FiMa-2015-Feb-08	275.1	24.1	275.1	16.9
FiMa-2015-Feb-13	275.3	22.7	275.1	24.0
FiMa-2015-Mar-03	273.1	35.3	274.6	29.4
FiMa-2015-Mar-06	275.2	22.2	275.1	16.4
FiMa-2015-Mar-13	274.9	19.9	274.9	21.7
FiMa-2015-Mar-18	275.1	23.7	274.9	24.5
FiMa-2015-Apr-10	275.2	15.8	274.9	24.0
FiMa-2015-May-05	275.2	23.7	275.1	14.1

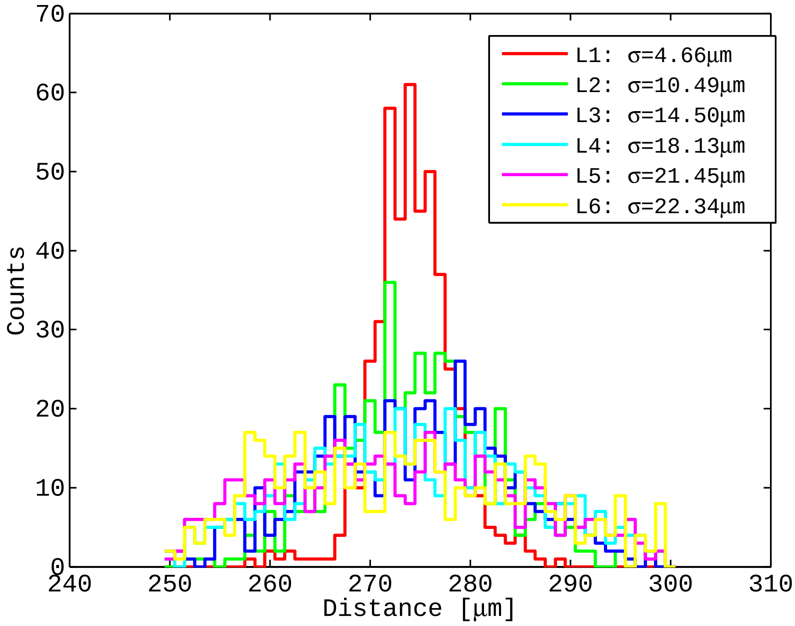

Figure 3.29: Distances between adjacent fibres in a typical fibre mat. The positioning of the fibres is best in the first layer where the fibres are guided by the thread of the wheel.

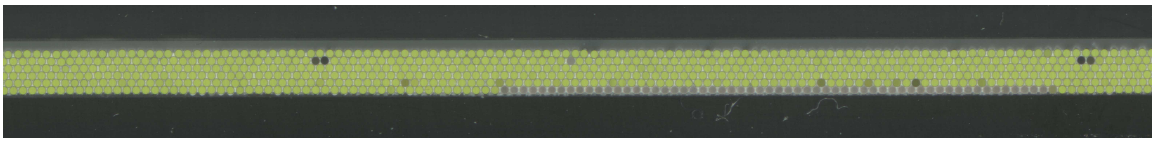

Figure 3.30: Extract of the photograph of the cross section of FiMa-2015-Mar-13. Multiple fibres were damaged in the first layer, the light guidance is blocked in these.

described in section 3.6. In figure 3.42 examples of photographs are shown for two mats. The fibre mat shown on the left (FiMa-Do-15-Mar-06) transmits light for all fibres inside the active area of the SiPM array, i.e. none of these fibres have been damaged. For fibre mat FiMa-Do-15-Apr-10 on the right of figure 3.42 on the other hand two fibres covering partially the active area of the SiPM show no light from the mirror side, i.e. these fibres have been damaged. An overview of this analysis for the fibre mats produced for the demonstrator module are shown in table 3.10. In total 5 fibres from the 8 fibre mats used for the demonstrator module show damages. These fibres are only partially inside the active region of the SiPM array as indicated by the shaded area in figure 3.42. Therefore a damaged fibre results only in an approximately 10% loss of photon yield for the outermost SiPM channel of the fibre mat. In addition it was observed that two fibres got loose at one edge of FiMa-2015-May-05. The reason for this is understood and the process was

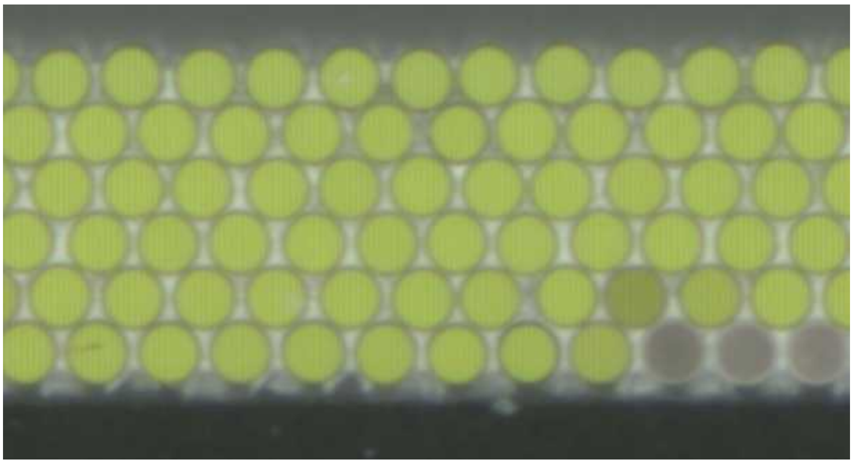

Figure 3.31: Extract of the photograph of the cross section of FiMa-2015-Mar-13 - zoom in. Multiple fibres were damaged in the first layer, three of these are visible on the bottom right.

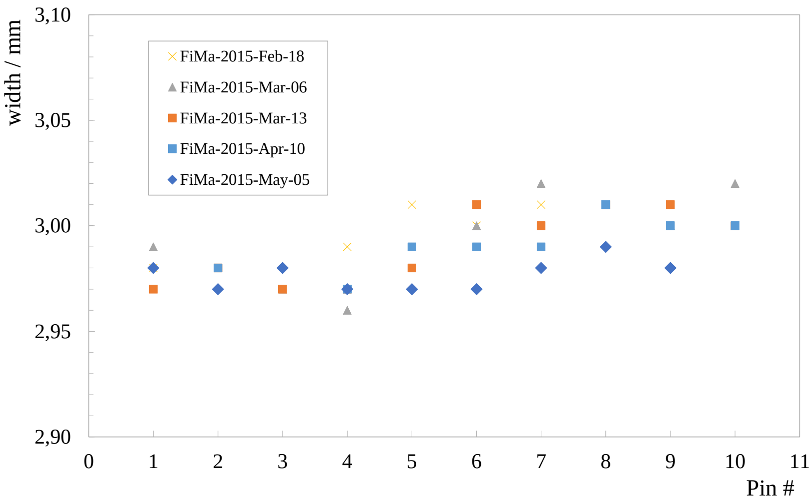

Figure 3.32: Width of the pins of five fibre mats produced for the EDR module. The absolute uncertainty of the measurements is 20 µm.

optimised. The achieved quality of the cut is already satisfying, nevertheless it is expected to improve using further developed tooling (see section 3.4).

While the fibre mats are intended to be straight by means of the alignment pins produced during winding, the relative straightness of the fibres within the casted mat with respect to these pins is unknown over the length of the fibre mat. Cross section images are only seen at either end of the fibre mat. Optical methods of measuring the fibres along the mat are very difficult as the fibres are transparent and they have been covered by

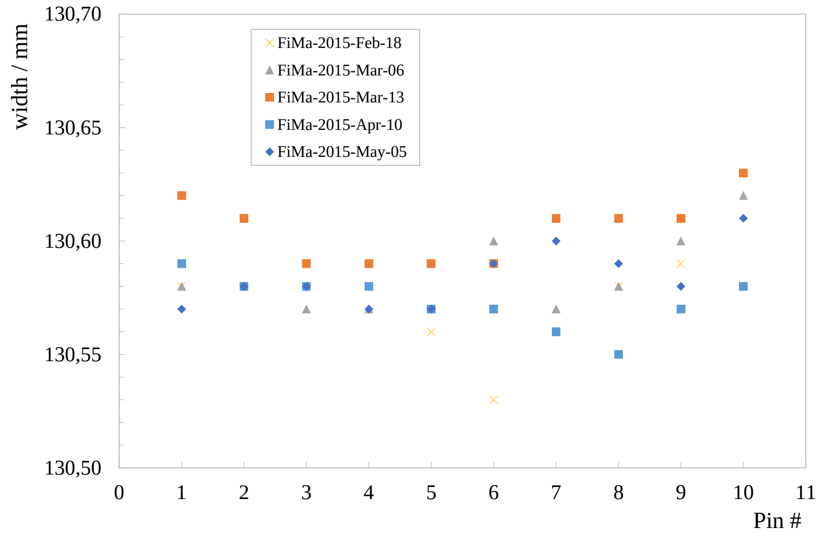

Figure 3.33: Width of five fibre mats produced for the EDR module.

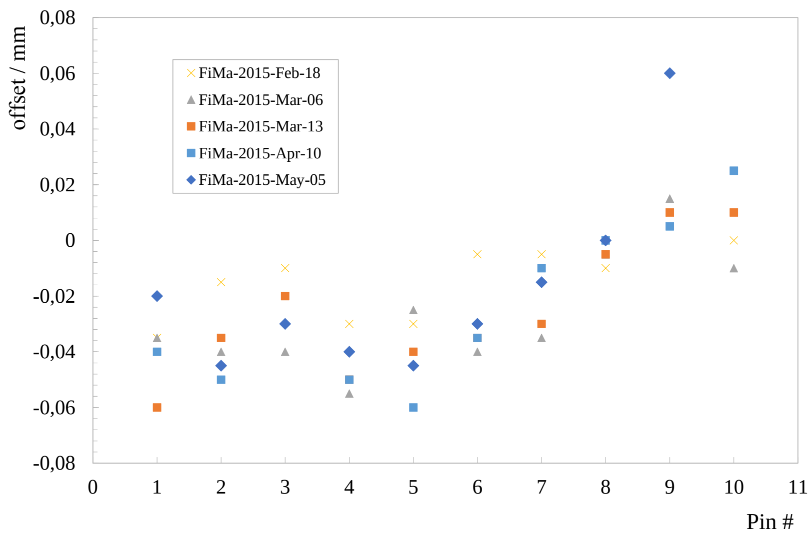

Figure 3.34: Offset of the pin position to the center of five mats produced for the EDR module. The offset from zero is not due to the offset of the pins, but due to the precision of the longitudinal cut. The reason for the systematic increase is known and can be corrected (see section 3.4).

titanium dioxide loaded glue. A dedicated setup was developed to determine the offset of the pins to the fibres. A collimated beta source is positioned on the fibre mat with the help of a pin. Since it is assumed that the pins are aligned to the fibres, aligning the beta source to these pins should excite the same set of fibres and produce the exact same signal

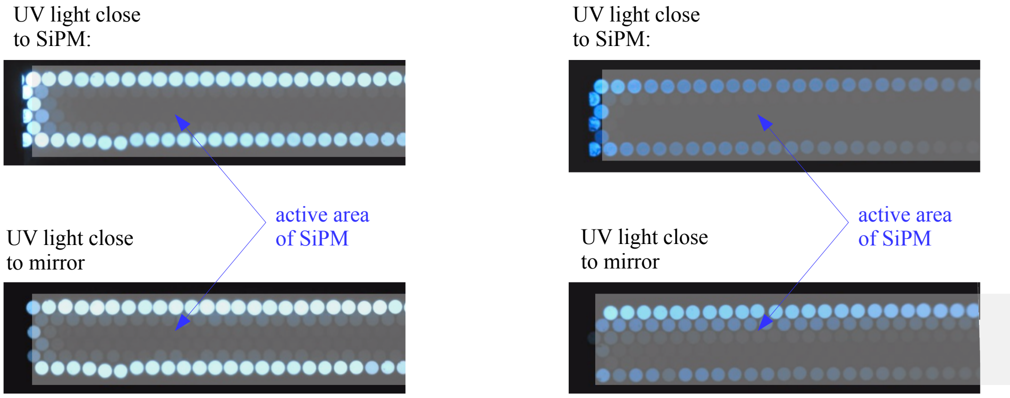

Figure 3.35: Photographs of edges of two fibre mats after the longitudinal cuts (left: FiMa-Do-15-Mar-06, right: FiMa-Do-15-Apr-10). The shaded area superimposed indicates the active area of the SiPM array. The upper two photographs have been taken with a UV light placed close the readout (SiPM) side. For the lower two photographs the UV source has been placed at the far end, close to the mirrors, due to the light attenuation the image is less bright. For FiMa-Do-15-Mar-06 all fibres inside the active area of the SiPMs transmit light from the far end, i.e. all fibres in the active region are intact. For fibre mat FiMa-Do-15-Apr-10 two of the fibres placed partially in the active region do not transmit light from the far end. These fibres are damaged.

Table 3.10: Overview over the analysis of the quality of the long cuts.

	left edge (dark/weak fibres)	right edge (dark/weak fibres)
FiMa-2015-Feb-13	0 / 0	0 / 0
FiMa-2015-Feb-18	0 / 0	2 / 0
FiMa-2015-Mar-03	0 / 0	0 / 0
FiMa-2015-Mar-06	0 / 2	0 / 2
FiMa-2015-Mar-13	0 / 2	1 / 1
FiMa-2015-Mar-18	not measured (used in different setup)	
FiMa-2015-Apr-10	2 / 1	0 / 0
FiMa-2015-May-05	0 / 2	0 / 0

distribution in the attached SiPM channels at all points along the mat. A diagram of the setup is shown in Figure 3.36. A more detailed description of the setup can be found in the appendix.

A histogram showing the number of events in each channel which pass a threshold is seen in Figure 3.37. A systemtic study of the repeatablity of the measurements indicates that the alignment can be repeated at each point better than 10 micron. 100k triggered events per point were recorded resulting in a statistical uncertainty in the mean of 3 micron. However, it was noticed that repeated placement of the bar over the pin results in a degradation of the positioning over time due to the wearing away of the relatively soft glue pins compared to the aluminium. As well, there is a 25 micron tolerance between the groove edges and pin, if the groove wall is not pressed against the pin sidewall.

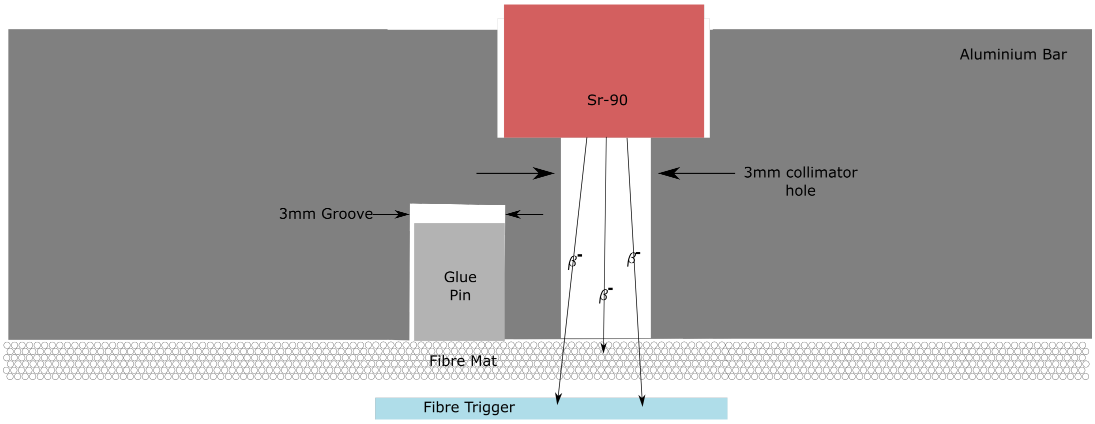

Figure 3.36: Schematic of the Sr-90 source based fibre mat straightness measurement.

This procedure was repeated at four points along the fibre mat length (more mats and more points will be repeated in the future) and the mean position of the collimated source was determined at each. The results are shown in Tables 3.11 for two separate mat measurements. The deviations from the first measurement point are shown in the tables. A min/max deviation of 33 micron is seen for the second mat, which was considered a fresh mat, i.e. having pins with their original size. The precision with which the first mat could be placed appeared to degrade over time, as this mat was repeatedly measured to test the method systematically. It is suspected that the pins are more worn through repeated alignment.

Summary

For the full size prototype eight fibre mats were built in a small serial production. The mats where produced in processes as close as possible to the expected serial production conditions. The achieved quality is already very good and within the specifications. Many of the steps could only be tested with dummy material before. The experience gained will help to improve the processes and tooling, with this the quality of the fibre mats can be improved and the reliability of the processes can be ensured.

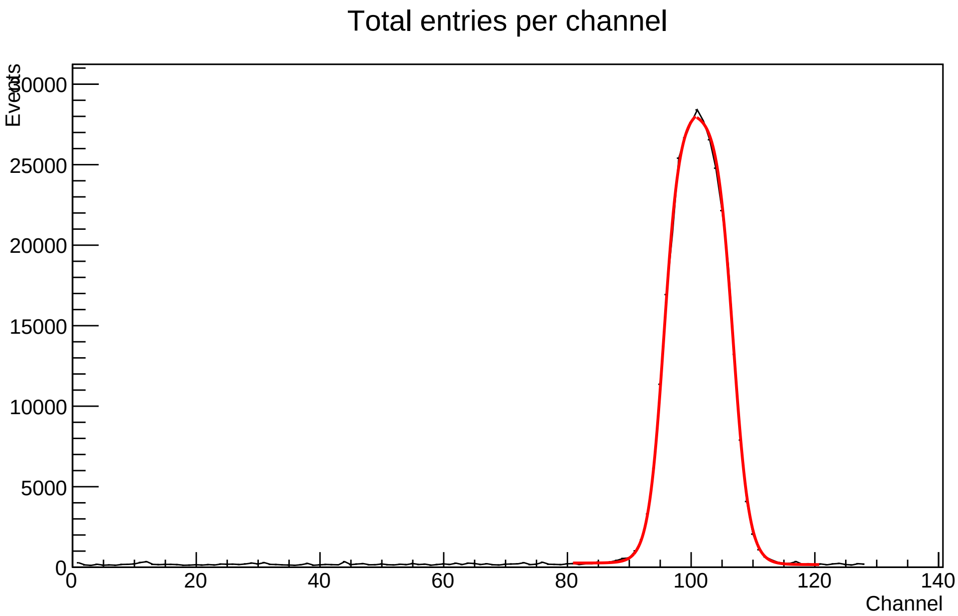

Figure 3.37: The number of triggered events over threshold as a function of SiPM channel. The red curves are two separete fits (left side and right side) to a Fermi function.

Table 3.11: Results for Mat 1 (FiMa-Do-20150318) and Mat 2 (FiMa-Do-20150303) from the collimated Sr-90 measurements of the internal fibre straightness within a mat. Deviations from the 30 cm measurement are shown. It is suspected that the pins at 88 cm of mat 1 are worn from repeated measurements during the testing process.

Position (cm)	Deviation (μm)	
	mat 1	mat 2
30	-	-
88	21.0	20.3
150	-38.6	11.0
195	-25.5	33.0

3.6 Quality Assurance

In total about 1300 fibre mats, corresponding to about 10.000km of fibres need to be produced. To sustain a good and constant quality of the fibre mats quality assurance (QA) procedures are needed. Possible problems have to be identified during fibre mat production as early as possible. To cope with that high numbers of fibre mats to be produced the driving principle for the development of QA tools are simplicity and efficiency.
In the following, the QA measurements foreseen for the serial production are briefly described.

3.6.1 Online monitoring during winding

Once a fibre mat has been wound it is no longer possible to correct possible defects in the fibre mat matrix. Therefore it is mandatory to detect the occurance of defects online during the winding procedure. Examples for defects in the winding process are given in figure 3.38(a) and 3.38(b). Winding is a time-consuming process and it is not reasonable

(a) (b)

Figure 3.38: Two different defects which can occur during the winding process. In (a) the current fibre jumped in the wrong threat and leave an empty space. (b) shows a fibre lying in the wrong layer.

and affordable for a technician to monitor the process continuously. For that reason an automatic defect detection is needed. The detection of a defect has to trigger a halt to the winding process, allowing the operator manually to settle the problem.
To meet these requirements a system is under development including an industrial camera and a lens with a large magnification mounted to the winding machine. During the winding process the camera is moving along the wheel. Like this it monitors always the fibre actually wound. Images from the camera are processed in real-time by a pattern recognition software based on the open source library *OpenCV*. The detection of a defect triggers the halt of the winding machine. Figure 3.39(a) sketches the set-up, figure 3.39(b) shows a prototype mounted to the winding machine in Dortmund. An image recorded by that system is shown in figure 3.40

3.6.2 Optical scan of fibre mat cross section

After winding and unforming from the wheel the fibre mat is casted (see section 3.3) and cut to its final length. The quality of the optical cut is crucial to ensure a good transmission of the photons produced in the fibre to the SiPM. After performing that optical cut a high resolution image of the fibre mat cross-section is taken to judge its quality and to check for possible defects in the fibre matrix. Two approaches have been followed to take images of sufficient quality. The first approach uses a digital microscope to take photographs. As it is not possible to take an image of the entire fibre mat at once the microscope is moved across the fibre mat and several pictures are taken. These images are stitched to a single image. Optical rulers fixed to the fibre mat ensure a proper stitching of the images. In the second approach a scanner is positioned in vertical position in front of the fibre mat and the mat is scanned. Like this stitching of images is avoided, but the quality of the images is worse compared to the microscope set-up. The set-up's are shown in figure 3.41(a) and figure 3.41(b). A circle finding algorithm has been developed to recognize the fibres and determine the position and the radius of the fibres. Figure 3.42 shows an image

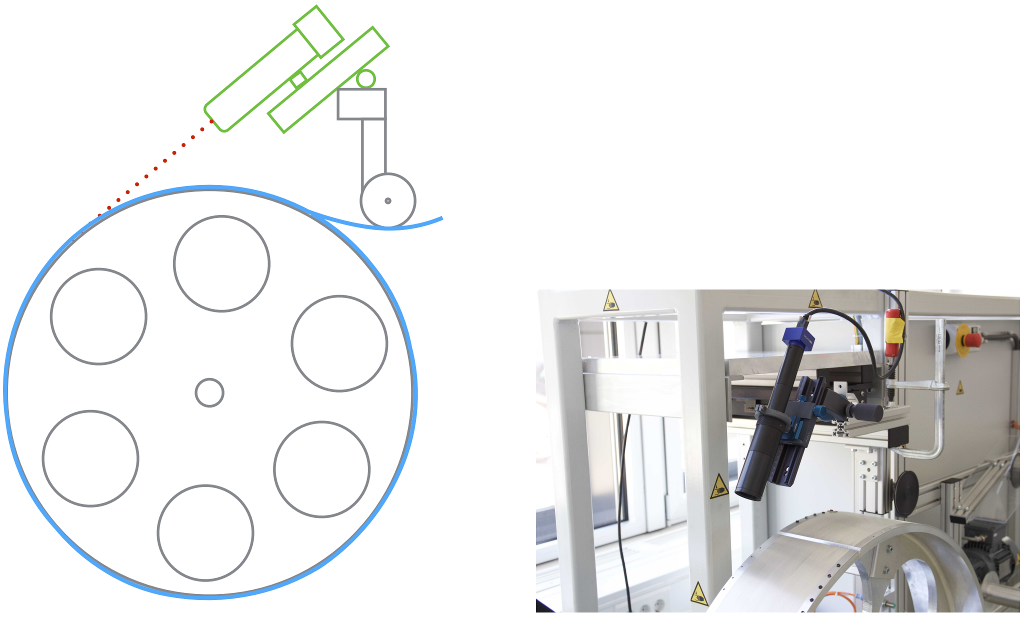

(a) (b)

Figure 3.39: Left: Scheme of the camera setup on the winding machine. The camera (green) will be placed on the same slide as the positioning spool and look tangential on the wheel. Right: Camera setup mounted on the winding machine.

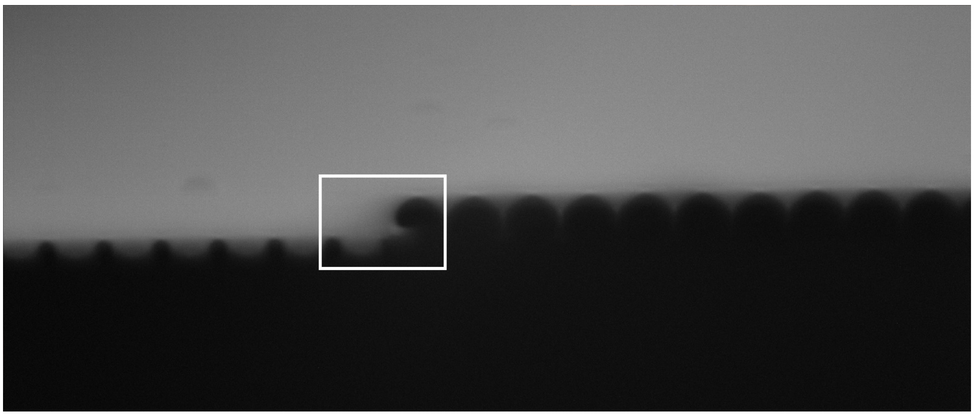

Figure 3.40: Screenshot of the online monitoring during the winding of the first layer. The white rectangle marks the area which is controlled. As soon as the newest fibre changes the position, this area will change and the error is detected.

taken by the microscope set-up with the result obtained by the circle finding algorithm superimposed. These results are used to display the position of the fibres inside the mat, histogram deviations from the nominal position and detect defects in the fibre matrix, e.g. missing fibres or fibres with a wrong diameter. A protocol is generated to allow a fast

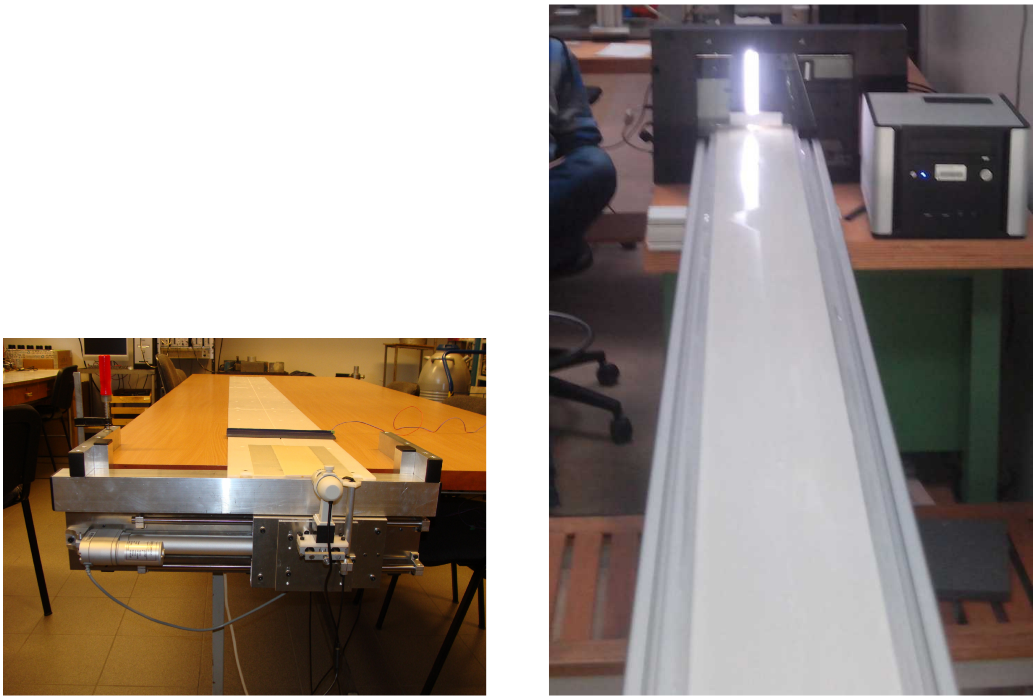

(a) (b)

Figure 3.41: Left: Microscope set-up for visual mat inspection. Right: Scanner set-up for visual mat inspection.

judgement of the fibre mat quality. The performance plots shown in figure 3.28 and figure 3.29 are generated using the microscope set-up. The optical scan is highly automized for both set-ups. The time needed to test a fibre mat is approximately 30 minutes.

3.6.3 Optical scan after longitudinal cut

During the longitudinal cut (see section 3.4.2) it has to be guaranteed that fibres inside the active area of the SiPM array are not accidentally damaged. Possible damages can be revealed using a camera or microscope and a UV source. Two pictures are taken for each edge of the fibre mat, the first with the UV source placed close to the end-piece used to mount the SiPM arrays. For the second photograph the UV source is placed close the mirrors. Damaged fibres will show UV light for the first photograph, but not for the second. The analysis of the quality of longitudinal cuts described in section 3.5 has been performed using that techniques, more details can be found in figure 3.42. This analysis demonstrates that the method is well suited to investigate the quality of the longitudinal cut and to detect possible problems and defects introduced by the longitudinal cut.

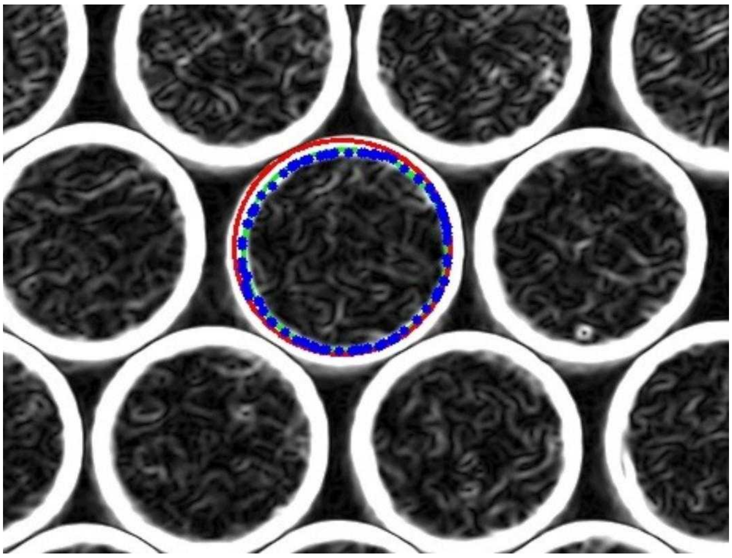

Figure 3.42: Detail from a microscope image of a fibre mat. Superimposed is the result of the circle-finding algorithm.

3.6.4 Metrology

In the subsequent module assembly fibre mats need to fit geometrically to the tools used for the assembly. Critical parameters need to be checked. To avoid time-consuming measurements templates will be built allowing a fast and simple verificaton of the geometrical parameters of the fibre mats.

3.6.5 Tests with ionizing particles

Before integrating fibre mats in detector modules a final test with an radioactive source is foreseen. A ^{90}Sr is used as the passage of a β-particle can be triggered by an external trigger (see figure 3.43). A measurement of the average photon yield for each SiPM channel is performed. Defects from the fibre mat matrix, a reduced reflectivity of the mirror or a bad quality of the optical cut results in a reduced photon yield. For that measurement a readout system based on the spiroc chip [**?**] is developed. It allows to readout a full fibre mat. The system will be used also to test detector modules (see section 4.7). Figure 3.44 gives an overview over the system.
Fibre mats have been tested with the SPIROC chip, but only one half of the active fibre is equipped with SiPMs. The profile of the photon yield from the ^{90}Sr source is shown in figure 3.45(a) for a fibre mat free from defects. The photon yield is not uniform as the particles cross the fibre mat perpendicular at the centre of the mat, while the incident angle increases to the edges. For the average photon yield per SiPM channel it is therefore expected that it decreases towards the fibre mat edge. It should be noted, that a contrary behaviour is expected if the photon yield of a cluster is plotted. For a cluster created by a

particle with large incident angle a higher photon yield is expected due to the larger path length. On the other hand the signal is distributed over a larger number of channels. Like this the average photon yield for a single SiPM channel is lower at higher incident angles. In figure 3.45(b) the response of a fibre mat is shown, that developed a crack during handling of the fibre mat. The crack is clearly visible as a drop in the average photon yield close to the fibre mat. These measurements show the capability of the method to detect problems in the fibre mat matrix. As the observable in that measurement is the absolute photon yield it is also possible to detect an overall loss of the photon yield, e.g. given by a bad quality of the mirror or the optical cut. Our study demonstrate that it is

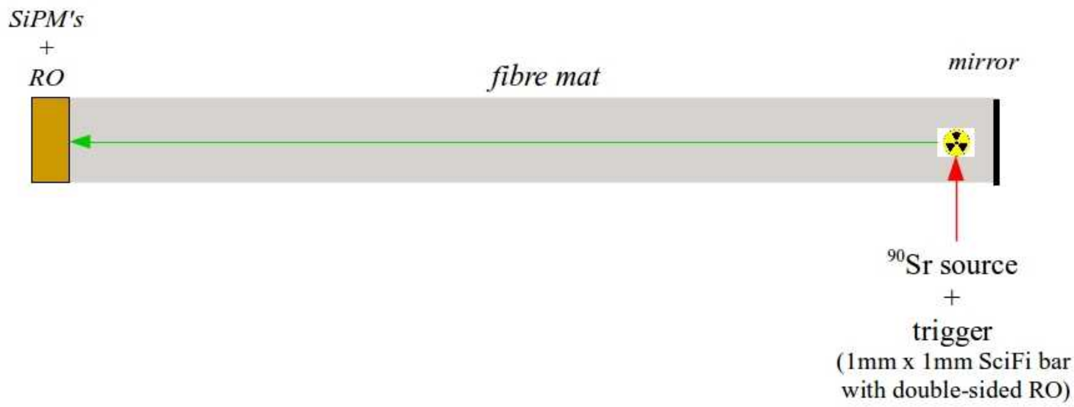

Figure 3.43: Sketch of the set-up used for the final test of fibre mats prior to their integration to a detector module.

possible to measure the photon yield across the entire fibre mat from a single location of the source. The source activity in the measurements was 3.7MBq, the measurement time is approximately 1 hour for one fibre mat.

3.7 Open issues and remaining development

The following issues are studied further:

- The online control of the fibre winding (see section 3.6) is still to be implemented as part of the winding machine and tested for reliability.
- The casting procedure requires multiple devices and needs a lot of time. A simplification of the method would also reduce the needed FTEs.
- The positioning pins stick well enough to the mat for simple careful operations. When using them too often (multiple testing steps) they tend to fall off. Increasing the pin footprint will make them more rigid. This could be included in the winding wheel or in the casting process.

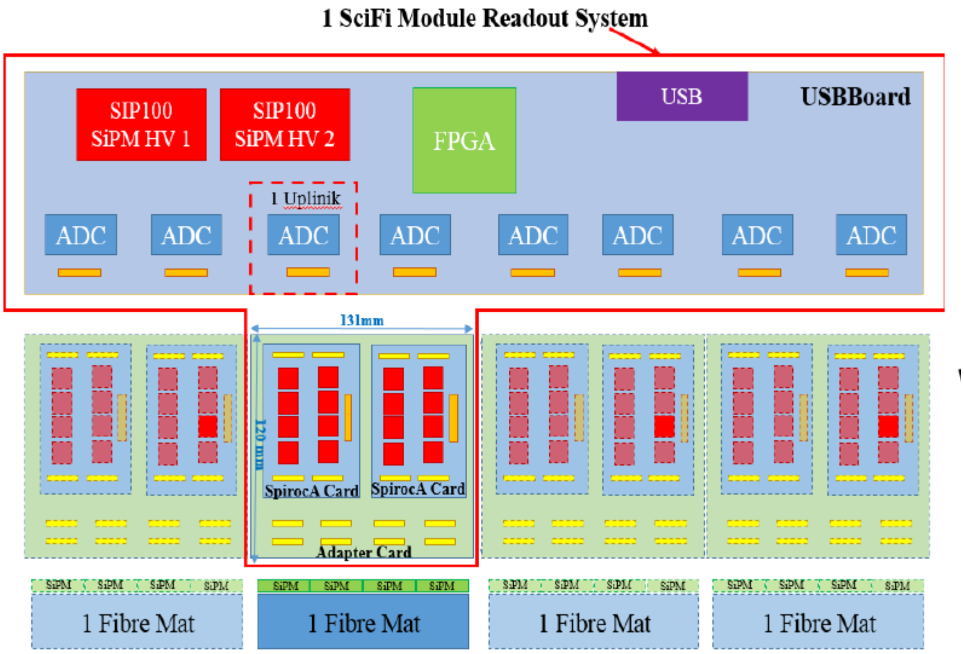

Figure 3.44: Sketch of the readout system used for the final test of fibre mats with ionizing particles.

- The mechanical stability of the mirroring requires some refinement, the connection to the fibre mats wasn't stable enough so far. In addition it was observed that the optical quality (gain in light yield) was not as expected for all fibre mats (test beam experience), probably due to attachment reasons.

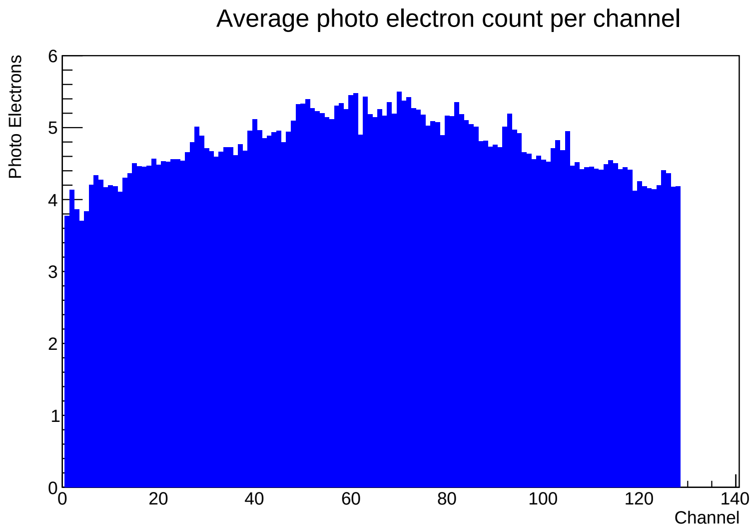

(a)

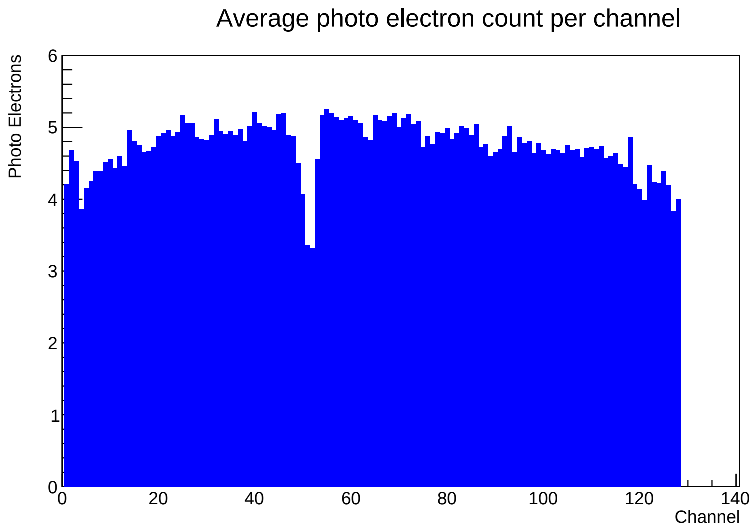

(b)

Figure 3.45: Top: Typical photon yield profile for a fibre mat. Half of the fibre mat is equipped with SiPMs. Bottom: Photon yield for a fibre mat with a crack close to channel #54.

Chapter 4

Fibre Modules

Each full SciFi Tracker detector plane is divided into 12 individual detector components, termed modules. Each plane will consist of 10 basic type modules and two modules which have been modified to fit around the beam pipe. The beam pipe modules are further discussed in detail in Section 4.1.1. A fibre module is the assembly of multiple mats into a rigid structure that can be mounted onto frames within LHCb and interfaced to the photo-detectors and the electronics. The major components are described more in detail in Section 4.2. Each module consists of:

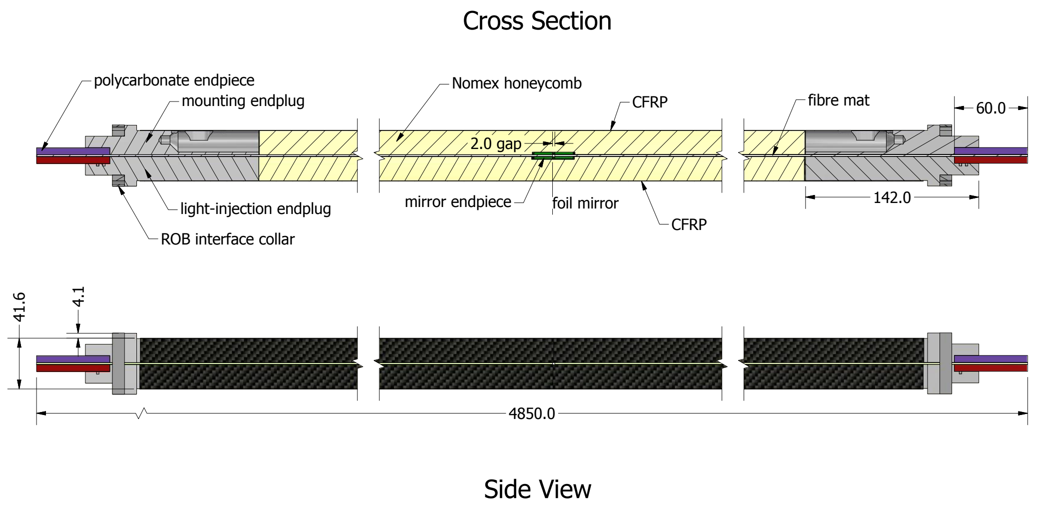

Figure 4.1: A sideview and cross-sectional cut through the centre of the module. The components are indicated in the figure.

- Four aluminium endplugs of which there are two types:
  - two endplugs contain the light injection system for calibrating the gain of the SiPMs

– two endplugs contain the mechanics for mounting and aligning the module to the C-Frame

- Eight finished fibre mats with endpieces and mirrors
- Two half-panels which are made from a honeycomb core and single carbon-fibre skin

The stiffness and stability of a module is ensured by sandwiching the finished fibre mats between the two half-panels (4.85m x 0.525m) such that the carbon fibre skins are separated by 41.5 mm. A drawing and cross section of the module is seen in Figure 4.1. The endplugs are slightly wider than the panel by a couple mm to allow for the ROB interface collar.

The precision placement and alignment of the mats with respect to one another is done by means of a full size (5m x 0.53m) template, machined from single plate of aluminium at very high precision. The template gives the precise alignment of the detector modules and the reproducibility is intrinsically guaranteed. This is done by alignment pins that are part of the fibre mat and the corresponding alignment holes and grooves in template (see figure **??**). Like this, the alignment is transferred from the pins produced during winding of the fibre mat, via the cast mat, to the final detector module and C-Frame. The mats have a centre-to-centre distance of 130.8 mm, as shown in Figure 4.2, leaving a 0.15-0.2 gap between them. This gap allows for the tolerances of the long cut on the mat and lies between the SiPM array gap such that no additional acceptance is lost.

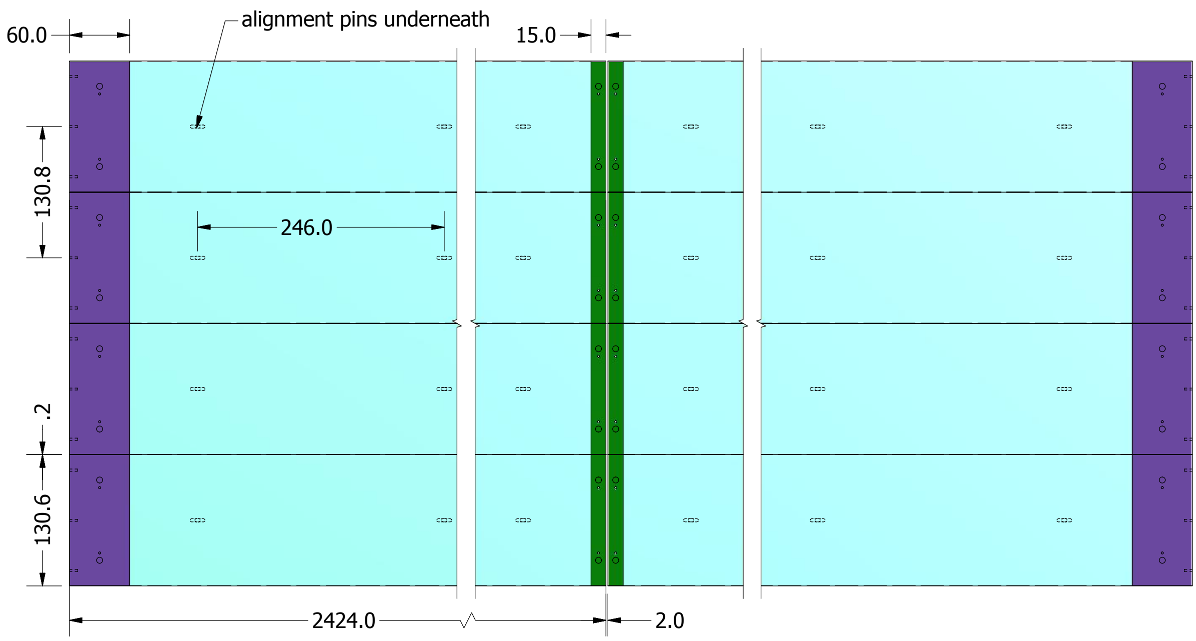

Figure 4.2: A drawing of the placement of eight fibre mats with respect to each other. The template ensures this position with better than 50 micron precision.

4.1 Module Assembly

The module assembly steps are described below and shown in the flowchart in Figure 4.3. The times for each step are shown in Table 4.1.

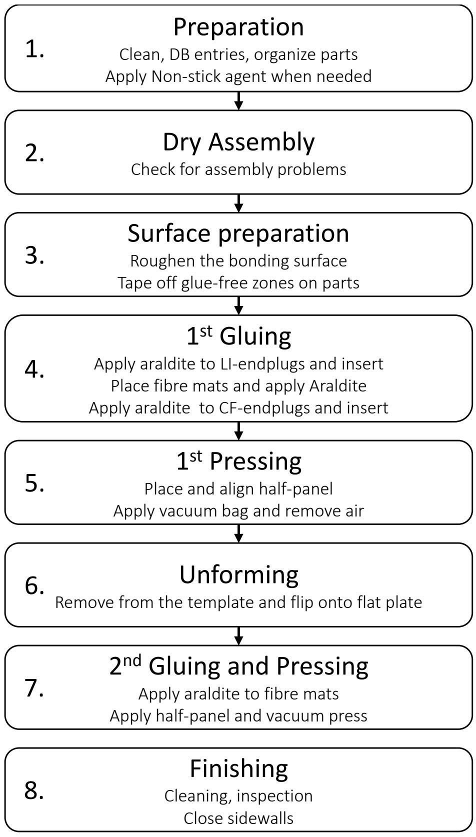

Figure 4.3: A flowchart of the steps to assemble a module. Details are explained in the text.

General Preparation Time is included for organization of components, entering material into the database and other miscellaneous details.

Template Preparation The first step of any module assembly is to clean the template, removing any residual glue and dirt. This is a 30 minute process. The non-stick agent that has been applied to the template must also be refreshed after every 3-5 assemblies. This is a 12 hour process. The fumes from this are quite aggressive and an air filter must be worn over the nose and mouth during application while the room is ventilated. A more localised ventilation system might also be constructed.

Dry Assembly The second step in the assembly is to ensure that all the components for a given module assemble correctly and that there are no surprises. geometrical anomalies, excess glue in certain regions of fibre mats or damages during transport can interfere with the assembly process. All the parts are gathered at the assembly table and put together to check everything.

Surface Preparation The ensure that the components have a good bond and will not separate later, the bonding surfaces of the aluminium endplugs and the casted fibre mats are roughened with sandpaper. The grit and dust must be cleaned off afterwards with a soft cloth and isopropyl alcohol.

In order to prevent excess runoff of the araldite glue from interfering with the readout box interface, fibre ends or sidewall finishing, certain surfaces must be covered with removable silicon tape which does not leave a residue.

1st Glueing Approximately 450g of araldite glue is applied to this surface of the fibre mats and endplugs. The glue is applied to the endplugs with a foam paint roller creating a thin layer of glue that will bond to the carbon fibre skins of the half-panel. Given the orientation of the alignment holes of the cold-bar and SiPMs in the Read-out box, it required to put the light injection endplug in the template first before the fibre mats.

The remaining glue is applied to the fibre mats and spread evenly over the surface such that every honeycomb cell wall will form a glue bond with the fibre mat. A minuscus should form at this glue bond, pulling the glue up the cell wall.

1st Pressing Now that the glue is applied, the first carbon-fibre / honeycomb half-panel is placed square on top of the fibre mats. Once this is done, the vacuum foil and frame are placed over the module and the air is removed with a vacuum pump. This is left to harden for 8 hours under vacuum and then left overnight.

Unforming The bonded half-module must be removed from the template without damaging it. This step must assure that no fibre mat pins are pull off or the rest of the panel is otherwise damaged. Once it is safely removed, it must be turned over onto a flat aluminium plate in order to bond the second half-panel. The panel after unforming is shown in Figure 4.6.

2nd Gluing & Pressing This is similar to the previous gluing and pressing steps, but the half-panel applied here must have pockets in the honeycomb made to accommodate the fibre mat pins. This is done simply with a scalpel.

Finishing The module must be cleaned of excess glue from runoff and checked for defects. Additionally, the sidewalls require closing with an adhesive foil to make the module light-tight. The fibre mat edges at the outside are still exposed to light before this stage. Any additional holes must be found and filled as well.

Figure 4.4 shows an exploded view of the assembly before the 2nd Pressing where the eight fibre mats are placed onto the alignment template along with the endplugs and the first half-panel. Figure 4.5 shows the corresponding production step while constructing the 5 m dummy module where the fibre mats were replaced with polystyrene sheets.

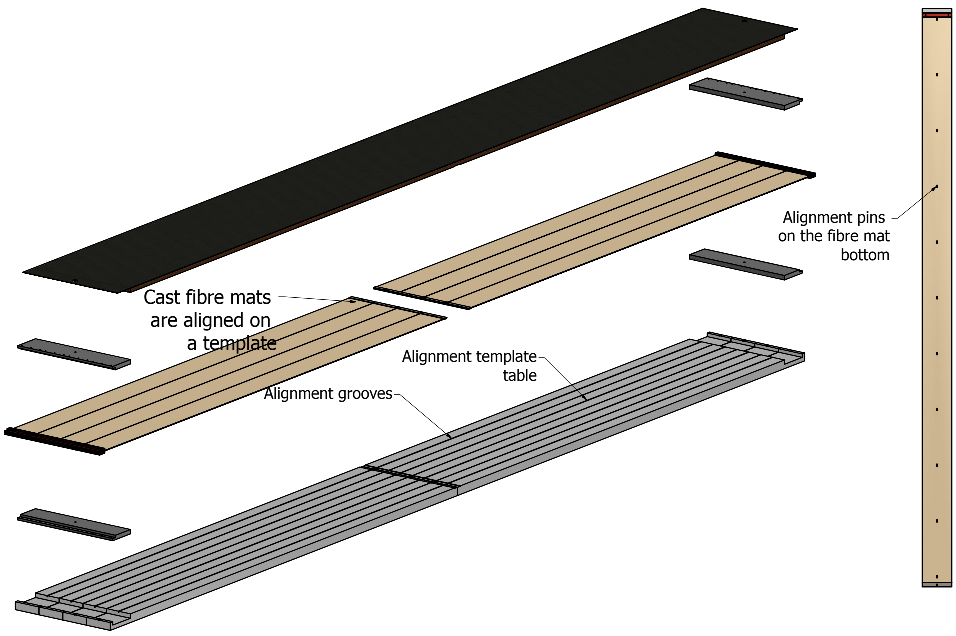

Figure 4.4: Exploded view of the first half of the module assembly.

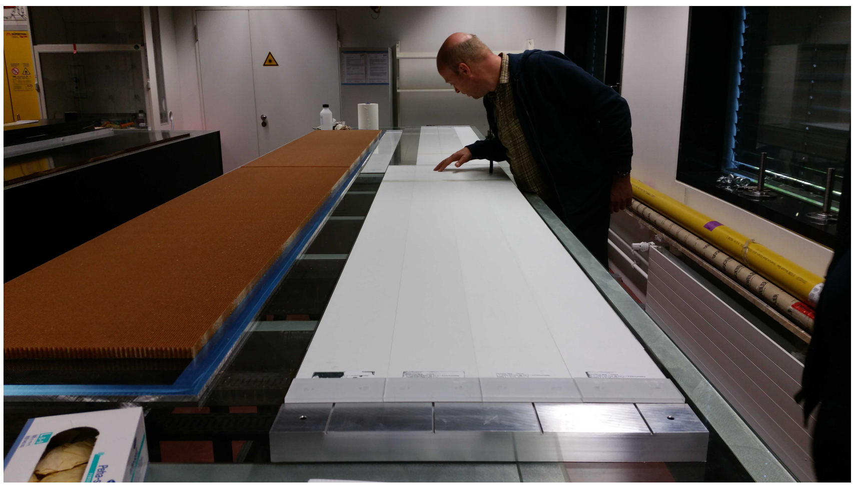

Figure 4.5: A photo of seven of eight dummy mats with endpieces which have been placed in the template. The 5 m honeycomb panel is visible on the left. The grooves in the template are visible and continue under the mats.

The temperature and relative humidity of the assembly room is monitored in 15 minute intervals and recorded on a server. The nominal values for the lab in Heidelberg are RH $= 40 \pm 5\%$ and the temperature is 20.7 ± 0.5 degrees Celsius. If the relative humidity is too high, the glues will not harden as well, and the temperature fluctuations will cause thermal expansions of the long templates.

Table 4.1: Summary of steps assembling finsihed fibre mats into full 5 m modules. The refreshing of the non-stick agent occurs every few module assemblies.

Step	Item	Time	People
0	**General Preparation**	1 hr	2
1	**Template Preparation**	30 min	2
*	(Refresh Non-stick agent)	(2 hrs)	2
2	**Dry Assembly**	1 hour	2
3	**1st Gluing**		-
	prepare glue	10min	1
	apply glue to mats	20 min	2
4	**1st Pressing**		-
	place top half-panel	10 min	2
	vacuum press and cure	10min + overnight	2
5	**Unform and flip**	30 min	3
6	**2nd Gluing**		-
	prepare glue	10 min	1
	apply glue to mats	20 min	2
7	**2nd Pressing**		-
	place top half-panel	10 min	2
	press and cure	10min+overnight	2
8	**Finishing**	1 hour	2
Total		∼5hours+2 nights	-

4.1.1 Beam-pipe module

There are two possible configurations that will affect the shape of the modules that will accommodate the beam-pipe. The diameter of the beam-pipe is on the order of 20 mm. If the half-layer of each tracking plane is symmetric, two modules on either side of the detector are also symmetric and will require the fibre mat nearest the beam-pipe on the top and bottom halves to be modified, along with the half-panels. A step-like structure equal to the width of the SiPMs could follow the circle of the beam-pipe, maximizing the detector acceptance. A symmetric layer would mean that both half-layer frames could open the same distance. However, currently in LHCb, the Outer Tracker half-layers are asymmetric, as there is infrastructure in the way that does not allow for both layers to be opened equally. A similar asymmetric structure for the SciFi modules would not allow the SiPM step cutout on both sides of the beam pipe and would require that the inner two fibre mats on the top and bottom to be modified in their length. It would be possible to have the step structure in one fibre mat, but this would increase the asymmetry in the acceptance. The symmetric and asymmetric configurations are shown in Figure 4.7. To construct these modules, slighly different endpieces for the modified mats would be required, as well as the assembly template which matches these modules. It is also possible that different panel

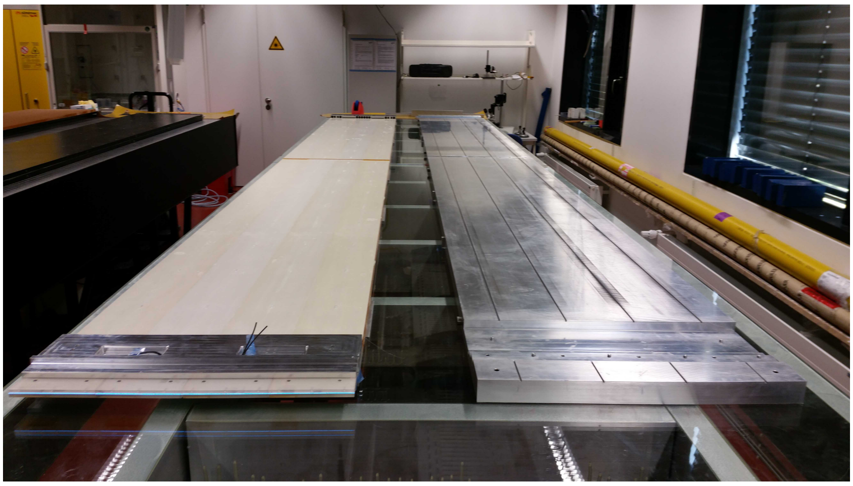

Figure 4.6: An module after unforming lies on the flat plat on the left. The assembly template with grooves can be seen on the right.

supports are needed to improve the stability of these beam-pipe modules. The design and engineering of these modules is an outstanding item.

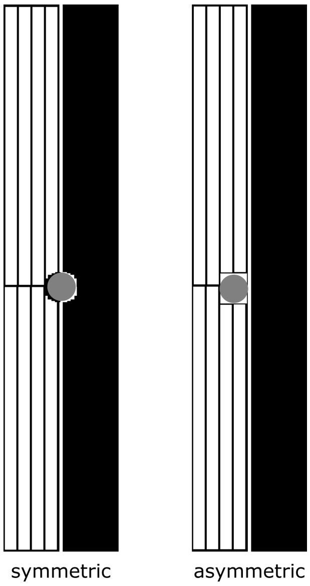

Figure 4.7: The cutout of the beam-pipe modules for a symmetric plane and an asymmetric plane. The mats nearest to the beam-pipe must be modified along with the module to accommodate the beam-pipe. The circle illustrates the beam-pipe.

4.2 Module Components

The type, number and the estimated costs of the components required to produce the modules for the SciFi tracker are shown in Table 4.2. The total cost of the module is estimated to be 20.4k Euro each, and we assumed that we will have approximately a 5% loss during production of modules due to unforeseen problems. The extra fibre mats lost here are not accounted for in any losses mentioned in the fibre mat chapter. Estimates for the endplug costs are based upon 50/Eur per hour of 5-axis CNC machine time. The costs for the half-panels are based on preliminary quotations from two separate manufacturers.

Table 4.2: The components of the SciFi detector modules. Costs are expressed in Euros. Extra module production of 5% is assumed to account for losses during module production.

Component	Number required	Extra	Total	Cost/item	Cost/module
fibre mats	1152	58	1210	1.85k	14.8k
half-panels	288	15	303	2.3k	4.6k
LI endplugs	288	15	303	250	500
M endplugs	288	15	303	250	500
assembly glue	124 kg	6 kg	130 kg	60	45
Total					20.4k

4.2.1 Endplugs

The endplugs, made from aluminium[1], serve multiple roles. The endplug provides the bonding surfaces from which the carbon fibre and fibre mats hang from. The endplugs provides part of the interface to the Readout-Box (ROB), which must be sealed against the endplugs. One type of endplug provides the mounting and alignment interface to the C-Frame. The second type of endplug contains the light injection system for injecting light into the fibre mat polycarbonate endpieces. Both types of endplugs have identical outer geometries with additional features machined into it. Material has been removed where possible to reduce the mass of the endplug. The endplug types and interfaces are discussed below.

4.2.1.1 Light injection endplugs

The SiPMs require a source of light distributed uniformly along the channels in order to determine the single photoelectron signal gain. Light from a VCSEL (vertical-cavity surface-emitting laser) is routed into the interior side of the endplug through a plastic multi-core optical fibre. A path for the fibre has been milled and bored through the body of the endplug. On the interior edge where the surface contacts the transparent endpieces

[1] EN AW-5083 (AlMg4.5Mn0.7)

of the fibre mats, the multi-core fibre is spliced with a 2 mm clear plastic optical fibre which is the length of the fibre-mat width. This clear fibre has a fine narrow cut through the cladding along its length such that injected light will leak out from the scratch and into the polycarbonate endpiece. One VCSEL output and fibre is needed for each fibre mat. A drawing of the light-injection endplug can be seen in Figure 4.8. The endpieces acts as a light mixer as well and improves the uniformity of light transmitted to the SiPM. The amplitude of the VCSEL can be tuned to compensate for the variations in the transmission, coupling, and intrinsic VCSEL output. A detailed explanation of the light injection electronics can be found in the SciFi Electronics EDR when it is available. The light injection endplug has a mass of 2.17 kg.

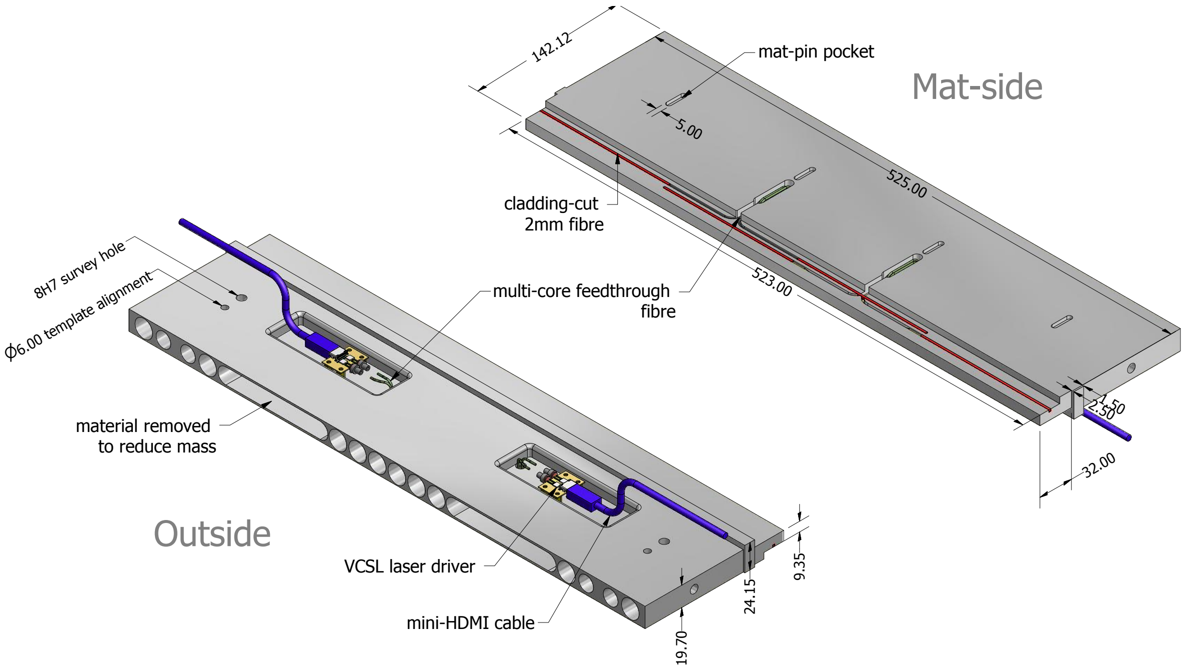

Figure 4.8: An illustrative drawing of the light injection endplug. Construction drawings can be found on EDMS.

4.2.1.2 C-frame mounting endplugs

The module must be placed with precision on the C-Frames in LHCb in such a way that additional forces are not applied to the modules which would result in a deformation of the panel. The mounting endplug allows for kinematic mounting such that all six degrees of freedom of a rigid body are constrained at once. Further discussion regarding the interface to the C-Frame is in Section 5.2. The mounting endplug has a mass of 1.82 kg.

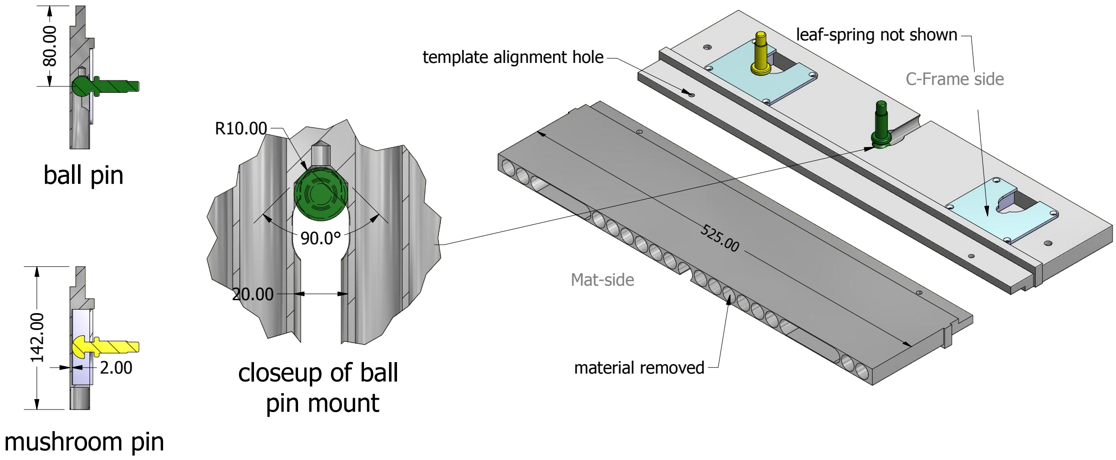

Figure 4.9: An illustrative drawing of the C-Frame mounting endplug. Construction drawings can be found on EDMS.

4.2.2 Half-Panels

Two 0.53m x 4.85m half-panels are placed on opposite sides of the fibre mats to provide the strength and stiffness. A honeycomb core is chosen for its low mass (32 kg/m^3), fire and smoke properties. Each half-panel consists of a honecomb core 19.8 mm thick with a single 0.2 mm CFRP skin bonded on one side[2]. This allows us minimize the material budget of the detector, while ensuring it is strong and stiff once both half-panels have been bonded. The panel nominally uses 100 g/m^2 of araldite glue for bonding each layer (as in the FACC prototype panels).

It is foreseen, but bot yet included, to have a thin black foil between the carbon fibre and honeycomb in order to increase the light-tightness of the half panels. It has been noted that there are a significant number of pinholes in the carbon fibre skins as a result of the slight inmperfections in the crossweave of the carbon fibre fabric.

The pins of the fibre mat require a pocket or a groove to accommodate all the pins in one half-panel. However, these need not be precise as the panel need only be made square with the rest of the module to +- 0.5 mm and the slits play no role in the alignment. The additional endpieces needed for the mirror end of the fibre mat require an accommodating space is need there as well, but again, does not to be precise.

Full 5 m panels have been supplied for the EDR prototypes by two German companies, ADCO GmbH (who also participated in the test-beam module panel production), and Crosslink GmbH. The panels were found to have a flatness better than 50 micron, along their 5 m length, as shown in Figure 8.5. The Crosslink panels, which showed a similar

[2] When being laminated only on one side, honeycomb compared to Rohacell has the advantage of staying flat.

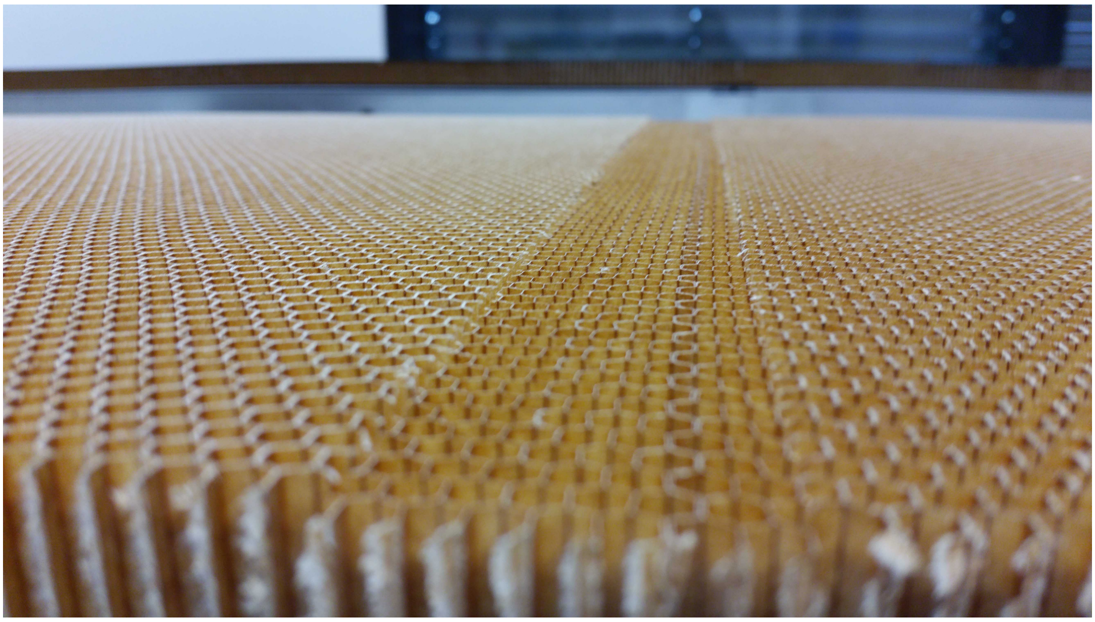

Figure 4.10: The cutout for the mirror endpiece in the honeycomb of the half-panel.

flatness, were used for the dummy module, and the ADCO panels were used in the fibre module.

The flatness of a half-panel delivered by ADCO GmbH was measured with the laser and beam camera setup. See Section 8.1 in the Appendix for details on the laser setup. The panel flatness results are presented in Figure 8.5. The minimum/maximum deviation is ±50 μm from a straight line fit with a standard deviation of 30 μm.

4.2.2.1 Carbon fibre reinforced polymer (CFRP) skin

A single carbon fibre reinforced polymer skin of 0.2 mm thickness is bonded on one side of the honeycomb. Along the length of the half-panel, the carbon fibre skin extends past the honeycomb, such that it can be bonded to the endplugs. Nominally it is 0.2 mm thick and 200g/m^2. The CFRP uses a phenolic resin and a twill weave fabric.

4.2.2.2 Honeycomb

A density of 32 kg/m^3 was chosen as a balance between low density and better compression and plate shear modulus. A lower density of 24 kg/m^3 is also available. Typical variation for core-to-core thickness is +/- 0.100 mm over 2.5m. The density of the core has a variation of ±10% as specified in the data sheet[3]. The Nomex honeycomb will meet the ‘’self extinguishing” classification of FAA Air Crash Worthiness Rules and Regulations Section 25.853. Source: Hexcell HRH-10 data sheet.

[3] It is not known if this is min/max or the standard deviation

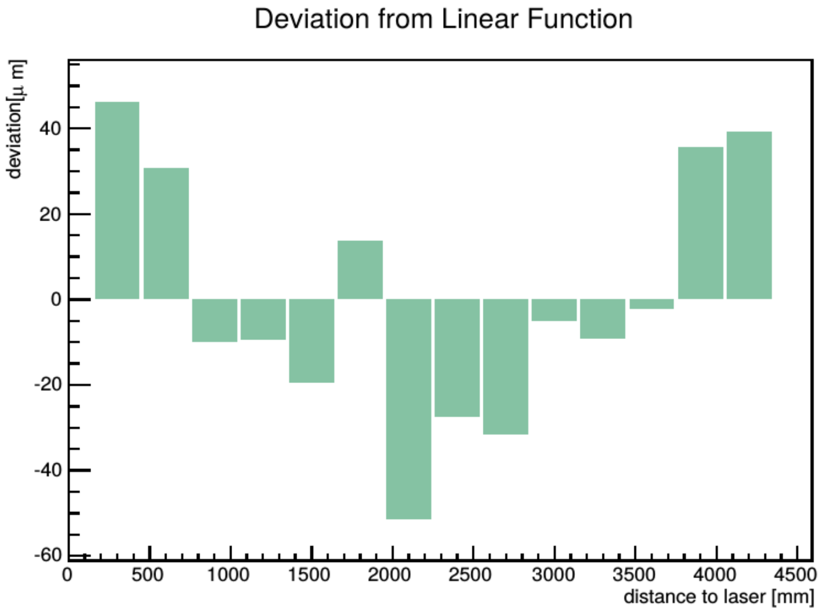

Figure 4.11: Flatness of a half-panel, produced by ADCO GmbH, as measured with the laser measurement setup.

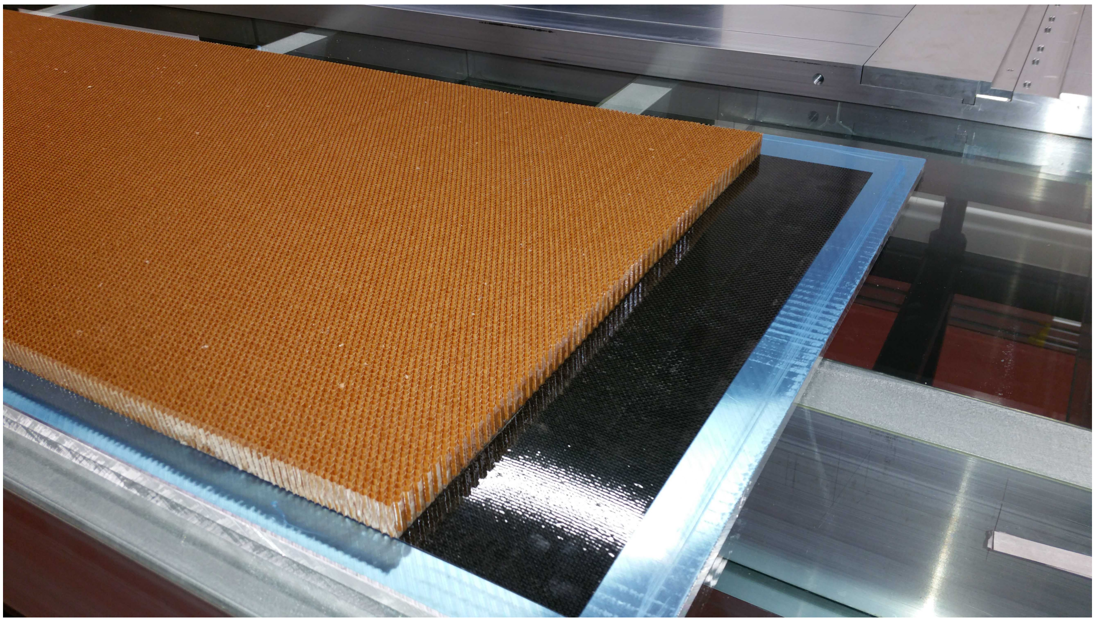

Figure 4.12: A single honeycomb half-panel. The honeycomb does not cover 95mm at each end. This excess carbon fibre will be bonded to the endplugs.

4.2.3 Material Budget

The panel material has been chosen to provide the maximum strength while having the lowest material budget. A sandwich of two 0.2 mm carbon-fibre reinforced polymer (CFRP) layers separated by two 20 mm layers of light core material (Nomex® honeycomb,)[4] on either side of the scintillating fibre mats produce a simple, light and robust tracking module. The endplugs lie outside the detector acceptance and are not considered here. Given the large volumes of material in the entire SciFi Tracker, the honeycomb core is chosen for its low density and excellent fire, smoke and toxicity (FST) properties. The other materials in the detector are also chosen to meet CERN radiation and safety requirements.

Table 4.3: The material budget for a single module. Core material budgets for 32 kg/m^3 Nomex are listed. The fibre mat is for a 6-layer thickness. The fibre mat glue contains $Ti0_2$ while the casting glue does not. The average thickness of the panel assembly glue is listed. A miniscus will form from the glue at the honeycomb cell walls increasing the thickness there and reducing it in the centre of the cell. The thickness agrees with the volume and mass used. The last column indicates whether the property has be measured (M) or estimated (E).

Material	Thickness(μm)	Layers	X_0(cm)	X/X_0 (%)	Meas./Est.
Nomex Core	20000	2	1310	0.305	M
CF skin	200	2	23.3	0.172	M
Panel assembly glue	75	4	36.1	0.083	Est.
Fibre mat	1350	1	33.2	0.407	M
Casting glue	120	2	36.1	0.066	M
Total	42290			1.02	

The prototype module material budget is shown in Table 4.3. The total radiation length for this design is X/X_0= 1.02% for one module of 6-layers of fibre or 4.1% for one tracking station of four module layers. The majority of the material budget is a result of the fibre mat, as described in the TDR. The glue used during winding contains TiO_2 while the casting glue does not, but both are a variant of Epotek 301, a low-outgassing epoxy. The IT and OT would be replaced completely by the nearly uniform SciFi Tracker which would contribute approximately 12% of a radiation length to the LHCb detector [5] .

The total mass per module is shown in Table 4.4. Measurements of test modules have indicated that the emasured mass is usually within a couple percent of expectation.

[4] Nomex is a registered trademark of E.I. du Pont de Nemours and Company (DuPont®).

[5] Total radiation lengths should be compared to the Inner and Outer Tracker material budgets. The OT has a material budget of 0.744% per layer plus 0.191% for sidewalls, which is 3.17% per station [9]. The IT contributes between 2 and 7% per station. Averaged over the T-stations, and averaged over ϕ and for $2.0 < \eta < 4.8$ for minimum bias events, a particle sees around 17.5% of a radiation length coming from the IT and OT material [10].

Table 4.4: The mass of a single module. The mass of the glue is taken from the weight used in production. The light injection endplugs eachs weigh 2.17 kg and the the mounting endplugs each weigh 1.82 kg. Uncertainties in the mass are less than a few percent.

Material	ρ (kg/m^3)	Mass (kg)	% of Total
Nomex Core	32	3.02	15.1
CF skin	1540	1.53	7.6
Panel assembly glue	1160	0.86	4.3
Fibre mat	1180	4.10	20.4
Casting glue	1200	0.74	3.7
Polycarbonate pieces	1200	1.8	8.9
Aluminium Endplugs	2700	8.0	39.9
Total		20	100

4.2.4 Tooling

The overall length of the modules creates some difficulty in production, as machines and other readily available tools of this size are not standard or are very expensive. The following tools where developed to handle modules of 5 m in size.

4.2.4.1 Tables

To construct a flat working surface of 6 m in length, two separate 3 m glass surface tables were constructed, as shown in the drawing in Figure 4.13. Each consists of a steel frame with three adjustable posts on the top which hold the glass table top. The glass top is made from two sheets of 1 cm thick glass separated by and aluminium profile structure. The glass table top is assembled separately on a flat granite surface by placing the first glass sheet on the granite surface, then adding the aluminium profiles. The second glass sheet ensures that any bi-metal effects are reduced by making the structure symmetric. After some initial adjusting of the table mounting points the measured flatness of the table is shown in Figure 4.14. The data points are collected along the length of the aluminium template on the left and right side. The min/max deviation from the best fit horizontal plane is +157/-87 micron with a standard deviation of 52 micron. The flatness of the table will be improved in further iterations.

4.2.4.2 Template

The template is machined from a single 6 m plate of an aluminium alloy[6]. Pockets for the endplugs are machined into the template along with the grooves for fibre mat pin and reference holes for surveying. The template can be seen in Figure 4.6.

[6]EN AW-5083 (AlMg4.5Mn0.7)

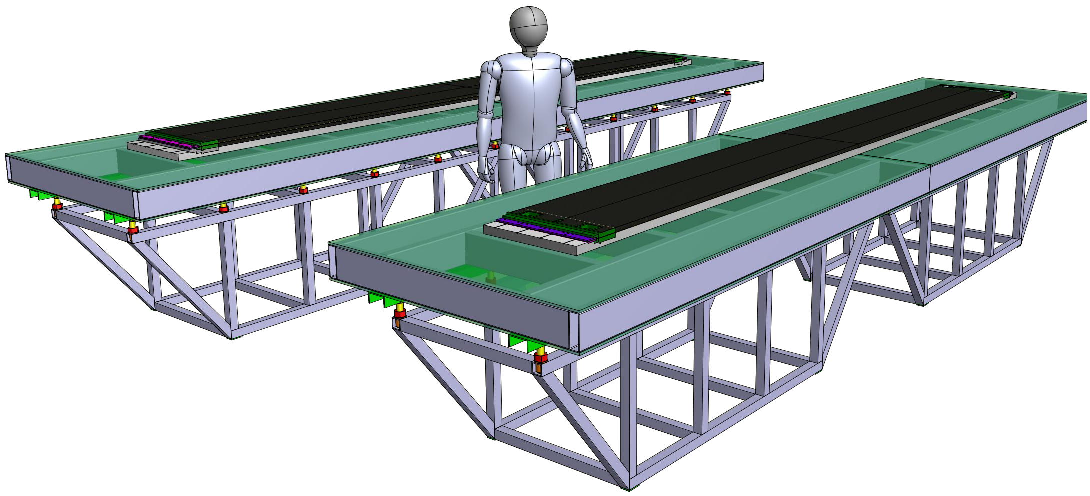

Figure 4.13: An illustration of the two glass tables placed end-to-end to make a 6 m table. A second set of tables is shown behind the figure. The template and assembled half-panel is shown on top of the two tables.

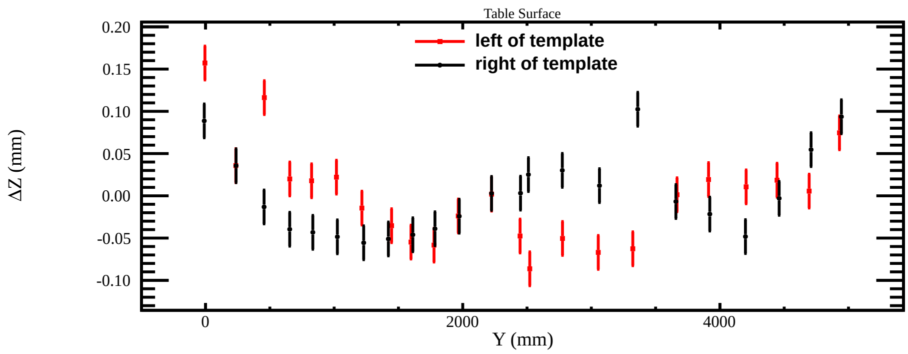

Figure 4.14: The flatness of the glass table as measured by CERN EN/SU/EM with the laser theodelite.

Surface Flatness The template was surveyed with the laser setup shown in Sectionappendix:lasersetup, as well as by the CERN EN/SU/Experiment Metrology (EM) Group [7] using a laser theodelite measurement. The results are shown in Figures 8.4 and 4.16. Both results show similar structures, with similar deviations from flatness. The laser/beam-camera measurement shows a min-max deviation of ± 45 μm while the CERN theodelite measurements shows +95/-52 μm. However, the CERN

[7] Metrologist: Pascal Sainvitu. Unit Leader: Jean-Christophe Gayde.

measurement covers a larger area at either end of the module where the largest deviations occur. The RMS of the residual from a best fit flat plane is 31 μm for the CERN survey measurement.

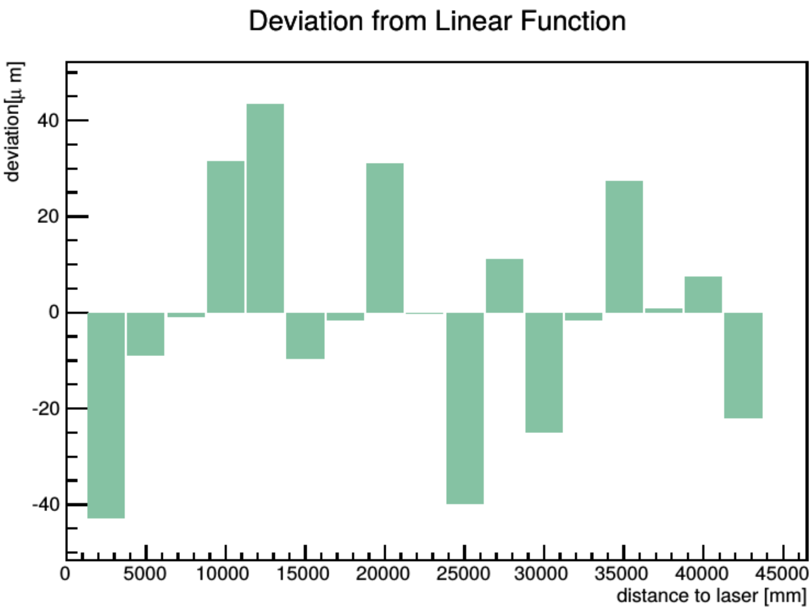

Figure 4.15: The flatness of the aluminium template as measured with the laser and beam camera.

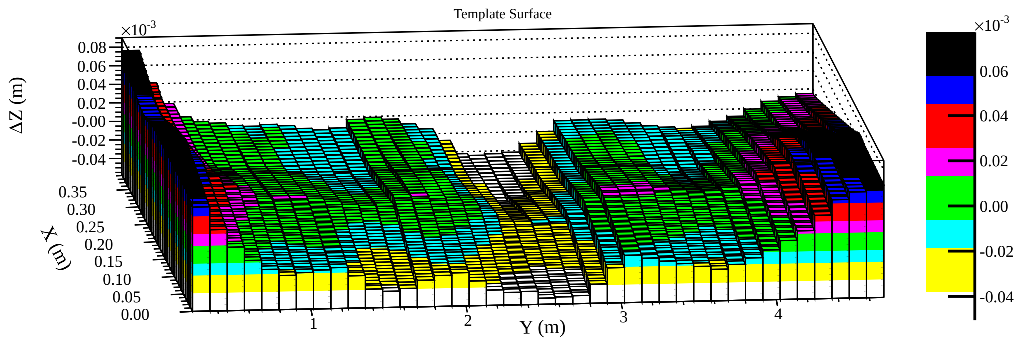

Figure 4.16: The flatness of the aluminium template as measured by CERN EN/SU/EM.

Groove Linearity As it is important that the grooves which receive the mat alignment pins are straight with respect to one another, the linearity of these groves was also measured by the CERN EM group. The difference in the measured position from its specification are shown in Figure 4.18, where a straight line fit through the first groove defines the Y-axis and the template surface defines the horizontal. Aside from one outlier in Groove 1, the min/max deviation is +/-35 μm with RMS values approximately 15 micron for each groove. The uncertainty in each data point is given as 20 μm. Within error, no overall shape is visible.

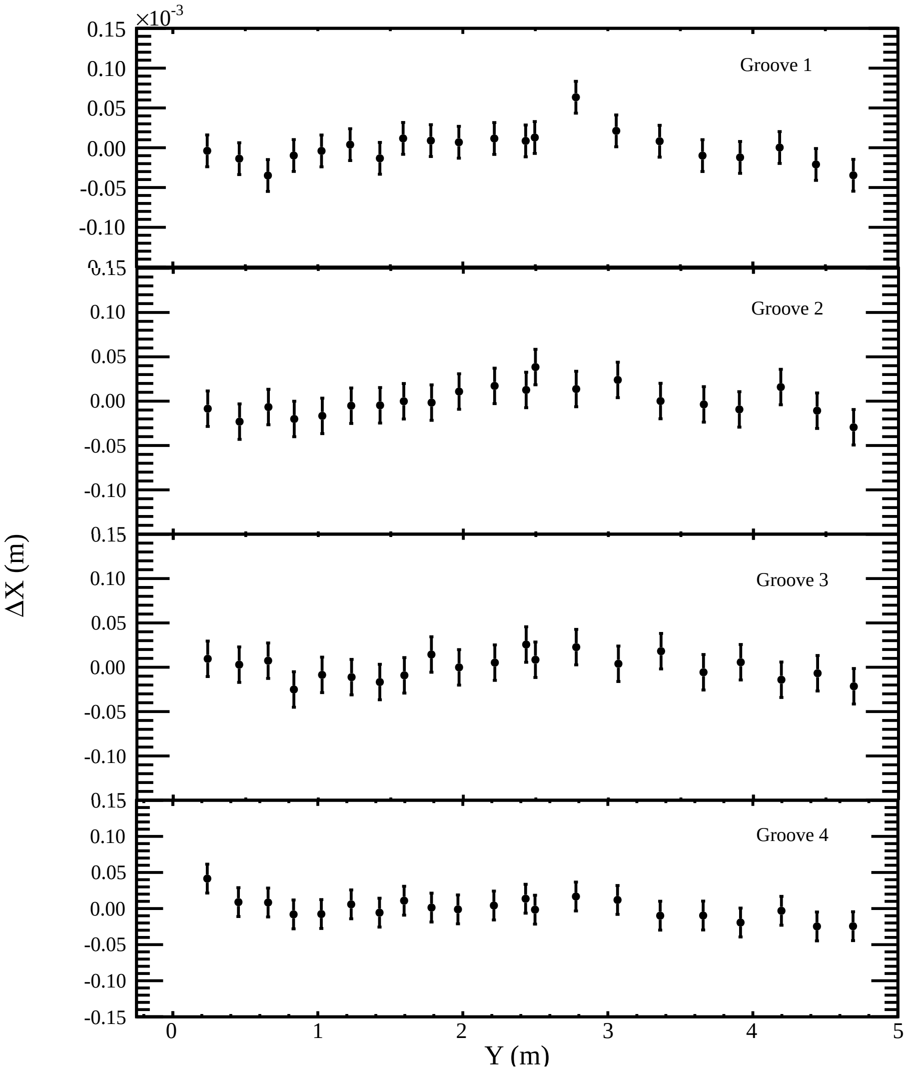

Figure 4.17: The linearity of the four template grooves as measured by CERN EN/SU/EM.

4.2.4.3 Vacuum pressing

The pressure applied to the panel during bonding is done via vacuum pressing. An aluminium profile box frame with a sealed rubber ring underneath holds a loose reinforced plastic foil on top. Once the half-panels have had the glue applied, the vacuum foil box is placed over the template and panel and vacuum is applied via a vacuum pump. As the seal is not perfect, a large volume of air is continuously removed. The overall pressure can

1528 be coarsely adjusted by the opening of a valve. It is unknown what the exact pressure
1529 applied to the panel is, currently.

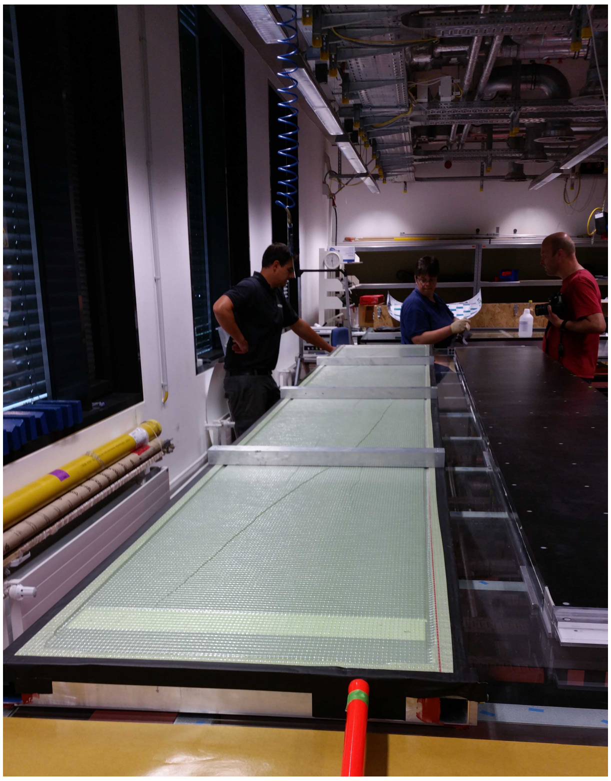

Figure 4.18: The vacuum press assembly overtop of the panel during the first pressing step.

Table 4.5: Summary of the estimated costs for tooling at two module assembly centres.

Item	Quantity	Cost/Item (EUR)	Cost (EUR)
module alignment template	2	6k	12k
flat assembly tables	8	1k	8k
Quality Assurance Mechanics	2	1k	2k
Quality Assurance Electronics	32	??	??
Total (EUR)			22k + ??

1530 ## 4.3 Finite element calculations

1531 A series of finite element analyses of the final module has been carried out to investigate
1532 the mechanical stability properties and the behaviour under various thermal loads. Tow

different panel thicknesses have been studied: The standard 4 cm thick panel as discussed in this report, and, optional, a 5 cm thick panel. The mechanical stiffness of the panels is of great importance for the reconstruction of the particle trajectories through the panel stack. The thermal load cases chosen are such that might occur during the assembly of the modules. In addition to the mechanical loads modal analyses have been done, which also give indication for the stiffness of the panels. A more detailed analysis can be found in LHCb-PUB-2015-007 [11].

The analyses have begun with the determination of the material properties. To this end in a first step the properties of the fibre structures – fibre mat and carbon fibre face sheets – have been evaluated and then laminates of the fibre layers and the glue layers, that are used to bond the individual layers, were put together. The properties of the Nomex honeycomb were determined by modelling a unit cell of the honeycomb and applying unit displacement in the x, y, z directions. The reaction forces are then used to calculate the mechanical constants.

Mechanical properties. The mechanical stability is studied with several kinds of loads by looking at the magnitude of the displacements under

- a line load of 10 N across the centre of the panel,
- own weight,
- air draft of Beaufort 2,
- lifting the panel at one corner only,

and with a modal analysis (see figure 4.19).

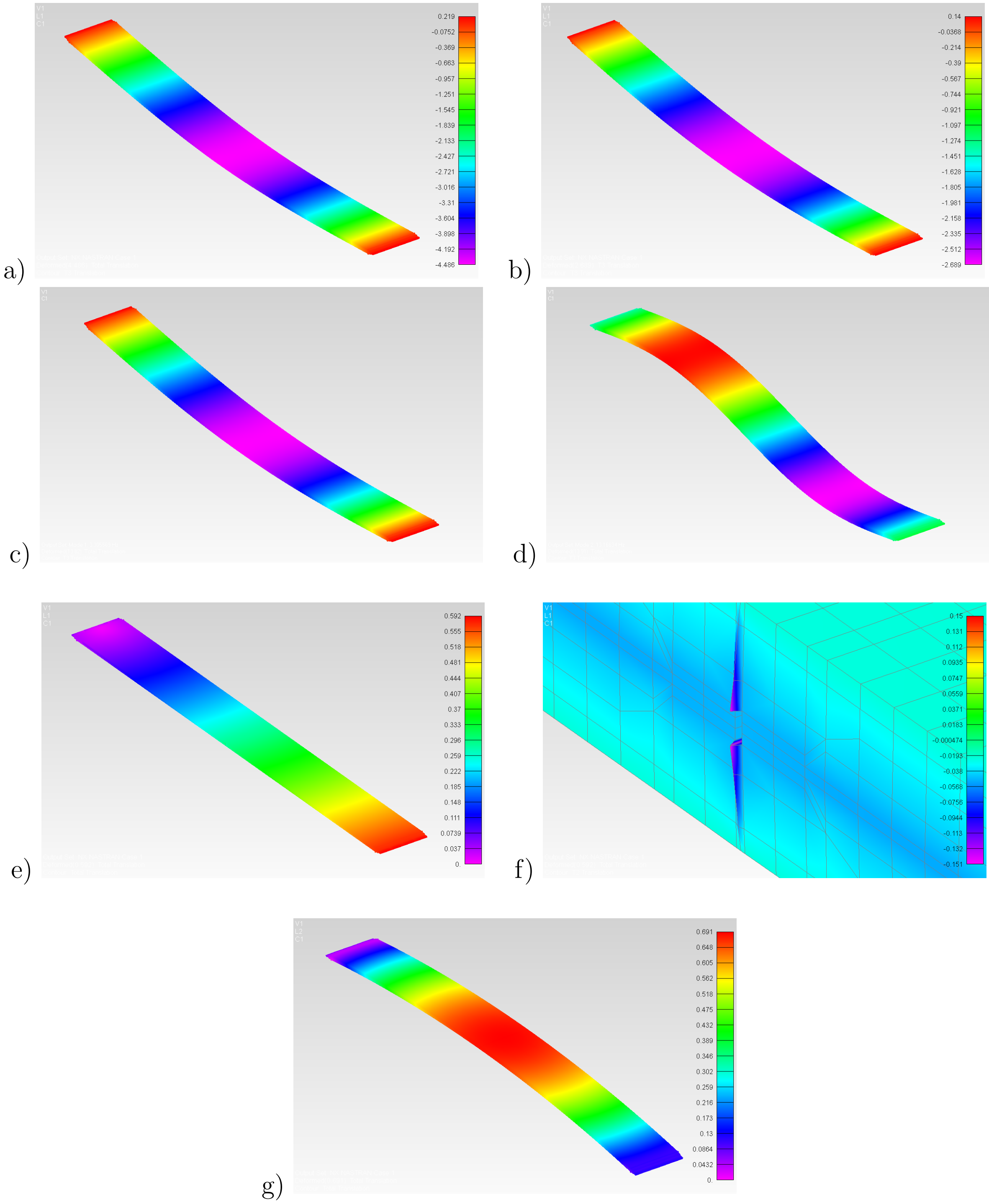

Figure 4.19: Numbers in brackets are for 5cm panel option. a) Deformation of the panel through a line load of 10 N. Max deflection 4.49 mm (3.09 mm). b)Deformation of the panel through air draft (Beaufort 2). Max deflection 2.7 mm (1.86 mm). c) First eigenfrequency 3.3 Hz (3.86 Hz). d) Second eigenfrequency 13.2 Hz (15.34 Hz). e) Deformation of the panel through a temperature difference of +5 C. f) Detail of the deformation in the centre gap of the panel through a temperature difference of +5 C. g) Deflection of the panel through a temperature difference of 2 C between the two skins

Thermo-mechanical properties. During the assembly of the panels various thermal influences might interfere with a stress-free structure. Frozen internal stresses lead to warped and twisted panels, particularly in the case where they are mounted only at the ends. Investigated load cases are (for the 4 cm panel version only):

- all nodes 5 C warmer than during assembly,
- SciFi-mat is 2 C warmer than the outer skins,
- one Skin 2 C warmer than the opposite one,
- lower half of the panel 5 C warmer than during the production.

The last case was studied to determine whether the vacuum table, that is used to assemble the module, keeps the module straight on its surface.

None of the investigated load cases shows any critical deformations or stresses. All strains are in the order of tenths of a millimetre and the stresses remain below 12 MPa. The deformations through the applied forces (own weight, air draught, torsion) are tolerable although a better rigidity would be desirable. As expected the 50 mm panel option is preferable as the stiffness is concerned. It has to be balanced against the radiation length difference of nearly 0.1

4.4 Survey strategy and integration of targets

After discussion with the Experiment Metrology group at CERN, it is foreseen to integrate the necessary precision holes and targets into the modules during production in order to simplify the procedure of surveying the modules and frames in the LHCb pit. Given the layout of the detector, the only way to see the modules while they are in the closed position is from the side. This necessitates the need for the use of theodolite laser measurements and the necessary reflectors. Photogrammetry requires visual access from multiple angles, which would not be available when the frames are closed. Currently the modules have several 8H7 holes in the endplugs in order to accommodate the holder for these cube corner reflectors. It is also foreseen to add an additional hole in the centre of the half-panel face in order to hold one of these reflectors. It would be possible to measure the deflections and distortions of certain modules while they are closed in magnet-on and off scenarios.

4.4.1 Survey results of the 5 m dummy module

The CERN SU/EM group was invited to Heidelberg to measure the flatness of the overall module in different conditions. The dummy module, produced as the first mechanical prototype, contained four precision holes in each corner of the module in the endplug, for precision reference. Photogrammetry was determined as the best way to determine the overall shape of the module given the sensitivity of the module when it is hanging vertical. The surface of the module was covered in rows of retro-reflective stickers and coded markers. For each module measurement, 50-100 images were made with a calibrated digital SLR camera. Software then reconstructs the position of the camera and the retro-reflective stickers to a precision of 20 micron in X, Y and Z. When mounted in the vertical, the ball pin mount was used such that no additional forces were applied to the module aside from internal stresses. A thick foam was used in place of a flat spring to constrain the endplug against the mushroom pin.

The following configurations of the module were measured with select results shown below:

- Day 1: Flat on the table.
- Day 1: Hanging off-vertical on the kinematic mount (2 ball pins and 1 mushroom pin). The wall that it was hanging from was discovered to be 20 mm off-vertical over 5 m.
- Day 2: Repeat off-vertical measurement
- Day 2: Corrected vertical measurement
- Day 2: Apply 0.5 kg of force on lower right hand corner
- Day 2: Apply 1.0 kg of force on lower right hand corner
- Day 2: Apply 2.0 kg of force on lower right hand corner

- Day 2: Remeasure on the flat table

The results of the measurements of the module as it was hanging in the corrected vertical position on the frame is shown in Figure 4.20. The min/max deviation is from a fitted reference plane +98/-2473 micron with a standard deviation of 893 microns. The negative curvature indicates the curvature in the the direction of the wall. While the curvature is disappointing, it was not unexpected. Similar curvature was seen in the Outer Tracker modules, up to 7 mm. If all modules are similar, an effort will have to be made to align neighbouring modules in the centre against a common reference, such as a carbon fibre honeycomb panel 1 m from the top and bottom of the frames. Further investigations will have to be made into the cause of the internal stresses as well as any additional contributing forces, such as the off centre mounting.

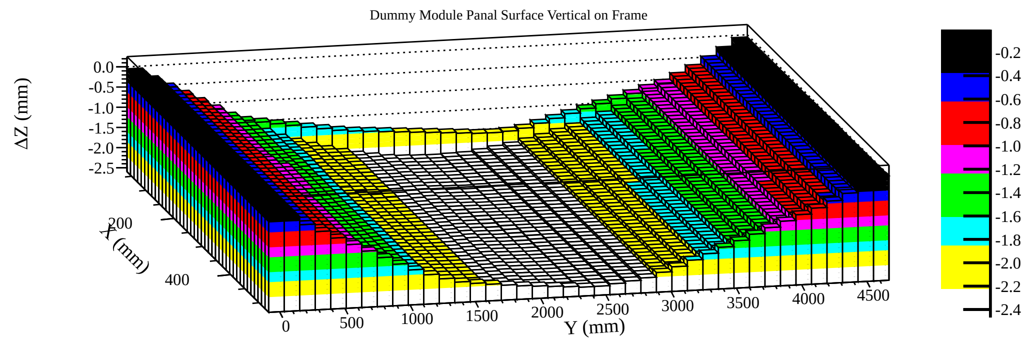

Figure 4.20: The results of the photogrammetric measurements of the dummy module while hanging in the corrected vertical position on the demonstration frame, as measured by CERN EN/SU/EM.

The difference from the nominal vertical position on the frame where a 10 N force was applied in the direction away from the wall, using a pulley and a mass, is shown in Figure 4.21 . The min/max deviation from the nominal vertical position is +330/-700 micron with a standard deviation of 224 microns. The panel appears to twist along the central axis, which was expected, as it is constrained in this axis. This measurement is meant to mimic asymmetric forces applied on the ends such as the ROB cabling and other infrastructure. Movement in the top endplug was not unexpected as the stiff spring required was instead replaced with a soft foam sponge which deformed under some minimal load. If torsional forces on the module are too great in the full SciFi detector, a second mushroom pin can be used at the top and bottom, instead of the spring, to over-constrain the module on the frame.

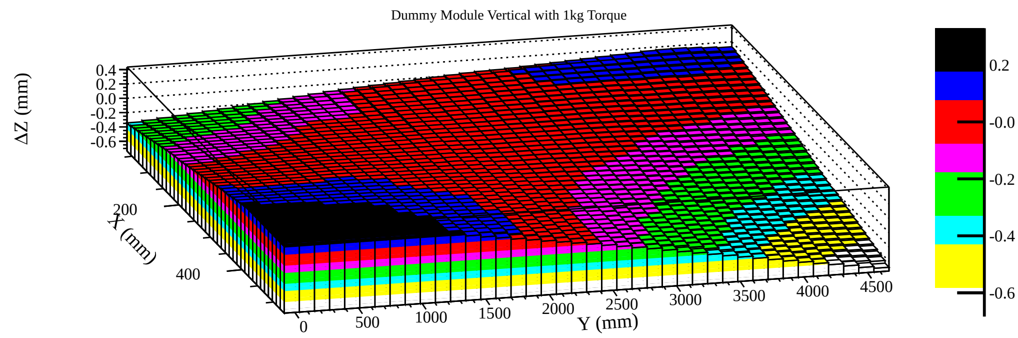

Figure 4.21: The difference of the photogrammetric measurements of the dummy module hanging vertically and vertically with 10 N of force applied on the bottom right corner, as measured by CERN EN/SU/EM.

4.5 Production plan and logistics

4.5.1 Sites

It is forseen to have two assembly sites where the work is split between Heidelberg and NIKHEF. The fibre mats will be shipped from the fibre mat production centres to the Module Assembly centres for the final steps of module production, including the long cuts of the mats, panel bonding and module finishing.

4.5.2 Schedule for Production

As the modules each require eight fibre mats and five production sites, at full production speed, will produce 20 mats per week, it seems likely that a production rate of two to three modules per week will be achieved. A buffer of mats produced by the slightly lower consumption rate of mats compared to production will allow for interruptions in mat winding to not affect the module production. Given the ramp up of mat production starting with the PRR in February 2016 and the five winding centres each being brought online shortly thereafter, the PRR for the first Module Assembly centre will likely occur in May of 2016 with the production targeted to be completed by July 2017. See Chapter 7 for general planning schedules.

4.6 Shipping and Logistics

Given the large size of these objects, their total cost and the non-reparable nature of the modules, large crates that can fit multiple objects will have to be produced that will protect multiple modules from punctures and other damage as well as excessive humidity and water during transport and storage. The reduce risk of loss, the number of modules in each crate should likely be smaller than or equal to five. With an estimated value of

20k EUR each, this is 100k EUR or less of modules in each crate. Thought should also be given to insuring these during transport.

It should be foreseen that the modules are also shipped and sealed individually in plastic bags.

Shipping to the final frame integration site (likely CERN) can then begin early in 2017 with the modules already produced until completion.

4.7 Quality Assurance

Items to be checked during quality assurance:

Light Tightness The scintillating fibre must be protected from external light. In the production process, a foil has been integrated into the half-panel and the sidewalls are also closed with a separate external foil. This must be checked after production and shipping by looking for signals with a full array of randomly triggered 16 SiPMs. Each production site is equipped with this electronics setup containing two USB boards and 16 SPIROC front-end boards. Two such systems would be required to read-out each end simultaneously.

Geometry The module dimensions should meet specification within defined tolerances. No excess glue should be on important interface surfaces or extend past the defined boundaries.

Light Yield A light yield measurement using a Sr-90 source with the trigger below the module can be used (similarly to the bare fibre mat) to ensure that the fibre mats have not been damaged during the module assembly reducing the light yield. This would likley only need to be done at one location for each mat near the mirror.

4.8 Safety considerations

Refer to document regarding the use of plastic and other non-metallic materials at CERN with respect to fire safety and radiation resistance IS41 https://edms.cern.ch/document/335806/1.02 .

The polystyrene based scintillating fibre mats do not meet the IS41 specifications for fire safety on their own. However, they have been sandwich between Nomex honeycomb cores, which are self-extinguishing. The carbon fibre skins are also embedded in a phenolic resin which meets fire safety standards. The sidewall enclosure foils will also need to meet fire safety specification in order to completely enclose the module.

A burn test of a test module or dummy samples is foreseen in the near future, but is an outstanding item.

4.9 Open issues and remaining developments

Beam Pipe Modules The asymmetry of the detector layers has not been determined yet. The construction and the stability of these modules has also not been determined.

Light Tightness A module which contains all the foreseen light tightness features has not been completed. It is planned to include a thin black foil in the half-panels, and finish the sides with an additional more robust black foil to protect against punctures and wear.

Safety The safety measures required for installation of this module are not completely understood. A burn test has not been conducted yet.

Chapter 5

Interfaces

The module must interface with two different systems. First, the ROB which contains the silicon photomultipliers SiPMs, the cooling and readout systems must be placed onto the module with some precision at either end, with and against gravity. Inside the ROB, the SiPMs are mounted on a cold bar, which must be aligned with respect to the fibre mats and sit flat against the face of the mats and endpieces.

The second system that the module must interface with is the C-Frame. The multiple modules must be stable and flat with respect to each other on each frame and must allow for tolerances and distortions in the frames. The C-Frame design is planned to be similar to that of the Outer Tracker in LHCb.

5.1 The Module and ROB

The connection between the ROB and the module, as well as the cold bar and the endpieces, must allow for the tolerances of the production of the modules as well as the ROB, the positioning of the endpieces within the module, the thermal expansions (contractions) of all the components at -40 degrees Celcius, the positioning of the cold bar, etc. It is foreseen that a cold-box should be able to be removed in the LHCb cavern and the box self-aligns the SiPMs to the fibre mats.

5.1.1 ROB

The ROB is mounted onto the module using a machined aluminium collar which has a single continuous surface around the module end. A drawing indicated the interfaces is shown in Figure 5.1. The interface collar is bonded to the top surface of the two endplugs. This single surface allows for sealing the ROB against light and moisture penetration, as the two aluminium endplugs otherwise have a gap between them where the fibre mat passes through. The tolerances in stacking the multiple layers of the module do not allow for this gap to be bridged by the endplugs alone. The ROB is constrained to the collar by 14 threaded bolts.

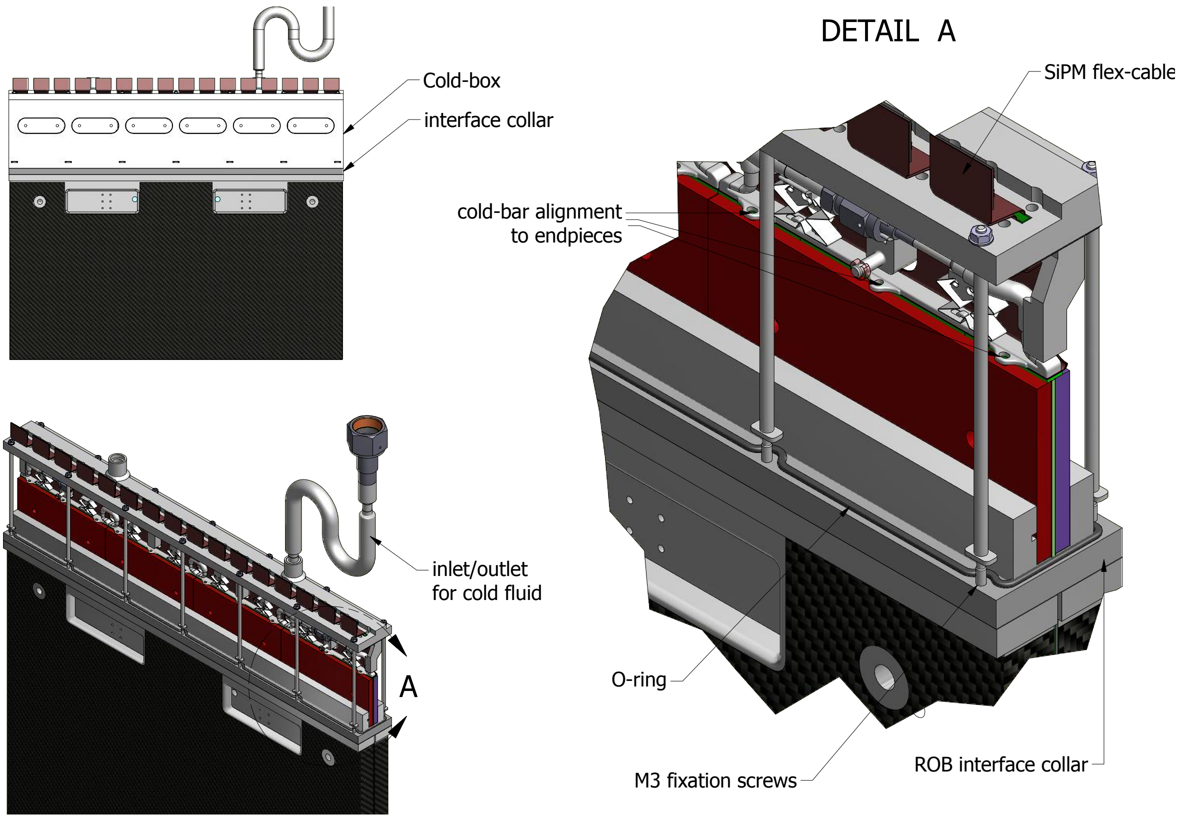

Figure 5.1: The Read-out Box (ROB) attached to the module (only the cold part of the box is shown). The interface collar is shown between the ROB and module. The alignment holes aligning the cold-bar to the endpieces is also indicated.

5.1.2 SiPMs, Fibre Mats and and Endpieces

The second important interface system is where the connection between the endpiece and the SiPM. The SiPMs are bonded and aligned to the cooling bars in the lab. The cooling bars contain alignment holes which match to the pins inserted into the endpieces of the fibre mats which are exposed at either end of the module. The central long-hole constrains the movement in the X coordinate. The outer two long-holes constrain the movement in Z. A spring behind the cold bar holds SiPM in Y. This is also visible in Figure 5.1 on the right-side cutout. The relative alignment of the arrays and the overlapping gaps between mats and modules is visible in Figure5.2. The 0.150 mm(0.2mm) gap between fibre mats lies between the 0.460 mm gap between the active silicon of two neighbouring SiPM packages. The gap between every SiPM package is currently designed to be 0.110 mm. The tolerances between arrays and the package dimension (32.59 mm) dictates that groups of four arrays are 130.8 mm as a unit, which coincides with the mat width of 130.65 and its spacing of 0.150 mm.

KETEK arrays Special consideration for the endpiece design and production must

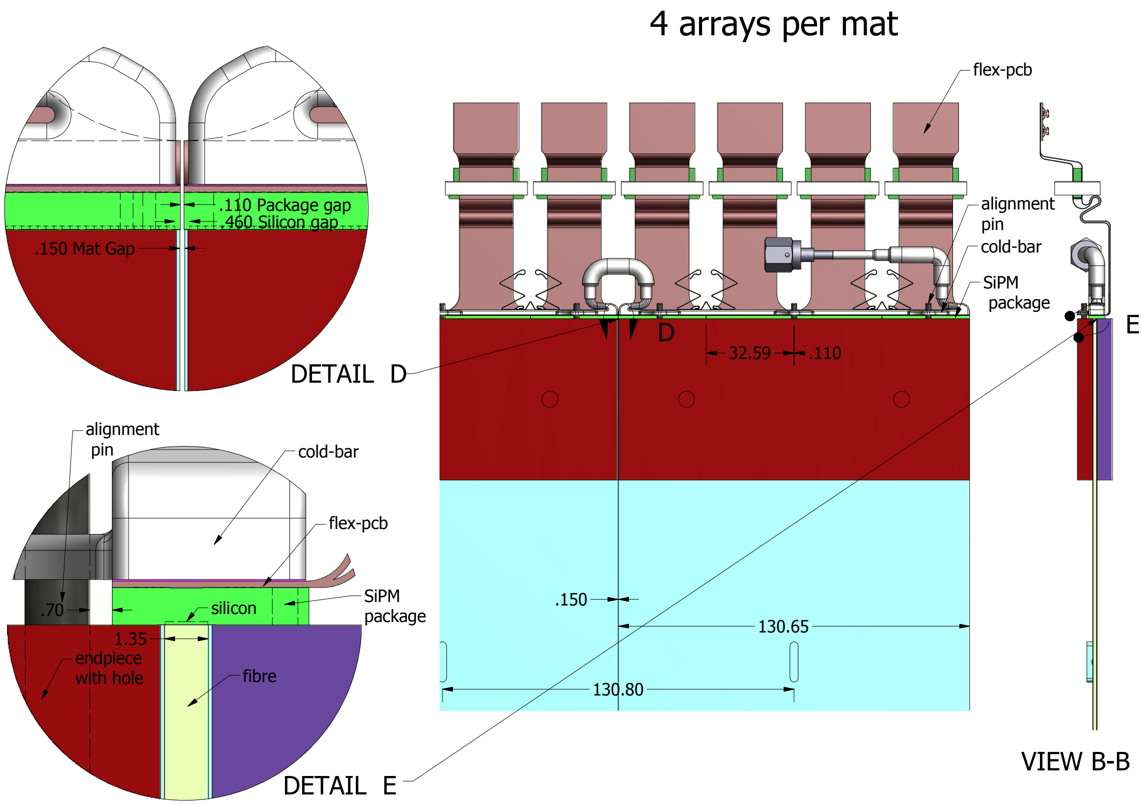

Figure 5.2: The interface with the cold-bar and SiPM arrays. Four SiPM arrays match each fibre mat. The section of the cold-bar is aligned to each fibre mat by three alignment pins which match three long-holes. The gaps between arrays and mats are shown in detail.

be made if KETEK SiPM arrays are used which have the glob top over the bond wires at a height larger than the face of the glass covering the silicon. Hamamatsu arrays have a flat surface across the face of the package and require only the diamond milling across the end of the fibre mat, as shown in Figure 5.3. Using the KETEK arrays would require a second milling of the endpiece and fibre mat in order to accomodate the bond wires. The interface for the KETEK array is shown in Figure 5.4.

Additionally, the size of the SiPM package has become larger in design since the EDR design of the endpiece was finalised and would require modifications for production in order to accommodate the alignment pins.

Further details regarding the SiPMs can be found in the SiPM and Electronics EDR when it becomes available at the beginning of 2016.

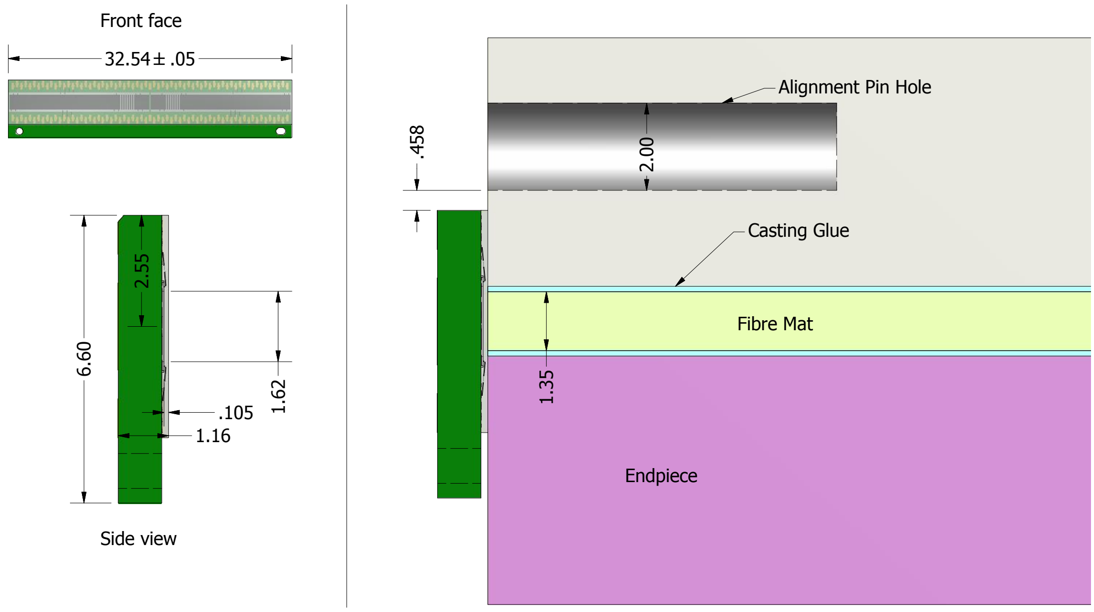

Figure 5.3: The interface with the Hamamatsu SiPM array. This interface is much simpler as the face of the endpiece must only be finished flat. However, the larger package has also reduced the space between it and the alignment pin.

5.2 The Module and the C-Frames

The mounting endplug inserted into the module, shown previously in Figure 4.9 contains several features in order to mount this detector module on a frame. Within each mouningt endplug, in the center, is a 20 mm diameter cylindrical hole, which ends in a cone. One either side of this cylinder is a space milled out forming a flat plate. One the top part of the C-Frame, for each module, there are one adjustable pin with a sphere on the end (ball pin), and one pin with a mushroom-like head (mushroom pin). The bottom part of the frame holds one ball pin. The placement of the two spheres will define the vertical axis of the module. As shown in Figure 5.5, the contact line of the cone inside the top mounting endplug sits on the top ball pin and constrains that point in X, Y and Z but is still able to freely rotate in the three angles. The mushroom pin next to it at the top constrains only rotations about Y. A flat spring on the opposite side must provide a force to press the module against this pin. The ball pin at the bottom of the C-Frame rests inside the cylinder of the endplug, allowing it to move in the vertical and rotate in Y, but constrains rotations of the module about X and Z. All constraints are indicated by the red arrows.

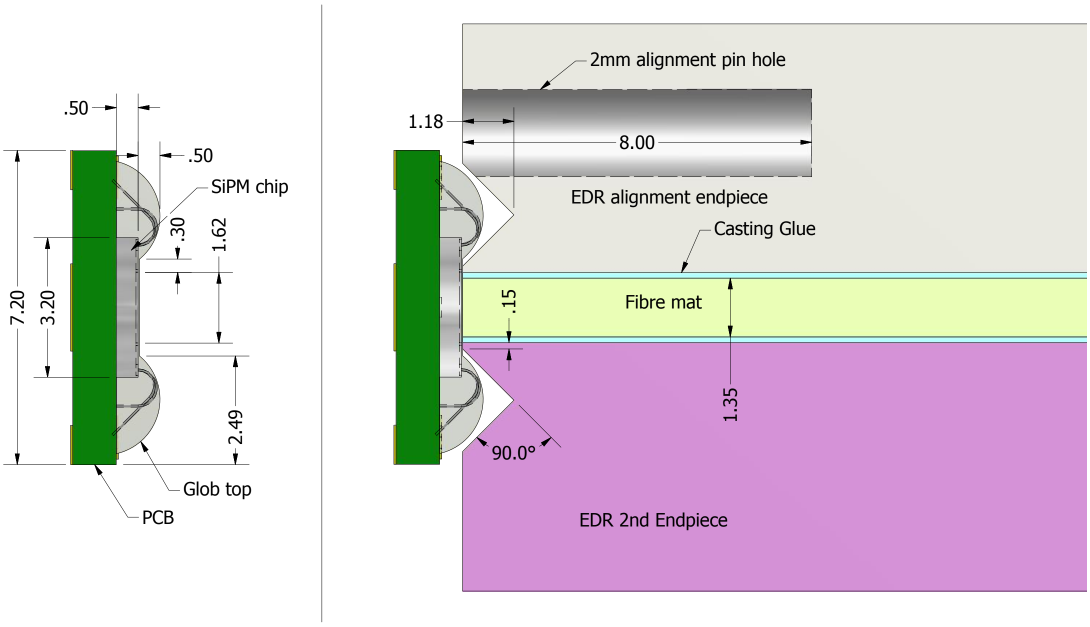

Figure 5.4: The interface between a proposed KETEK SiPM array package and the fibre mat endpiece. A triangular cutout is shown in order to accomodate the bondwires. With the current EDR module endpiece, there is a conflict with the alignment pin.

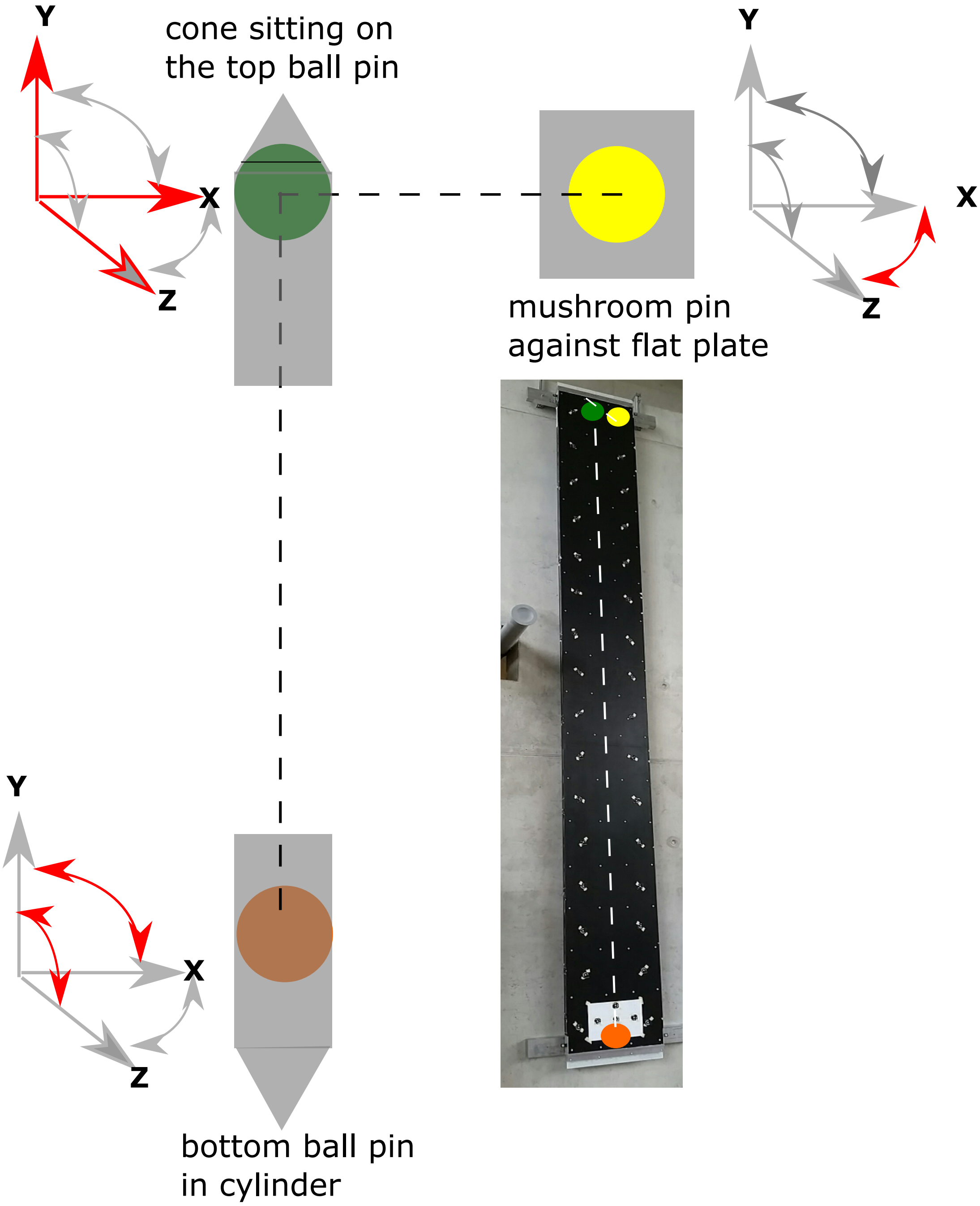

Figure 5.5: The kinematic constraints imposed by the mounting system. The red arrows indicate the direction or rotation that is constrained at that point. The green circle is the top ball pin. The yellow circle is the top mushroom pin. The orange circle is the bottom ball pin. The cone is indicate by the grey triangle and the cylinder by the grey rectangle over the ball pins. The flat plat is indicated by the grey square. A photograph of the module mounted on the prototype frame is shown in the bottom right and indicates the relevant points.

Chapter 6

Test Beam Results

The performance of the detector has been tested at the North Area SPS Test Beam Facility at CERN in May 2015 where 450 GeV protons from the SPS are directed to a target. The secondary beam mainly consisting of muons and pions with an energy of about 180 GeV is emitted in 5 - 10 s long spills, has a flux of 10^5 - 10^6 particles/second and is about 2 cm wide in the vertical and horizontal. The main goals of the May 2015 test beam campaign were the measurement of the single-hit efficiency, spatial resolution and light yield of a module which is, despite its smaller size, fully consistent with the technology described in this EDR. The light yield and attenuation length had been measured at previous test beams.

6.1 Experimental Setup

Four SciFi module prototypes were used during the testbeam. All modules are single fibre mats on honeycomb/carbon-fibre or similar supports, nearly 2.5 m in length, have 7 or 13 cm wide fibre mats, and 5 or 6 layers of fibres. A summary of the modules is shown in Table 6.1. The device under test (DUT) has a six-layer fibre mat with Kuraray 2015 fibres. SiPM arrays used are all Hamamatsu 2014 versions. The signal is read-out with SPIROC [12] readout chips and frontend electronics. The DUT was built following the EDR concept. The efficiency and resolution results obtained with the DUT are representative for the full size modules described above.

Table 6.1: The fibre modules in the testbeam.

Module	layers	width (cm)	mirrored
HD1	5	7	no
HD2	5	13	no
DUT (‘Slayer3’)	6	13	yes
CERN4	6	13	yes

The SciFi modules are mounted horizontally on a table that can be remotely moved horizontally and vertically. Two beam telescopes, allowing for a reference measurement of the trajectory of the beam particle, are placed directly before and after the SciFi table, an AMS silicon ladder telescope and the TimePix telescope, respectively. The TimePix telescope [13] has been developed as part of the LHCb VELO Upgrade project and consists of 8 layers of Silicon pixel detectors and achieves the best pointing resolution in the centre of the telescope of $1.54 \pm 0.11\ \mu$m. At the position of the SciFi modules, the resolution of the track reconstruction is estimated to be about 10 μm. The AMS telescope consists of three silicon strip detectors from the AMS experiment [14] each with a spatial resolution of about 10 μm. To ensure that both telescopes lie within the acceptence of the beam particles of an event, both telescope's scintillating triggers are required to fire in coincidence.

6.2 Calibration

To calibrate the digital ADC output of the SPIROC chips to the number of photo-electrons collected by each channel of the photodetector, light is injected onto the SiPM arrays with a pulsed laser in dedicated calibration runs between spills. The characteristic photo-peak spectra in the ADC distributions of all channels are described by the sum of equi-distant Gaussian functions. This distance is called the gain and corresponds to the number of adc-values per photo-electron. To supress the offset of the zero$^{\text{th}}$ photo-peak for which no photons have been collected, the mean adc-value of a dark pedestal run is subtracted from the data for each channel accordingly. Due to differences in the sampling time of the signal during a real physics run, the gain calibration is imperfect on the order of a couple percent. To correct for this fact, a similar additional calibration is performed using the p.e. distribution of the cluster channels in data.

6.3 Analysis

Three different thresholds in units of photo-electrons are applied to find the individual signal clusters and discriminate against noise. Every cluster is required to have at least one seed channel above seed threshold, neighbouring channels are added to the cluster as soon as they exceed the neighbour threshold and the accumulated charge of the whole cluster is to be larger than the sum threshold. Averaging over the collected charges of all clusters refers to the light yield for that specific run. Weighting the cluster channels x_i with their collected charge q_i gives the charge-weighted position

$$x_c = \frac{\sum_i q_i x_i}{\sum_i q_i} \tag{6.1}$$

of the detected cluster. With the PACIFIC read-out to be used in the full SciFi Tracker, the total collected charge information is not known. Only 3 bits indicating the three thresholds is transmitted from each channel. However, using the SPIROC information, one can assign an average charge for the specific threshold regions. A PACIFIC-like clustering can then be performed in the offline test beam analysis. The calculated position using this weighted thresholds is called the Pacific-like hit-weighted position $x_{Pacific}$.

Regardless of the method, each found cluster constitutes a potential hit of a beam particle in the detector. The cluster width corresponds to the number of channels included in the cluster.

6.3.1 Results

All the following results are taken with the device under test which is not tilted towards the beam but faces it vertically at 0°.

6.3.1.1 Determination of the light yield

Fig. 6.1 shows the collected charge distributions of all clusters at three different horizontal positions of the module. The left one is at the mirror, the central one is in the centre of the module length and the right one is 50 cm from the SiPM. Due to binning effects and range of the histogram the mean given in the histograms is only an estimate for the light yield. None of the values are corrected for SiPM pixel crosstalk. The calculated average light yields are given in Table 6.2

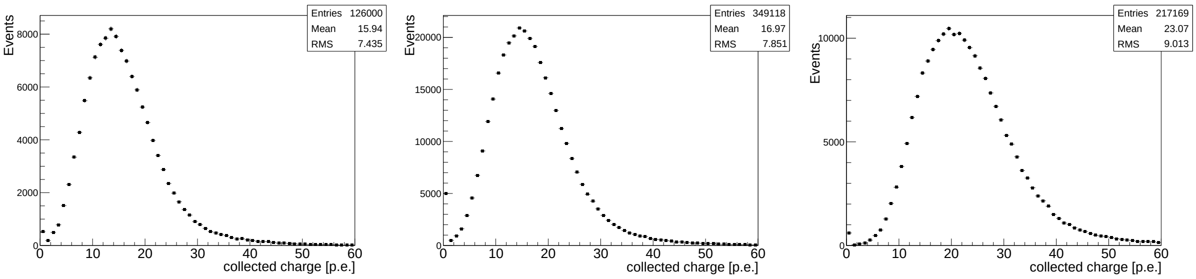

Figure 6.1: Collected charge distributions at the positions (left) at the mirror, (centre) at the centre of the module and (right) 50 cm from the SiPM. Not corrected for crosstalk.

Table 6.2: Average light yield at the mirror, at the centre of the module and 50 cm from the SiPM. Not corrected for crosstalk.

	at the mirror	centre	50 cm from SiPM
light yield [p.e.]	16.00 ± 0.05	17.04 ± 0.03	23.37 ± 0.05

6.3.2 Attenuation length

A finer position scan over the length of the modules with smaller data samples allowed for a measurement of the attenuation length of the modules without mirrors. The data are shown in Figure 6.2 with a single exponential fit to the data shown on the left, and a double exponential fit shown on the right. The single exponential shows an attenuation length of 328 cm from 100 cm to 250 cm from the SiPM. The double exponential fit has a short attenuation length component of 49 cm and a long component of 352 cm. These values agree with expectations from previous measurements of the 2010 fibres used in the module. It is reported that 2015 fibre from Kuraray and newer have attenuation lengths over 4 m, but has not been tested in test-beam conditions.

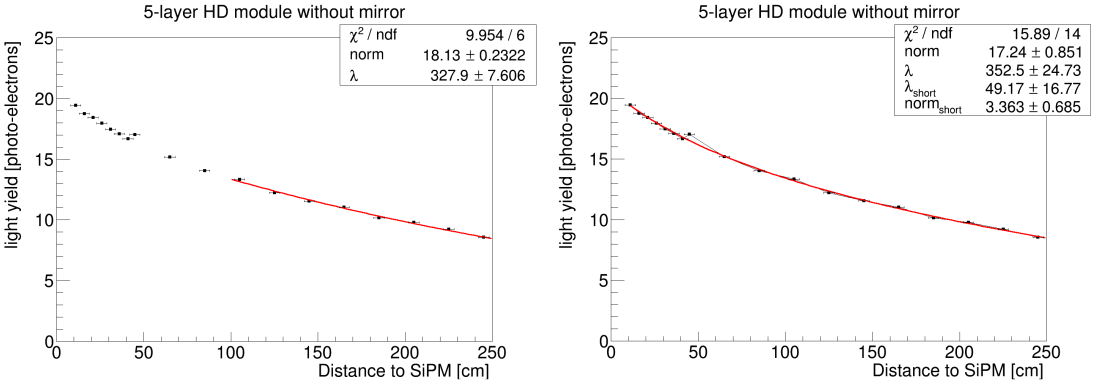

Figure 6.2: The attenuation length of 2.5 m testbeam modules. (left) A single exponential fit from 100 cm to 250 cm. (right) A double exponential fit.

6.3.2.1 Determination of spatial resolution

For the determination of the spatial resolution the residual of the SciFi cluster positions with respect to the reconstructed TimePix tracks are calculated where the TimePix tracks are required to exhibit a track $\chi^2/ndof$ smaller than 4. Tracks that are within the area of the gap between the dies of the SiPM are excluded. The distributions of the residuals using the charge-weighted mean and the Pacific-like hit-weighted mean as the SciFi cluster position are shown in Fig. 6.3, 6.4 and 6.5 for the three horizontal positions. They are described by the sum of two Gaussian functions with the widths σ_i weighted with their fractions f and 1-f. The effective resolution σ_{eff} when neglecting the resolution of the TimePix track is determined as the squared sum of the widths weighted with their fraction. Table 6.3 gives the results for the effective resolutions. Whereas the charge-weighted clustering benefits from an increase of total light yield, the resolution applying the Pacific-like hit-weighting one stays constant over the module. At the mirror, the charge-weighted resolution is better than 66.78 ± 0.23 μm and the hit-weighted resolution better than 73.27 ± 0.26 μm.

6.3.2.2 Determination of single-hit efficiency

The single-hit efficiency is determined by the ratio of the number of correctly reconstructed fibre clusters to the number of predicted TimePix tracks. It depends on the applied cluster thresholds and on the allowed distance from the cluster to the reference track. Accepting

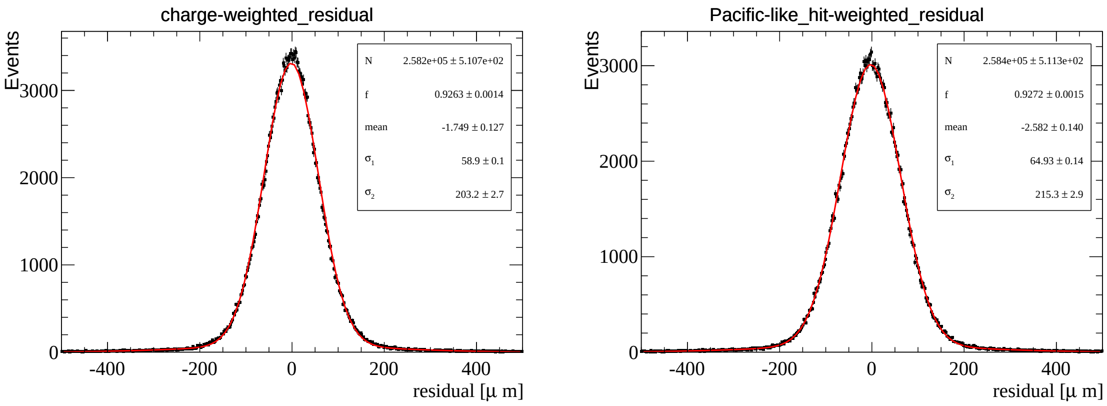

Figure 6.3: Charge-weighted (left) and Pacific-like hit-weighted(right) residual distributions of hits to the reconstructed TimePix track at the mirror.

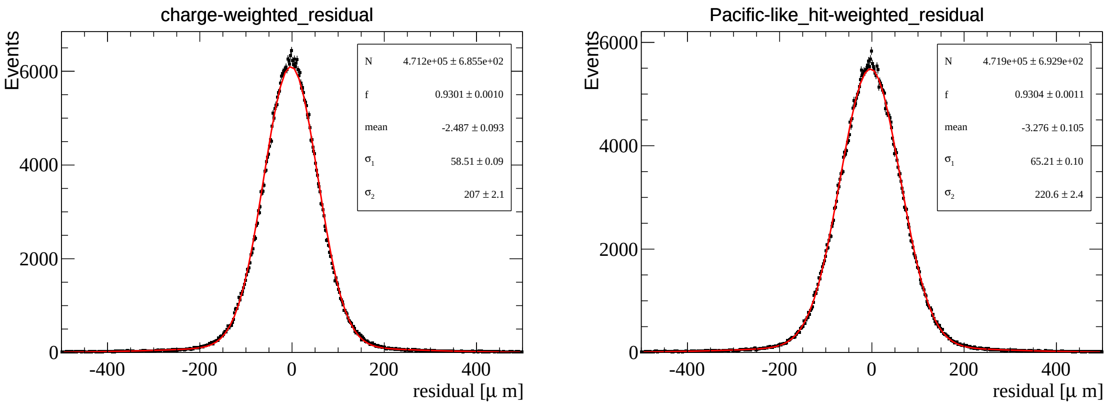

Figure 6.4: Charge-weighted (left) and Pacific-like hit-weighted(right) distributions of hits to the reconstructed TimePix track at the centre of the module.

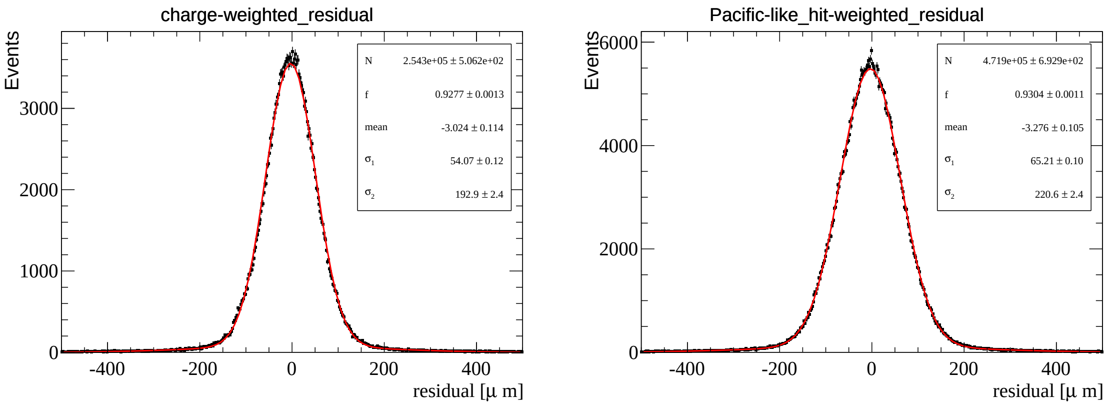

Figure 6.5: Charge-weighted (left) and Pacific-like hit-weighted(right) distributions of hits to the reconstructed TimePix track 50 cm from the SiPM.

all hits that are less than 5 channels away from the TimePix track, the left-hand side of Fig. 6.6 shows the single-hit efficiency as a function of the channel ID of the SiPM array

Table 6.3: Effective charge-weighted $\sigma_{eff,charge}$ and Pacific-like hit-weighted spatial $\sigma_{eff,Pacific}$ resolution when neglecting the TimePix telescope resolution at the mirror, at the centre of the module and 50 cm from the SiPM

	at the mirror	centre	50 cm from SiPM
$\sigma_{eff,charge}$ [μm]	66.78 ± 0.23	65.93 ± 0.18	61.22± 0.21
$\sigma_{eff,Pacific}$ [μm]	73.27 ± 0.26	73.18 ± 0.20	73.64± 0.20

for different seed thresholds. The beam traverses the module at the mirror. The neighbour threshold is chosen to be 1.5 p.e. For illustration purposes channel 65 corresponds to the gap between the two dies[1]. For the gap the efficiency decreases to 20%. To determine the efficiency way from the gap, a constant function is fitted to the efficiency pleateau of the channels left from the gap. The fit results are plotted against their corresponding thresholds on the right of Fig. 6.6. For the black graph, the sum threshold is chosen to be as large as the seed threshold whereas for the blue point the sum threshold is 4.0 p.e. as it is expected to be chosen for the future SciFi. The single-hit efficiencies 50 cm from the SiPM are shown in Fig. 6.7.

Table 6.4: The single hit efficiency for a given seed, neighbour and sum threshold for the DUT at the mirror (A). The text in bold is the foreseen thresholds for the LHCb Upgrade.

Seed	Neighbour	Sum	Hit Eff.
1.0	1.0	1.0	0.9993 ± 0.0001
1.5	1.5	1.5	0.9990 ± 0.0001
2.0	1.5	2.0	0.9972 ± 0.0002
2.5	1.5	2.5	0.9946 ± 0.0003
3.0	1.5	3.0	0.9990 ± 0.0004
3.5	1.5	3.5	0.9817 ± 0.0005
4.0	1.5	4.0	0.9693 ± 0.0006
4.5	1.5	4.5	0.9540 ± 0.0007
2.5	**1.5**	**4.0**	0.9866 ± 0.0004

6.4 Conclusion

A test module was built from a 6 layer casted fibre mat. The casting, endpieces and the mirror follow the design described above. The fibre mat was not irradiated before and was readout using 2014 Hamamatsu SiPM arrays with a PDE of 46%. A single hit efficiency of 98.7% near the mirror has been obtained. Near the silicon arrays, the hit efficiency increases to 99.95%. The resolution of the fibre mat using a Pacific-like threshold weighting

[1]The SiPM arrary comprises two dies, each with 64 channels.

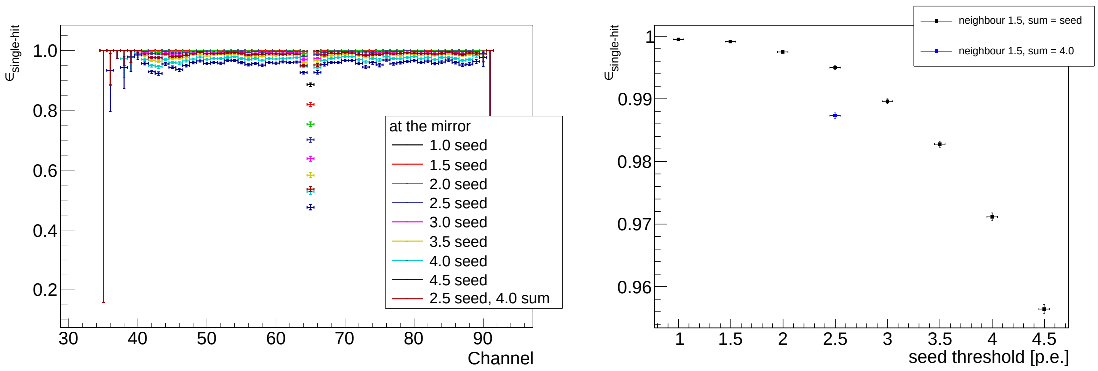

Figure 6.6: Single-hit efficiency vs. SiPM channels ID (left) at the mirror. For illustration purposes channel 65 corresponds to the gap between the two dies. On the right, the efficiency at the plateau for channels away from the gap is plotted against the seed threshold.

Table 6.5: The single hit efficiency for a given seed, neighbour and sum threshold for the DUT 50 cm from the SiPM (C).

Seed	Neighbour	Sum	Hit Eff.
1.0	1.0	1.0	0.9997 ± 0.0001
1.5	1.5	1.5	0.9997 ± 0.0001
2.0	1.5	2.0	0.9997 ± 0.0001
2.5	1.5	2.5	0.9996 ± 0.0001
3.0	1.5	3.0	0.9994 ± 0.0001
3.5	1.5	3.5	0.9991 ± 0.0001
4.0	1.5	4.0	0.9977 ± 0.0001
4.5	1.5	4.5	0.9962 ± 0.0002
2.5	**1.5**	**4.0**	0.9993 ± 0.0001

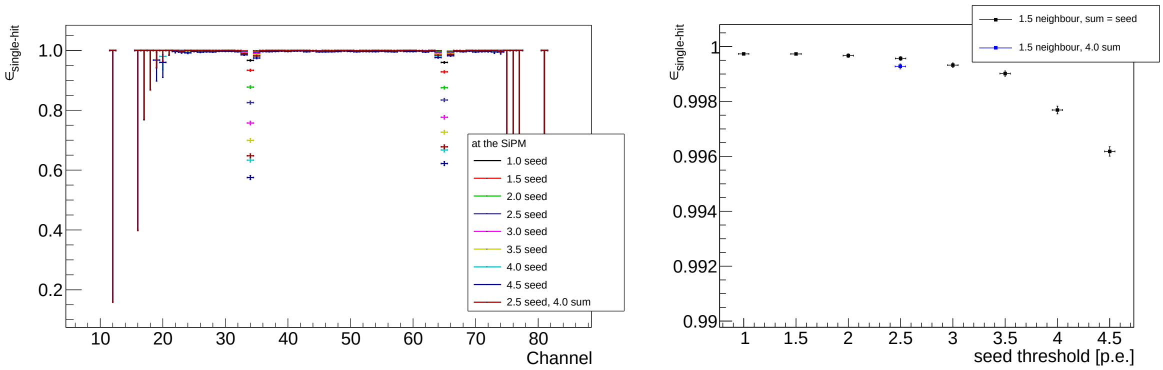

Figure 6.7: Single-hit efficiency vs. SiPM channels ID (left) 50cm from the SiPM. For illustration purposes channel 65 corresponds to the gap between the two dies. On the right,the efficiency at the plateau for channels away from the gap is plotted against the seed threshold.

procedure is 73 μm. The mean light yield near the mirror is 16.00 ± 0.05 photoelectrons and 23.37 ± 0.02 at a distance of 50 cm from the SiPM.

Chapter 7

General Planning, Production Schedule and Costs

Although the serial production is not part of the Engineering Design Review this section will give the details on the general planning, the production schedule and the costs.

7.1 General Planning

The long shutdown 2 (LS2) is scheduled to start in December 2018. With respect to the original planning the LHC shutdown is delayed by about 4 months. The Technical Board of LHCb collaboration however decided to treat the additional time as a reserve and to prepare for a detector installation starting in August 2018. Based on this assumption, Tab. 7.1 shows the schedule and milestones for the SciFi module production.

Table 7.1: Milestones for the fibre mat and module production.

Milestone	Date
EDR for modules	07/2015
Order winding machines	08/2015
Order winding wheels	10/2015
Order casting tools	10/2015
Order module tools	11/2015
Order fibres	11/2015
Order panels	12/2015
Start fibre mat production	01/2016
PRR fibre-mats	02/2016
Start module production	04/2016
PRR modules	05/2016
Finish mat production	07/2017
Finish module production	08/2017

7.2 Production scheme and task sharing

Mats and modules will be produced in specialized Winding and Module Assembly Centers. The task sharing between the winding centres and the module assembly centres is shown in Fig. 7.1.

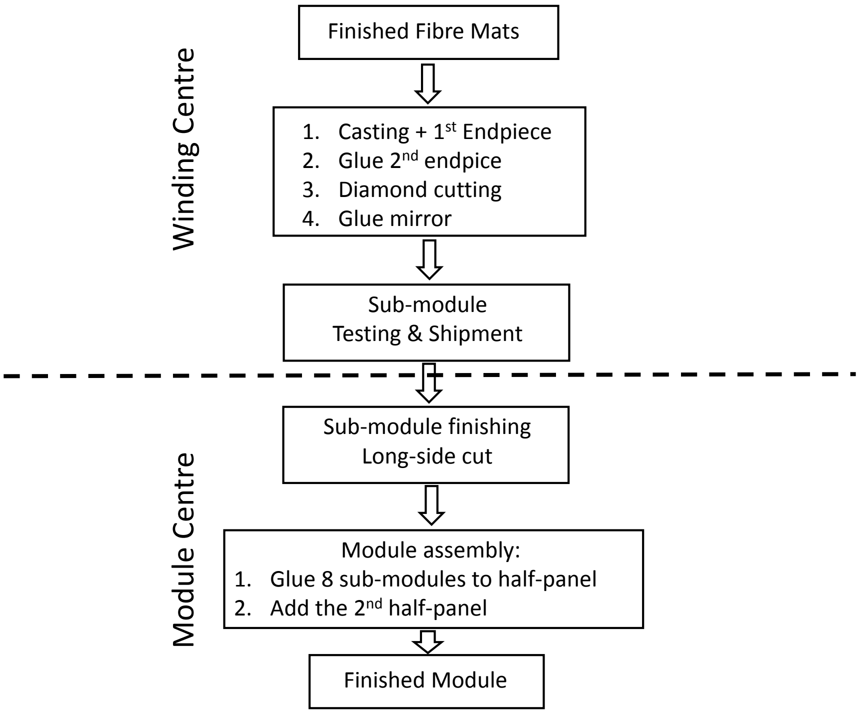

Figure 7.1: Task sharing between mat winding centres and the module assembly centres.

The task sharing allows to concentrate the tooling needed for the construction of a module (machine to cut the long-side edges of the mats, 5m gluing templates) in two module production centres.

7.2.1 Winding Centres

Adding the different production steps in Chapter 3 the total work-time to produce a finished fibre-mat at a Winding Centre (the long-side cuts will be done at the Module Assembly Centre) is about 21h (FTE). This time does not account for possible optimization of all production steps and in particular of the casting procedure. Table 7.2 also shows the waiting time for the different steps.

With a manpower of about 2.5 FTE technicians and assuming sufficient number of winding wheels and casting molds, a winding centre should thus be able to produce at 4 mats per week (5 working days). We hope however, that the effective man-power need to produce 4 mats per week can be reduced.

Table 7.2: Summary of the steps done at the WiC to produce a firbre-mat. Given times are FTE rounded to the nearest full hour.

Step	Item	Work time (FTE)	Curing/waiting time
1	Winding	10 h	36 h
2	Casting	8 h	72 h
3	2nd endpiece glueing	1 h	18 h
3	Optical cuts, mirrors, checks	3 h	18 h
Total		21 h	

In total we foresee 4 winding centres (Aachen, Dortmund, EPFL, Moscow). With the exception of Moscow the winding centres are assumed to have a single production shift. After a starting period, the winding centre in Moscow will be operated for two shifts per day and will produce the double amount of fibre mats compared to the standard centres.

We assume that the serial mat winding will start in the first winding centre in January 2016. We further assume a slow ramp-up of the mat production: In the first two months the centres will only produce 50% of their nominal production capacity. When the full production speed is reached the centres will all together produce 20 mats per week. This production speed requires 160 km of fibres per week, which is consistent with the assumed capacity of the fibre producer (250 km / week). Assuming 44 working weeks per year the mat production should be concluded by the end of July 2017.

7.2.2 Module assembly centres

The different steps done at the module assembly centre to build a module are summarized in Table 7.3

Table 7.3: Summary of the steps at a MAC to produce a final module. Given times are FTE rounded to the nearest full hour.

Step	Item	Work time (FTE)	Curing/waiting time
1	Long-side cuts (8 mats)	8 h	
2	Quality check of cut	4 h	
3	Module assembly 1st glueing	5 h	18 h
4	Module assembly 2nd glueing	3 h	18 h
Total		20 h	

If one module production template and two technicians are assumed per MAC, a production rate of two modules per week per production centre can be achieved. We foresee module assembly centres in Heidelberg and at NIKHEF. The module production should start in Heidelberg in April 2016 (timely after the mat production to have fast feed-back in case of problems) and NIKHEF should follow in May. With an assumed total production rate of 3 module per week and the given start dates the number of required fibre mats matches the production yield of the 4 winding centres. Assuming 44 working weeks per year the module production should be finished in August 2017.

The just-in-time arrival of the fibre mats at the module production centres require frequent transports. Seen the relatively compact size and the low weight of the mats a regular delivery also from the winding centre in Russia should be possible.

7.2.3 Quality Assurance

The high number of fibre mats that will be produced for the SciFi tracker require simple but effective quality assurance procedures during the serial production. These test procedures have been developed and applied during the production of the demonstrator module. The prototype setups used so far will be refined and identically setups will be provided to all production centres to ensure a common quality standard for the entire production.

The distributed production over several production centres also causes logistical problems. To cope with them a common data-base is under development. It provides fast access to the production information for the production managers, but it includes also simple masks for technicians serving as electronic process slips. The database contains the inventory of components, the status of production and results from quality assurance measurements.

7.3 Summary of Costs

The tables 7.4 summarizes the costs for the modules and the tooling as well as the total costs to produce the 144 detector modules. Here we assume a conversion rate between CHF and EUR of 1. The total cost of 3.6 MCHF matches well with the TDR assumption of 5.5 MCHF. NEEDS UPDATE.

Table 7.4: Summary of the total estimated costs per 5 m module for components (excluding institute-made tooling). Endpieces and Endplugs are injection molded cost estimates.

Item	Quantity	Cost/Item (CHF)	Cost (CHF)
Fibre Mats	8	1,850	14,800
Endpieces	16	9	144
Endplugs	4	92	368
Half-Panels (ADCO est.)	2	2,200	4,400
Glue	8	100	800
Total (CHF)			20,500

Table 7.5: Summary of the total estimated costs for institute-made tooling, assuming four winding centres and two module assembly centres.

Item	Quantity	Cost/Item (CHF)	Cost (CHF)
Winding Machine	4	75,000	300,000
WiC Casting Jig(s)	4	20,000	80,000
WiC: Glueing & Milling Jigs	4	2,000	8,000
WiC: Quality Assurance	4	10,000??	40000??
MAC: longitudinal cut jig	2	1,000	2,000
MAC: module alignment template	2	10,000	20000
MAC: flat assembly tables	8	5,000	40,000
MAC: Quality Assurance	2	10,000??	20000??
Total (CHF)			150,000 + 300,000

Table 7.6: Summary of total module costs including tooling and QA.

Item	Cost (CHF)
144 module	2,952,000
Tooling	450,000
QA	??
Total (CHF)	3,600,000 ??

Chapter 8

Appendix

8.1 Laser Setup

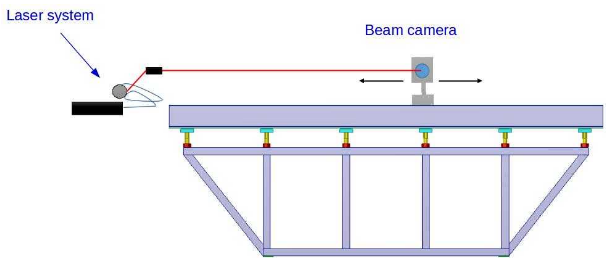

Figure 8.1: Diagram of laser setup with beam camera on the glass table.

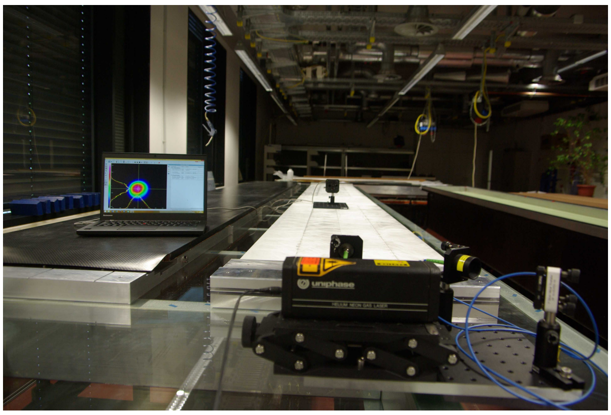

Figure 8.2: Photo og the laser setp on the dummy module.

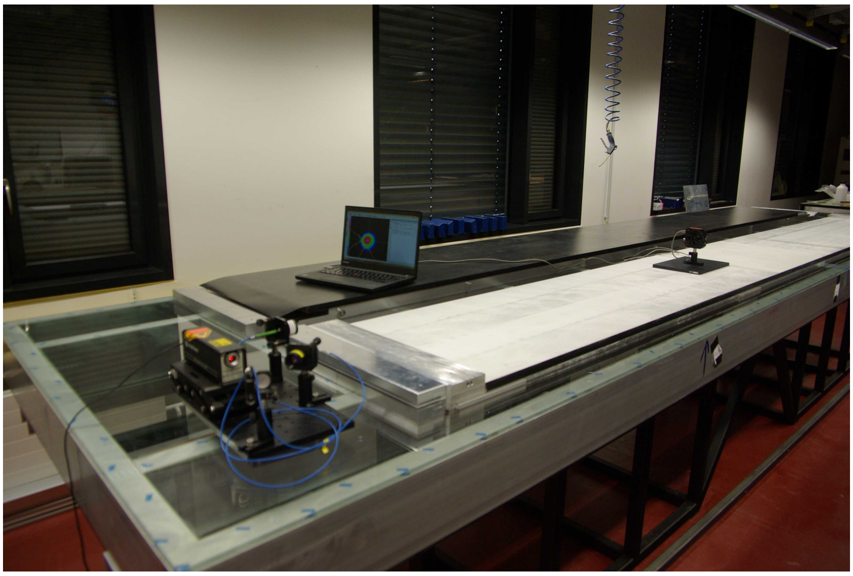

Figure 8.3: Photo og the laser setp on the dummy module.

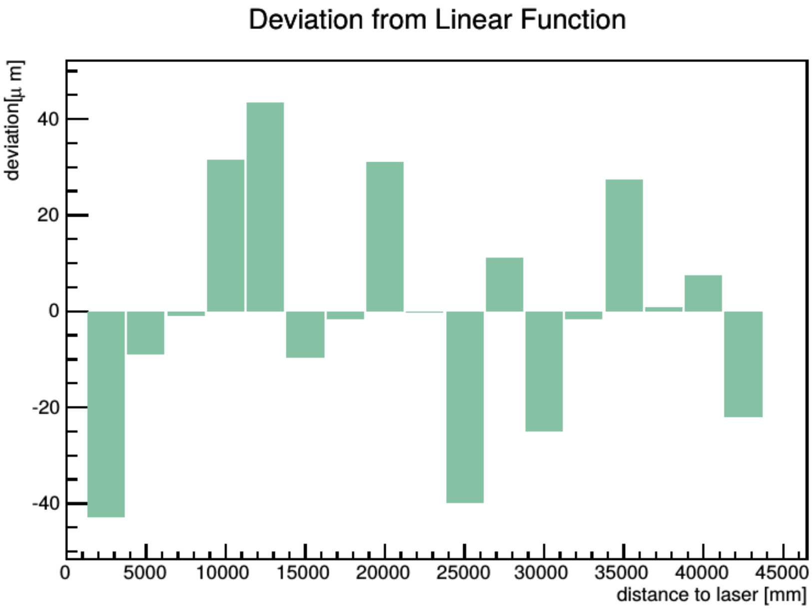

Figure 8.4: Flatness of gluing jig.

8.2 Fibremat straightness with a Sr-90 source

While the fibre mats are intended to be straight by means of the alignment pins produced during winding, the relative straightness of the fibres within the casted mat with respect

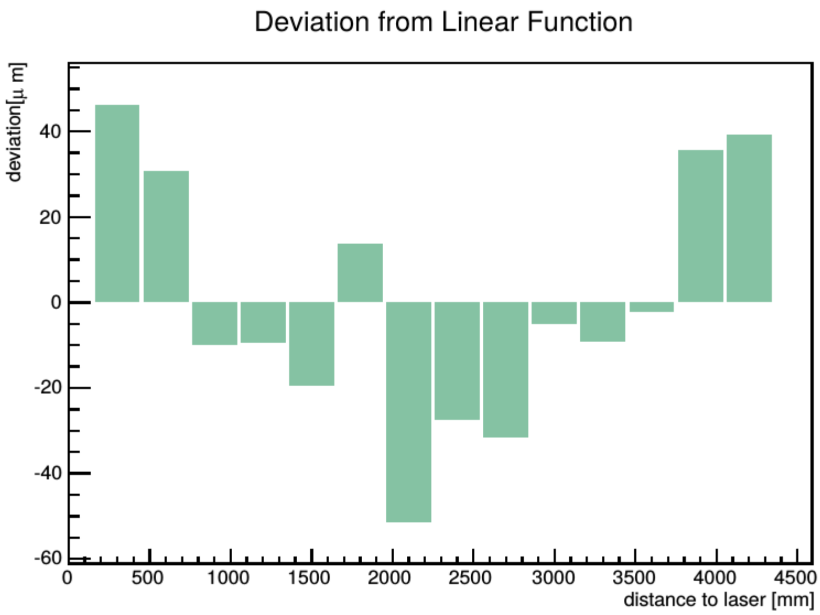

Figure 8.5: Flatness of half panels, produced by ADCO.

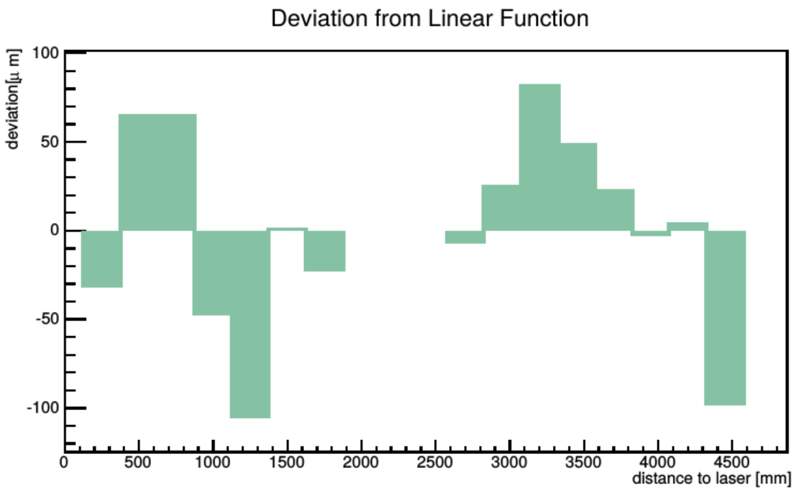

Figure 8.6: Flatness of detector half module, dummy module

to these pins is unknown over the length of the fibre mat. Cross section images are only seen at either end othe fibre mat. Optical methods of measuring the fibres along the mat is very difficult as the fibres are transparent and they have been covered by titanium dioxide loaded glue. The method developed in this section to measure the inter-mat straightness of the fibres involves aligning a collimated beta source with respect to the alignment pins above the fibre mat with a scintillating fibre trigger placed underneath the fibre mat .

Since it is assumed that the pins are aligned to the fibres, aligning the beta source to these pins should excite the same set of fibres and produce signal in the corresponding silicon photomultiplier channels, which are fixed at the readout end, producing the exact same signal distribution in the SiPM channels at all points along the mat. If the fibres move with respect to the pin, different fibres will be excited producing a shift in the signal (events above threshold) each SiPM channel sees.

A diagram of the setup is shown in Figure 8.7. An aluminium bar approximately 40 cm long with a 3 mm groove along the bottom is aligned along one edge of the groove to two of the fibre mat pins. A Sr-90 source is fixed in the bar above a 3 mm hole which collimates the beta particles. The particles with an energy high enough to pass through the fibre mat will be stopped in the scintillating fibre trigger placed below the collimator hole. The trigger fibres have single channel SiPMs at either end where the signals are passed through a discriminator and form a coincidence. The coincidence triggers the readout of the front-end electronics. A histogram showing the number of events in each channel which pass a threshold is seen in Figure 8.8. A Fermi function is fit to the left and right side of the distribution and is a good indication of the position of the edges. The mean of the distribution has also been found to be a precise indication of the position.

A systematic study of the repeatability of the measurements indicates that the alignment can be repeated at each point better than 10 micron. 100k triggered events per point were recorded resulting in a statistical uncertainty in the mean of 3 micron. However, it was noticed that repeated placement of the bar over the pin results in a degradation of the positioning over time due to the wearing away of the relatively soft glue pins compared to the aluminium. As well, there is a 25 micron tolerance between the groove edges and pin, if the groove wall is not pressed against the pin sidewall.

Results of the first measurements are shown in section 3.5.

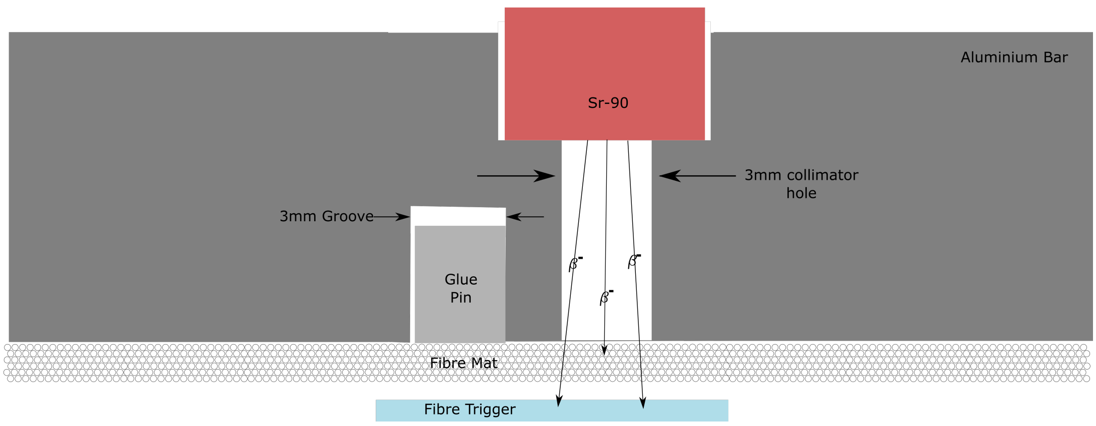

Figure 8.7: Schematic of the Sr-90 source based fibre mat straightness measurement.

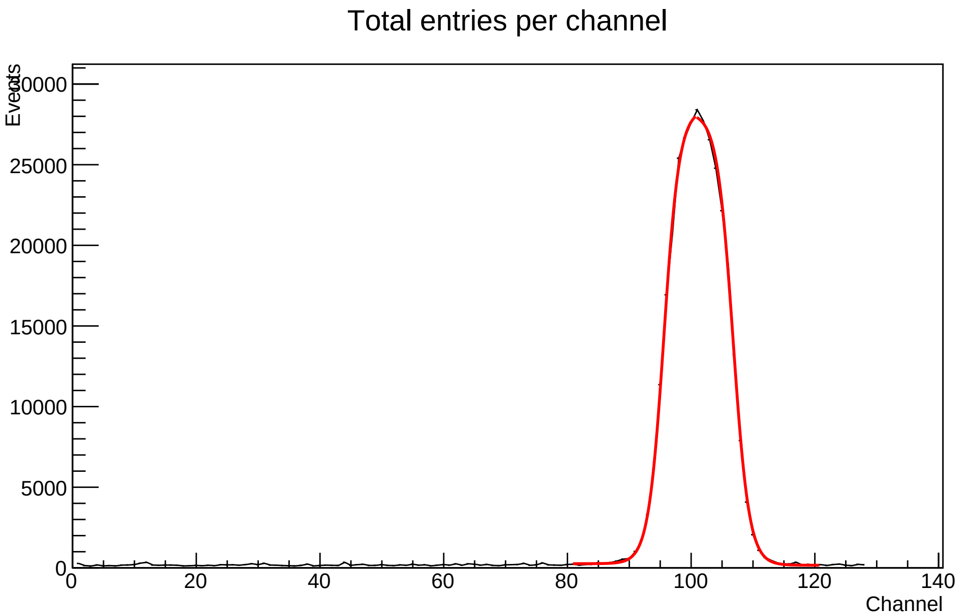

Figure 8.8: The number of triggered events over threshold as a function of SiPM channel. The red curves are two separate fits (left side and right side) to a Fermi function.

References

[1] LHCb collaboration, R. Aaij *et al.*, *Framework TDR for the LHCb Upgrade*, Apr, 2012.

[2] LHCb collaboration, *LHCb Tracker Upgrade Technical Design Report*, CERN-LHCC-2014-001. LHCb-TDR-015.

[3] C. Joram, *Technical specifications of the scintillating fibres*, Tech. Rep. LHCb-PUB-2014-019, CERN-LHCb-PUB-2014-019, LHCb-INT-2013-061, December, 2013.

[4] C. Alfieri, A. B. Cavalcante, and C. Joram, *A set-up to measure the optical attenuation length of scintillating fibres*, Tech. Rep. LHCb-PUB-2015-011; CERN-LHCb-PUB-2015-011, March, 2015.

[5] C. Alfieri, A. B. Cavalcante, C. Joram, and M. W. Kenzie, *"an experimental set-up to measure light yield of scintillating fibres"*, Tech. Rep. LHCb-PUB-2015-012; CERN-LHCb-PUB-2015-012, March, 2015.

[6] K. Hara *et al.*, *Radiation hardness and mechanical durability of kuraray optical fibers*, Nucl. Instrum. Meth. **A411** (1998) 31.

[7] C. Ponomarenko *et al.*, *Nanostructured organosilicon luminophores and their application in highly efficient plastic scintillatorst*, Nature Scientific Reports **4** (2014) .

[8] C. Joram and T. Schneider, *Mirroring of fibre ends for the LHCb SciFi project*, Tech. Rep. LHCb-PUB-2014-020. CERN-LHCb-PUB-2014-020. LHCb-INT-2013-060, CERN, Geneva, Feb, 2014.

[9] J. Nardulli and N. Tuning, *A Study of the Material in an Outer Tracker Module*, Tech. Rep. LHCb-2004-114. CERN-LHCb-2004-114, CERN, Geneva, Jan, 2005.

[10] V. Fave, *Estimation of the material budget of the Inner Tracker*, Tech. Rep. LHCb-2008-054. CERN-LHCb-2008-054, CERN, Geneva, Oct, 2008.

[11] A. Schultz von Dratzig, *"finite element analysis of the scifi-nomex-sandwich panels"*, Tech. Rep. LHCb-PUB-2015-007; CERN-LHCb-PUB-2015-007, RWTH Aachen, March, 2015.

[12] M. Bouchel et al, *Spiroc (sipm integrated read-out chip): Dedicated very front-end electronics for ilc prototype hadronic calorimeter with sipm read-our*, Nucl. Sci. Symp. Conf. Rec. (2007) .

[13] LHCb, *The Timepix Telescope for High Performance Particle Tracking*, .

[14] AMS 02, R. Battiston, *The antimatter spectrometer (AMS-02): A particle physics detector in space*, Nucl. Instrum. Meth. **A588** (2008) 227.